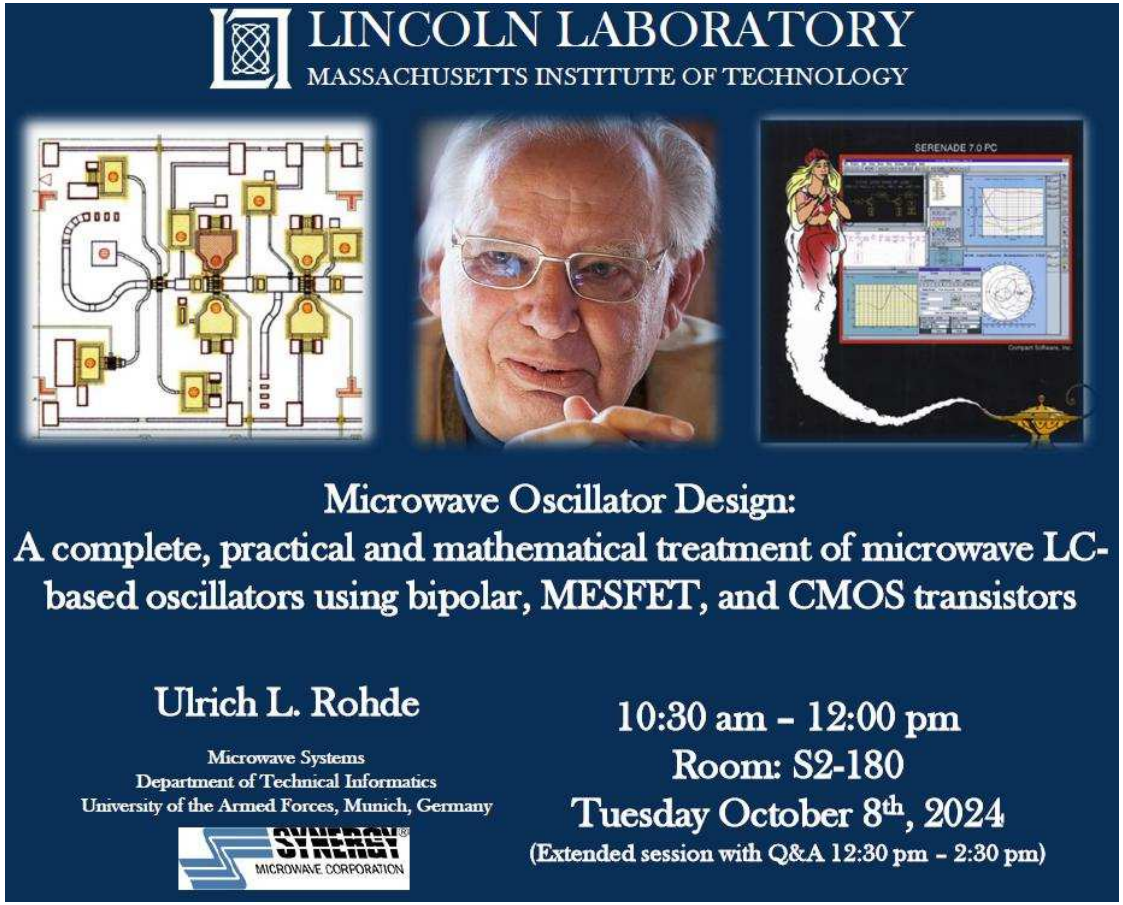

Based in part on the following books:

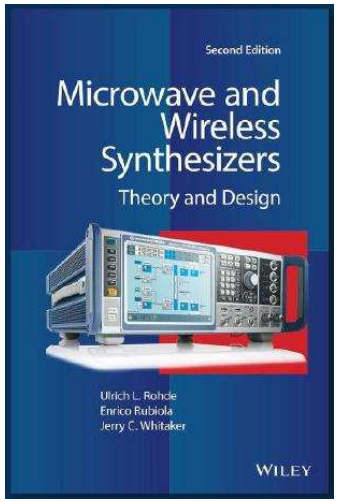

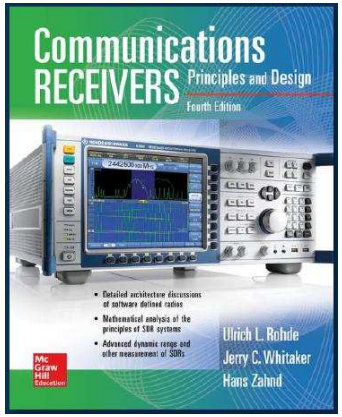

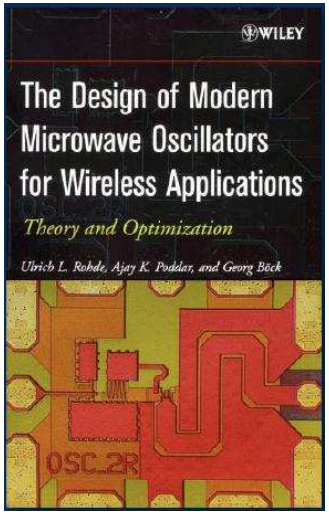

Zoom Link: https://mitll.zoomgov.com/j/1610670756?pwd=PvwQIth7sUhE2Da3pifaKHras72sby.1

der Bundeswehr Universität München

Abstract

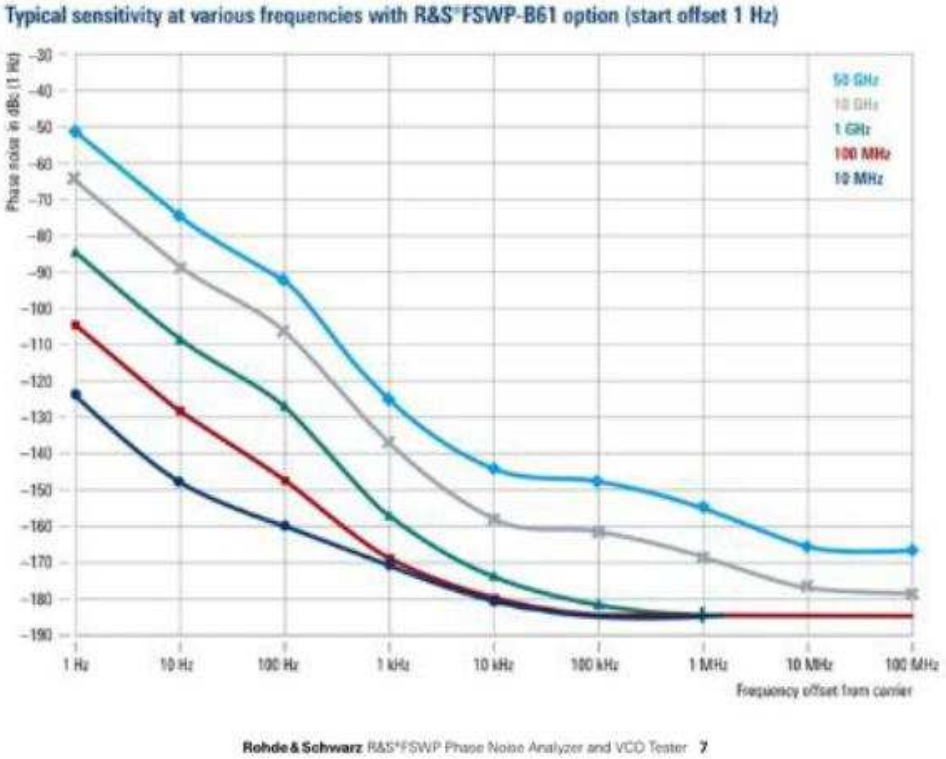

The design of RF/microwave oscillators has been and is the subject of many publications. Historically, oscillators have been designed to a large degree based on past experience with mostly successful designs and, to a lesser degree, on experimental data. High resolution test equipment for validation were also not available at the time. For a designer, however, it is preferable to start from a set of specifications and then apply a rigorous and an advanced mathematics-based design procedure. In this talk we show linear-data based, measured large-signal based and non-linear Bessel function based treatment of RF/microwave Oscillators. The LC-based oscillators such as bipolar, MESFET, and CMOS transistors and the resulting design of high-performance, low phase noise oscillators, from VHF crystal resonators to YIG oscillators and their measured data will also be discussed.

160 GHz Oscillator – Measured Phase Noise Plot

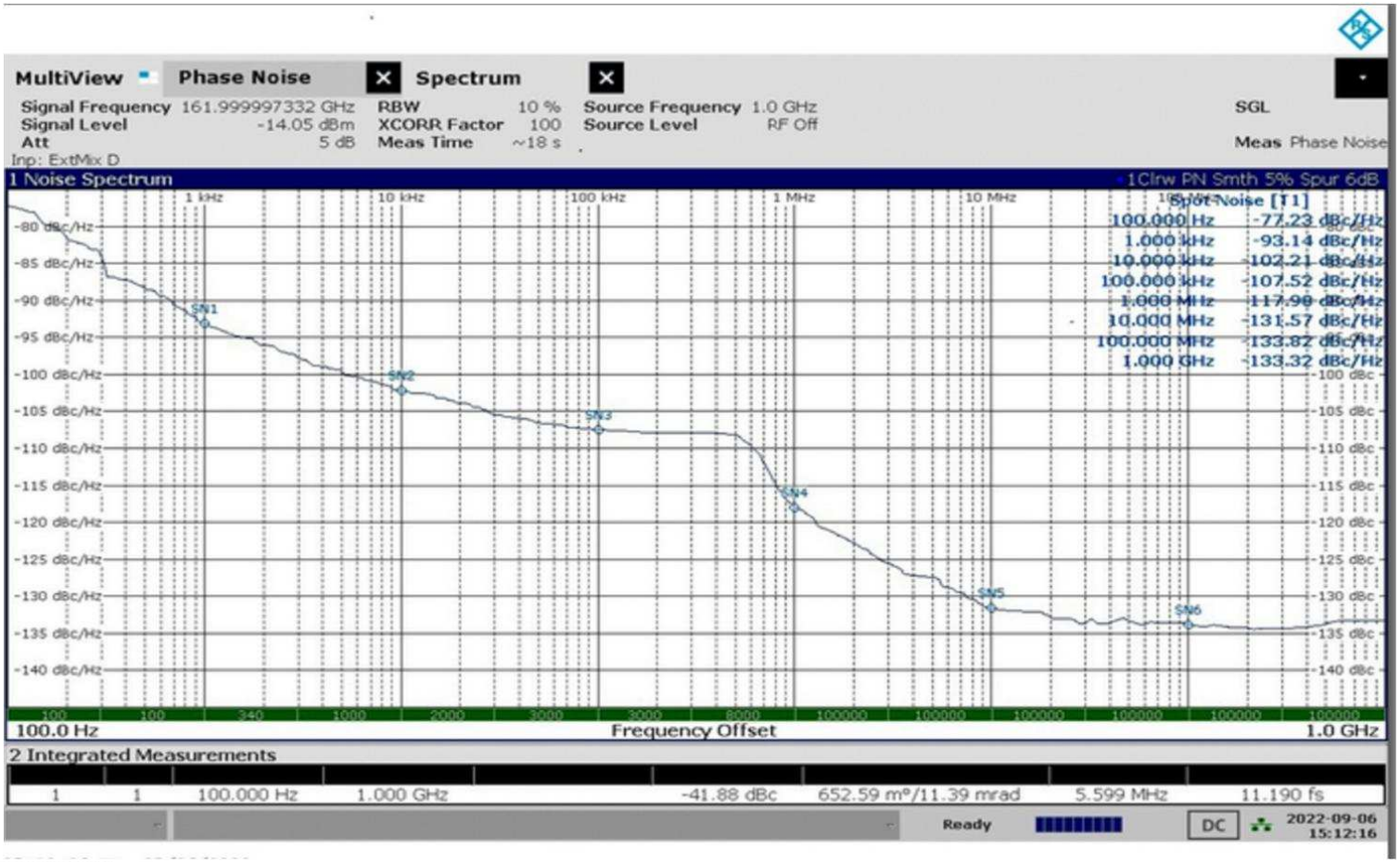

Outlook - 1

- **Introduction**
- **What is an oscillator?**
- **Introduction to Microwave Oscillators and Their Mathematical Treatment**
- **Transistor models and Noise Contributions**
- **Transistor Types**
- **Linear Approach to the Calculation of Oscillator Phase Noise**
- **Typical Microwave Oscillator (Colpitts Oscillator)**
- **Designing an Oscillator**
- **Tuning Diode Noise Contribution**
- **Designing an Oscillator based on Linear S-Parameters**
- **Large signal Operation of Oscillators (Colpitts/YIG)**
- **Classical Linear Two-Port Oscillator Design**
- **Microwave Resonators**
- **A Novel Tunable Active Spiral Inductor**
- **The Active Inductor Using a Gyrator**

Outlook - 2

- **Active Inductor Oscillator**
- **Synthesized Inductor Circuits**
- **Phase Noise Contribution of the Various Parts of the Oscillator Using an Active Inductor**
- **The Modern Time-Domain Behavior of an Oscillator**
- **Test Case: Design Example of a 100MHz crystal oscillator**
- **Phase Noise Analysis Based on the Negative Resistance Model**
- **Oscillator Phase Noise**
- **Design Examples of Oscillators for Best Phase Noise and Good Output Power**
- **Summary**

Introduction

- The following presentation will be a thorough practical and mathematical description of how to build optimized oscillators, mostly LC based, such as the one shown her in in Fig.1, but also with specific microwave resonators, crystals and other resonators.
- The oscillator below is from the MIMIC Program
- The acronym, “MIMIC” stood for Microwave/Millimeter-Wave Monolithic Integrated Circuits. The DARPA program manager was Dr. Eliot Cohen. In 2012 Eliot Cohen wrote an article on the MIMIC Program for IEEE MTT-S Microwave Magazine which is a good resource if you want to learn about this historic program. Here are the details:
- Eliot Cohen, "The MIMIC Program - A Retrospective", Microwave Magazine, June 2012, pp. 77-88

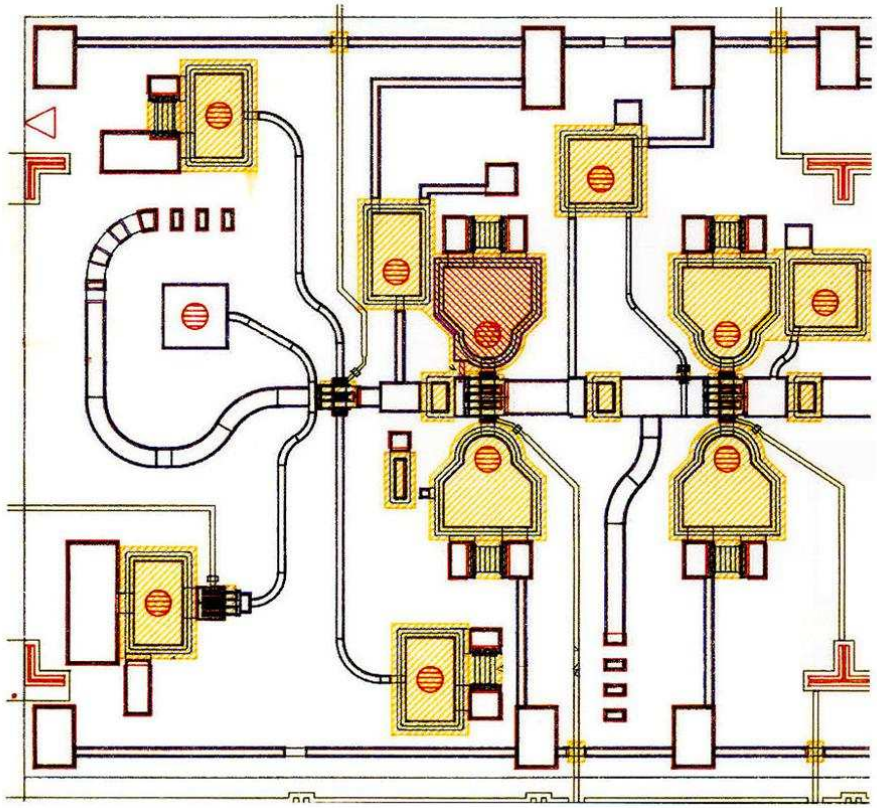

Fig. 1: Two stage FET based Microwave tunable Oscillator Built on GaAs Substrate

What is an Oscillator?

- An Oscillator is an Electronic Circuit that converts DC power to RF power, this can range from a few Hz to Tera Hz and higher
- An oscillator consists of an active device acting as an amplifier, a resonator, and a feedback circuit
- A small amount of energy feedback is needed to sustained oscillation and the majority of available energy appears at the output terminals
- Resonators can be LC based circuits, transmission line based, crystal, ceramic, dielectric resonator ,YIG (Yttrium Garnet) based, and others

For RF applications, the most relevant features besides size are:

- Output power
- Harmonic content
- Phase Noise
- Power consumptions, to name a few

Introduction

- The design of microwave oscillators has been and is the subject of many publications.
- To a certain degree, oscillators have been designed based on experimental data and experience, and the resulting performance has been measured and published.
- The designer, however, considers it important and useful to start from a set of specifications and then applies a synthesis procedure, which leads to a successful circuit.
- The following are popular transistor oscillator designs.
- **History**
  - The first time an oscillator became important was when Maxwell's Equations were to be experimentally proven. Heinrich Hertz made the first known oscillator. He used a dipole as the resonator and a spark gap generator as the oscillator circuit as shown in Figure 1-1.

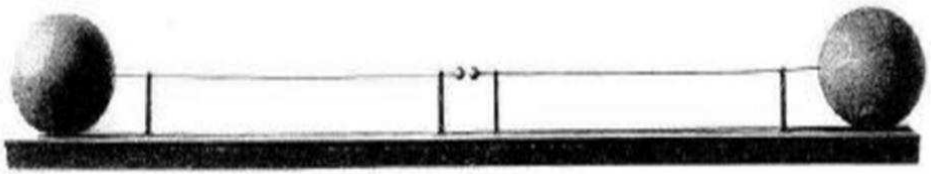

Figure 1-1 Original dipole made by Heinrich Hertz in 1887 using balls at the end to form a capacitive load (Deutsches Museum, Munich).

Introduction to Oscillators

- One of the most popular Oscillators is the Colpitts Oscillator

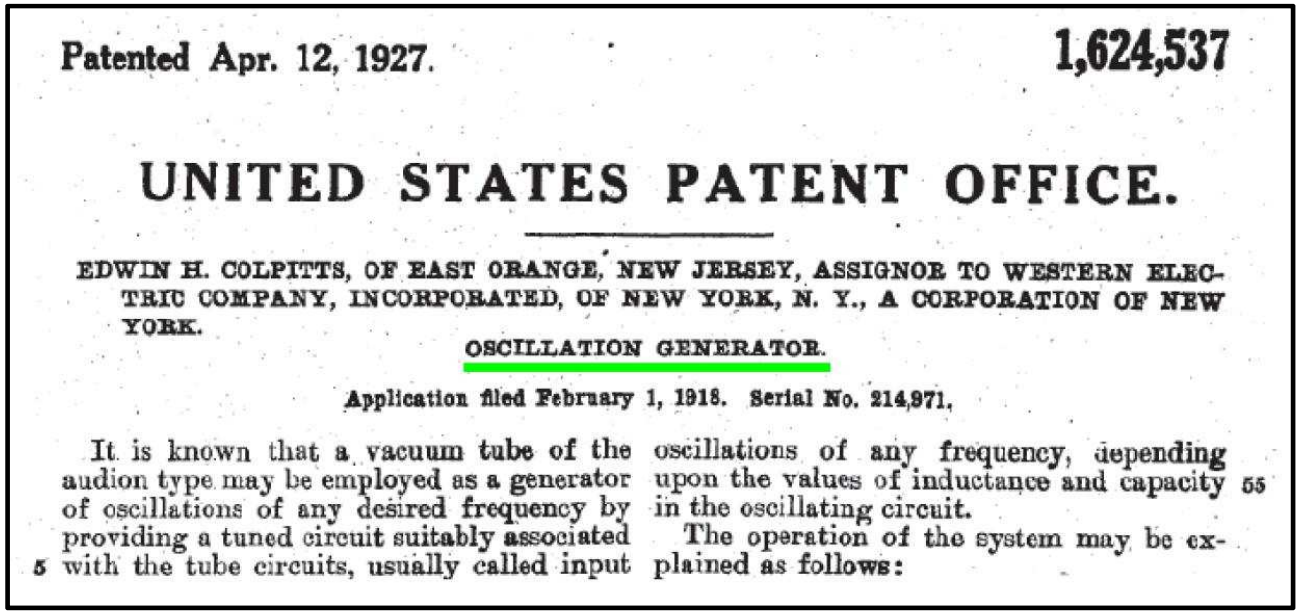

Patented Apr. 12, 1927. 1,624,537

UNITED STATES PATENT OFFICE.

EDWIN H. COLPITTS, OF EAST ORANGE, NEW JERSEY, ASSIGNOR TO WESTERN ELECTRIC COMPANY, INCORPORATED, OF NEW YORK, N. Y., A CORPORATION OF NEW YORK.

OSCILLATION GENERATOR.

Application filed February 1, 1918. Serial No. 214,971.

It is known that a vacuum tube of the audion type may be employed as a generator of oscillations of any desired frequency by providing a tuned circuit suitably associated with the tube circuits, usually called input oscillations of any frequency, depending upon the values of inductance and capacity in the oscillating circuit.

The operation of the system may be explained as follows:

- A Colpitts oscillator is based on a topology using one coil and two capacitors and is variation of Hartleys approach
- Hartley is using one capacitor and two coils. Hartley´s patent was filed in 1915 and issued 1920

Colpitts Oscillators

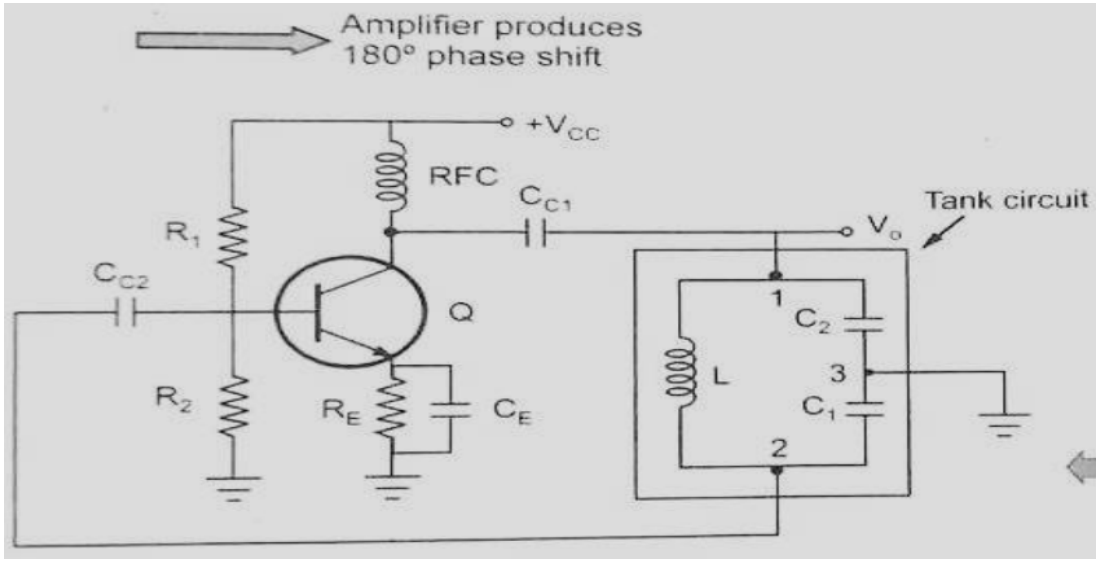

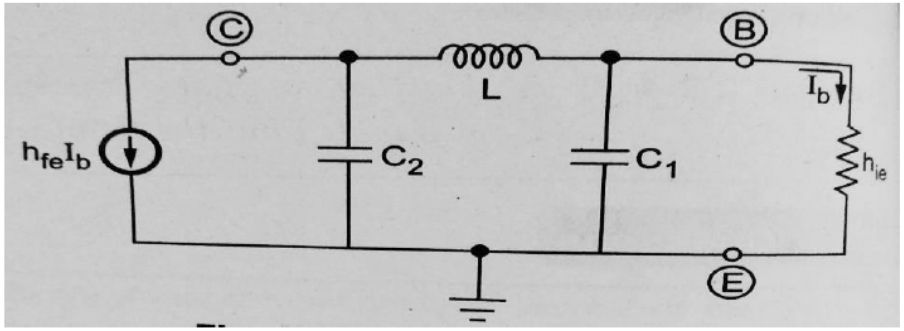

Colpitts oscillator equivalent circuit

Source: Microelectronics by J. Millman and A. Grabel

Introduction to Oscillators and their Mathematical Treatment

- Modern communications systems need oscillators as part of the design.
- In most cases these oscillators are part of a synthesizer and they are voltage-controlled, meaning that the frequency is determined by tuning diodes, frequently called varactors.
- For high performance circuits the Colpitts oscillator is most frequently selected
- The Colpitts oscillator comes in different flavors e.g.:
  - Figure 1a: Basis circuit with capacitive divider
  - Figure 1b: basic circuit with indictive divider
  - Figure 1c: basic circuit with a combination of both
- The important differences are the effective loading of the resonator circuit and also the way of tuning of the circuits resonance frequency.

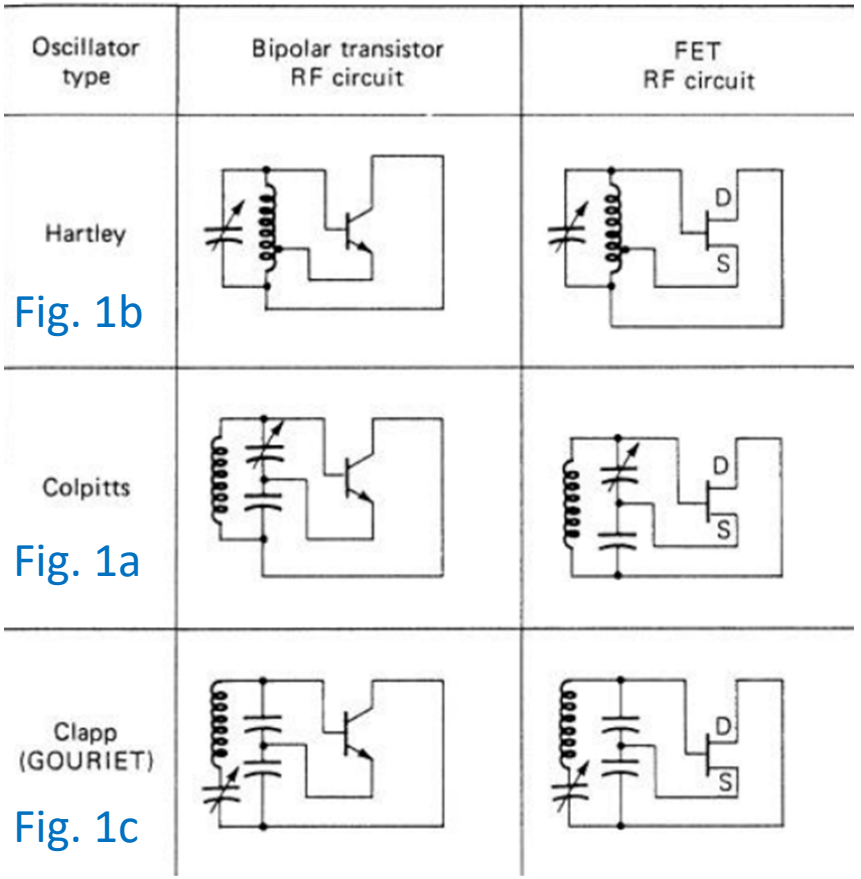

Transistor models and their Noise Contribution

- For the design of oscillators we are looking at members of bipolar and field-effect transistor families.
- In the case of the bipolar transistor, conventional microwave silicon transistors are manufactured with an fT up to 25 GHz, while the more advanced SiGe transistors take over from this frequency range.
- Today, SiGe transistors are available up to 900 GHz and are used as part of an RFIC. Their cousins, the heterojunction bipolar transistors (HBTs), based on GaAs technology, can achieve similar cut-off frequencies, but this technology is much more expensive for medium to large integrated circuits.
  - HBTs also have a higher flicker noise corner frequency.
  - SiGe transistors have a much lower flicker noise corner frequency and lower breakdown voltages (typically 2-3V).
- However, because of the losses of the transmission line in practical circuits, there is not much difference between HBT and SiGe oscillator noise as fT is the same.
- There is a similar competing situation between Bi-CMOS transistors implemented in a 0.062 micron technology and with GaAs FETs, specifically p-HEMTs.
  - The GaAs FETs have well-established performance with good models, and the Bi-CMOS transistors are currently being investigated as to what models are the best.
  - Also, there is the 1/f noise problem, specifically, with GaAs FETs more than with MOS transistors.
  - The 6 nm technology is somewhat impractical because of poor modeling. This means that many CAD predictions do not translate in a good design.

Johnson Noise

- The Johnson noise (thermal noise) is due to the movement of molecules in solid state devices called "Brown's molecular movements"
- It is expressed as $v_n^2 = 4kT_0RB$ (emf) volt $^2/\mathrm{Hz}$)
- The power of thermal noise can thus be written as
- Noise Power $= \frac{v_n^2}{4R} = kT_0B(W/Hz)$

It is most common to do noise evaluations using a noise power density, in Watts per Hz.

- By setting $B = 1$ Hz we get:

- For $B = 1$ Hz, Noise Power $= kT_0$

  by Thevinin, Noise Power $= 1.38 \times 10^{-23} \times 290 = 4 \times 10^{-23}$ W

Noise floor, noise power and more …..

- Noise floor below the carrier for zero dBm output is given by:

$$L(\omega) = 10\log\left(\frac{v_n^2/R}{1mW}\right) = -173.97\text{dBm or about } -174\text{dBm}$$

- In order to reduce this noise, the only option is to lower the temperature, since noise power is directly proportional to temperature.
- The Johnson noise sets the theoretical noise floor.
- The available noise power does not depend on the value of resistor but it is a function of temperature T. The noise temperature can thus be used as a quantity to describe the noise behavior of a general lossy one-port network.
- For high frequencies and/or low temperature a quantum mechanical correction factor has to be incorporated for the validation of equation. This correction term results from Planck's radiation law, which applies to blackbody radiation.

$$P_{av} = kT.B \cdot p(f,T), \text{ with } p(f,T) = \left[\frac{hf}{kT}/\left(e^{\left(\frac{hf}{kT}\right)} - 1\right)\right]$$

- where $h = 6.626.10^{-34}$ J $- s$, Planck's Constant (***Planck's Radiation Noise***)

Shottky / Shot Noise / Flicker Noise

- Schottky/Shot noise
  - The Schottky noise occurs in conducting PN junctions (semiconductor devices) where electrons are freely moving. The root mean square (RMS) noise current in 1 Hz bandwidth given by
  - $\overline{\iota_n^2} = 2 \times q \times I_{dc}\, P = i_n^2 \times R_L$
  - Where, q is the charge of the electron, P is the noise power, and I_{dc} is the dc bias current, R_L is the termination load (can be complex).
  - Since the origin of this noise generated is totally different, they are independent of each other
- Flicker noise
  - The electrical properties of surfaces or boundary layers are influenced energetically by states, which are subject to statistical fluctuations and therefore, lead to the flicker noise or $1/f$ noise for the current flow.
  - $1/f$ noise is observable at low frequencies and generally decreases with increasing frequency f according to the $1/f$-law until it will be covered by frequency independent mechanism, like thermal noise or shot noise.

    Example: The noise for a conducting diode is bias dependent and is expressed in terms of AF and KF.
- Transit time and Recombination Noise
  - When the transit time of the carriers crossing the potential barrier is comparable to the periodic signal, some carriers diffuse back and this causes noise. This is really seen in the collector area of NPN transistor.
  - The electron and hole movements are responsible for this noise. The physics for this noise has not been fully established.

Avalange Noise

- When a reverse bias is applied to semiconductor junction, the normally small depletion region expands rapidly.
- The free holes and electrons then collide with the atoms in depletion region, thus ionizing them and produce spiked current called the avalanche current.
- The spectral density of avalanche noise is mostly flat. At higher frequencies the junction capacitor with lead inductance acts as a low-pass filter.
- Zener diodes are used as voltage reference sources and the avalanche noise needs to be reduced by big bypass capacitors.

$$\langle i_{Dn}^2 \rangle_{AC} = 2qI_{dc}B + Kf\frac{I_{DC}^{Af}}{f}B$$

- The Af is generally in range of 1 to 3 (dimensionless quantity) and is a bias dependent curve fitting term, typically 2.
- The Kf value is ranging from $1\mathrm{E}^{-12}$ to $1\mathrm{E}^{-6}$, and defines the flicker corner frequency.

Bipolar Transistor

- The bipolar transistor has been known and used for many decades.
- Many scientists have explained its behavior, and probably the best analysis in the DC/RF area is summarized in [29].
- This summary is based largely on the Infineon transistor BFP520 as an example, but is applicable to other transistors also.

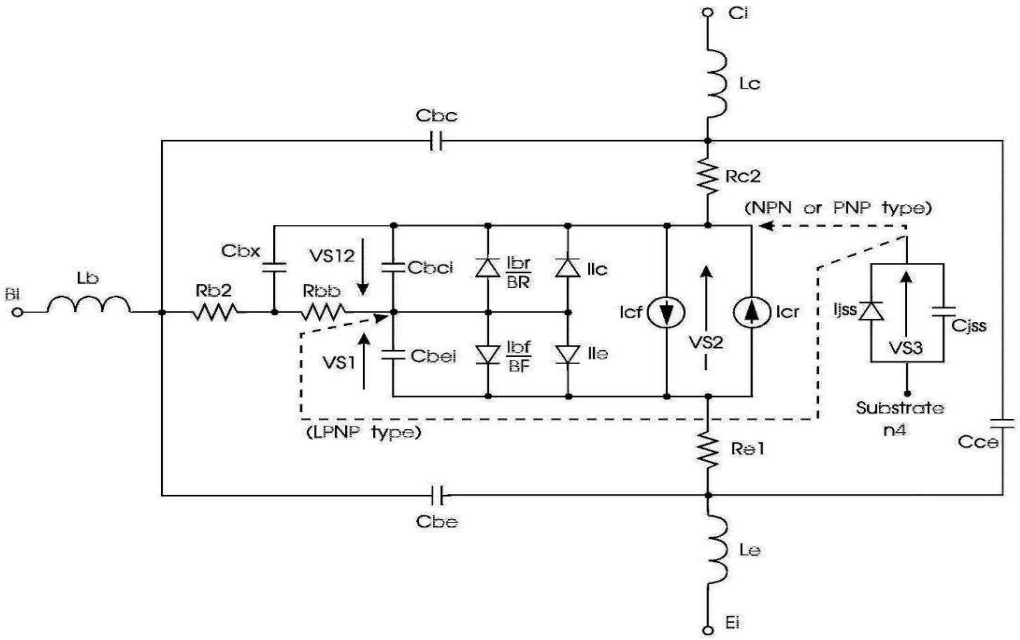

- equivalent circuit for a microwave bipolar transistor. It deviates from the SPICE implementation by having two base-spreading resistors

Noise Model of the Bipolar Transistor

Let Δf be the bandwidth (usually normalized to a 1Hz bandwidth). The noise generators introduced in the intrinsic device are shown below, and have mean-square values of:

$$\left\langle i_{bn}^2 \right\rangle = 2qI_B\ \Delta f + \mathrm{KF}\frac{I_B^{\mathrm{AF}}}{f^{\mathrm{FCP}}}\Delta f$$

$$\left\langle i_{cn}^2 \right\rangle = 2qI_C\ \Delta f$$

$$\left\langle i_{Rbb}^2 \right\rangle = \frac{4kT}{R_{bb}}\Delta f$$

$$\left\langle i_{Re1}^2 \right\rangle = \frac{4kT}{RE1}\Delta f$$

$$\left\langle i_{Rc2}^2 \right\rangle = \frac{4kT}{RC2}\Delta f$$

$$I_B = \frac{I_{bf}}{BF} + I_{le}$$

$$I_C = I_{cf} - I_{cr}$$

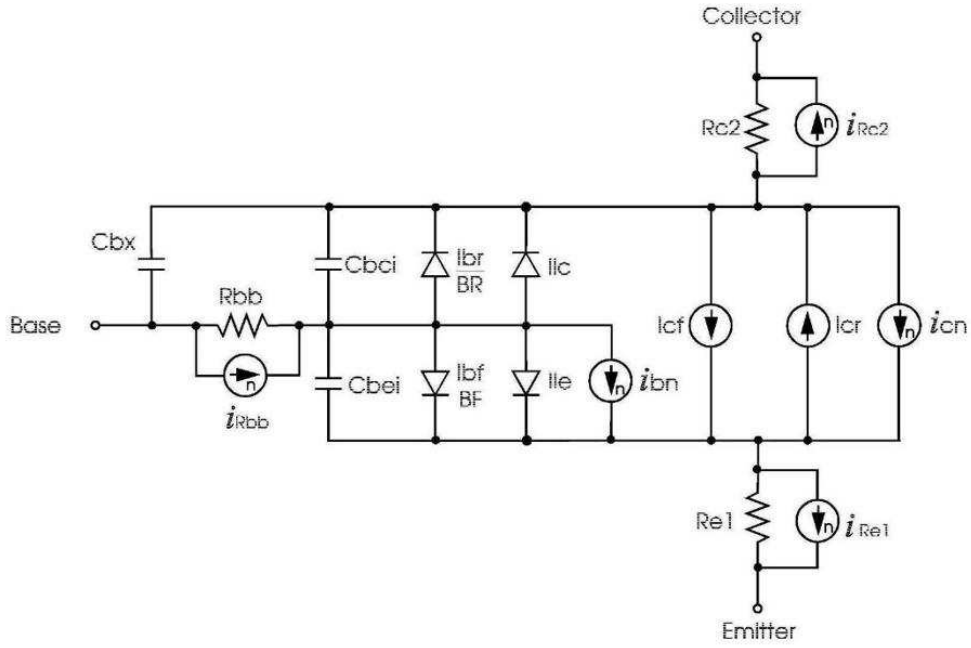

Field-Effect Transistors

- For RF applications, there are three types of transistors which can be used.
- The first is a junction FET, which have been shown to be useful up to 1 GHz at most. Their fairly high input capacitance of about 1pF and large feedback capacitance of about 0.1pF limits their use. They have been mentioned here only for completeness.
- The other two FETs of importance are members of the GaAs FET family and the BiCMOS transistors. Recent advances in technology have push the BiCMOS process close to 1009 GHz if the BiCMOS transistor is built on SiGe technology.
- For the purpose of modeling GaAs FETs, there is a large number of models available, and the list is longer if company or university internal models are added.
- The following models are popular with CAD tools.
  - Chalmers (Angelov) Model
  - Modified Materka-Kacprzak Model (low noise)
  - Physics-Based MESFET Model

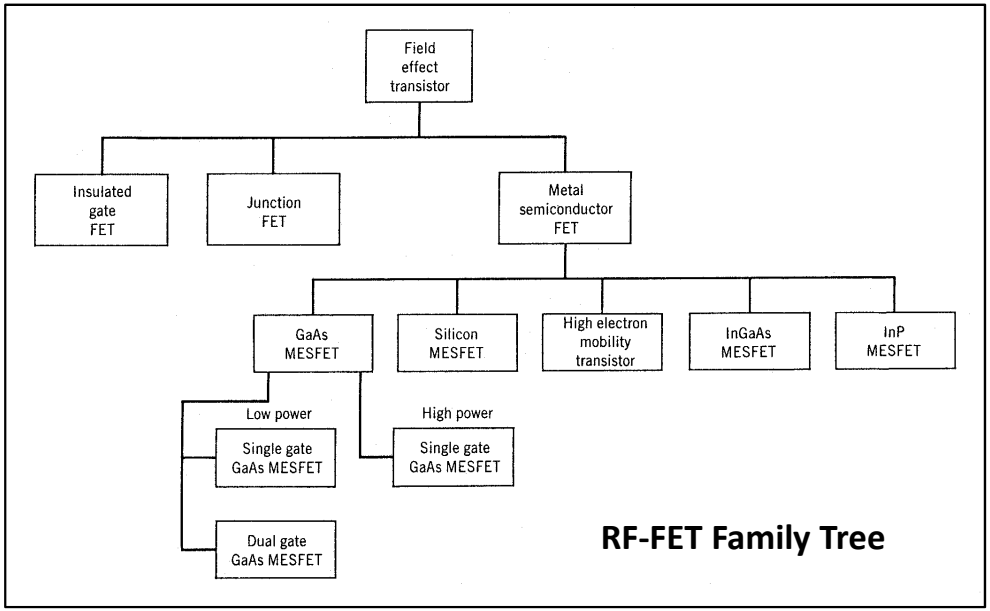

RF-FET Family Tree

Field-Effect Transistors

- Their properties and different model equations can be found in the CAD user's manual.
- As an example, the Ansoft Designer's reference manual gives all the details and references on how the model was implemented.
- It is difficult to obtain a reliable parameter extractor for the models. Probably, the most popular model for commercial application is the Angelov model.
- The model for which good parameters can be extracted with reasonable effort is the Materka model. It requires a DC/IV curve tracer and a network analyzer which operates up to 84 GHz.

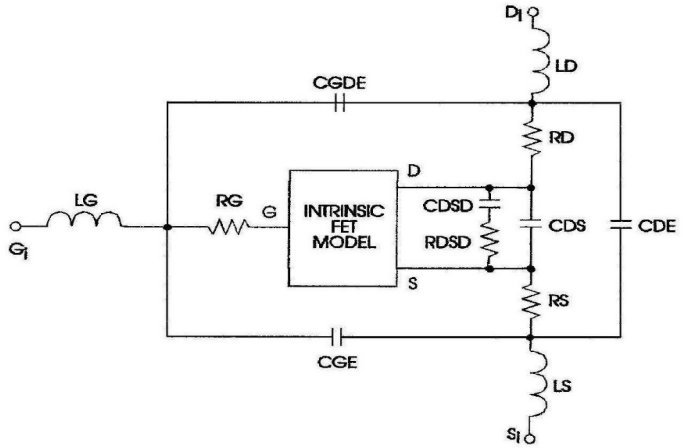

- Topology of the extrinsic model for all intrinsic models

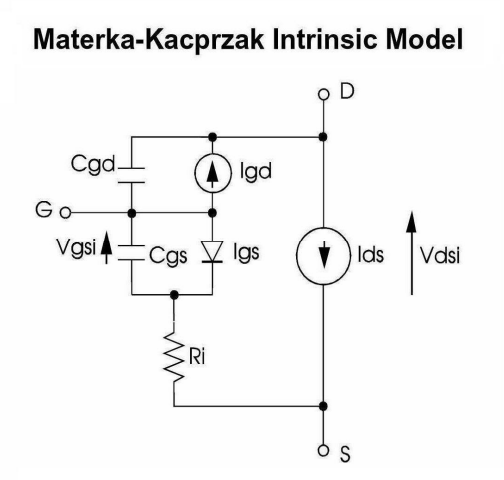

- Topology of the intrinsic model

NMOS Mosfet

- The model shown in this Figure is the popular but simple MOSFET model and has been implemented in this configuration and in most of the simulators (ADS from Agilent, Designer from Ansoft, and Microwave Office from AWR to name a few).
- Addressing the model Level 3, here are the parameters extracted for an LDMOS device which works up to several GHz and was used for a 2 GHz oscillator.

L = 0.12um	W = 0.15mm	CBD = 0.863E-12
CGD0 = 166E-12	CGS0 = 246E-12	GAMA = 0.211 + IS = 6.53E-16
KAPA = 0.809	MJ = 0.536	NSUB = 1E15
PB = 0.71	PBSW = 0.71 + PHI = 0.579	RD = 39 RS = 0.1
THET = 0.588 TOX = 4E-8 U0 = 835	VMAX = 3.38E5 + VT0 = 2.78	XQC = 0.41

- The data provided above was supplied for a LDMOS device.

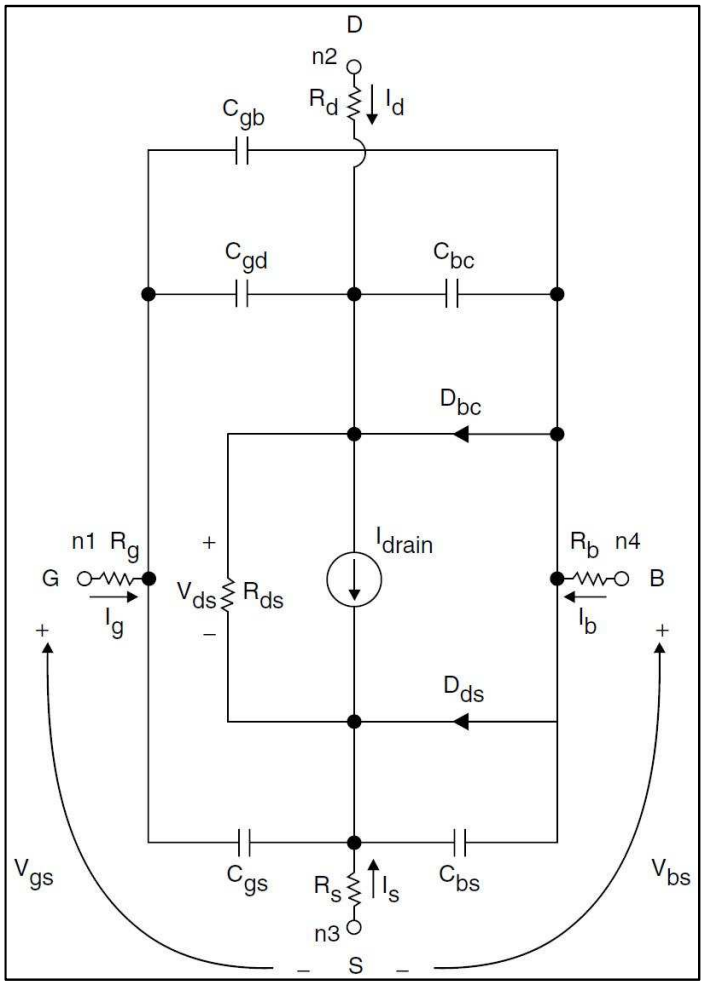

intrinsic model for an NMOS MOSFET.

NMOS Mosfet – Noise Model

Let Δf be the bandwidth (normalized to 1 Hz). The noise generators introduced in the intrinsic device are shown below and have mean square values of:

$$\langle i_{dn}^2 \rangle = \frac{8kTg_m}{3}\Delta f + \mathrm{KF}\frac{i_D^{AF}}{f^{FCP}}\Delta f$$

$$\langle i_{Rgn}^2 \rangle = 4\frac{kT}{R_g}\Delta f$$

$$\langle i_{Rdn}^2 \rangle = 4\frac{kT}{R_d}\Delta f$$

$$\langle i_{Rsn}^2 \rangle = 4\frac{kT}{R_s}\Delta f$$

$$\langle i_{Rbn}^2 \rangle = 4\frac{kT}{R_b}\Delta f$$

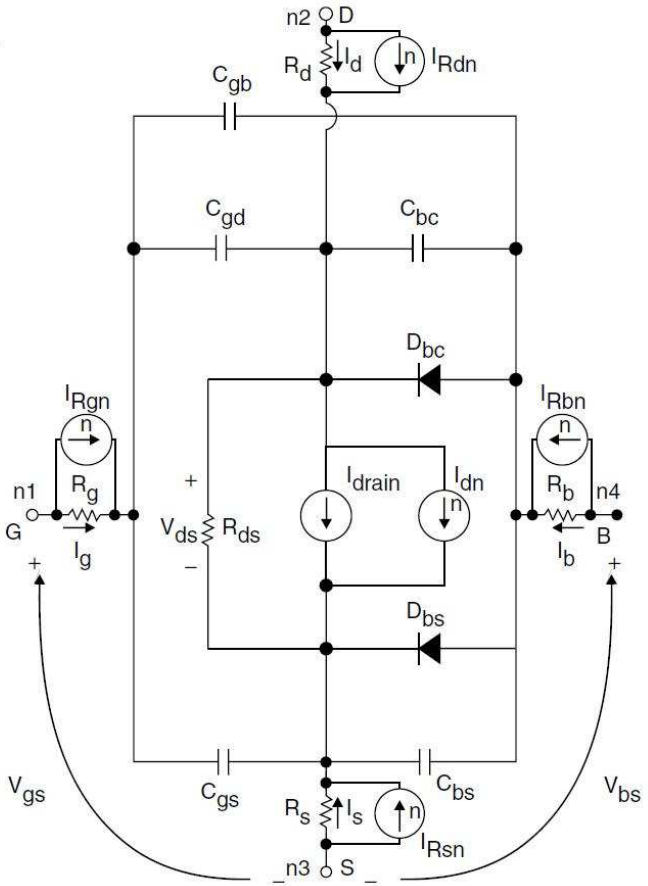

Noise model of a MOSFET transistor (not showing extrinsic parasitics). Current sources with "n" are noise sources

NMOS Mosfet – Noise Model

- For the RFIC application, the BISIM Model 3V3 is the model of choice. The figure here shows the MOSFET model representation
- While for the purpose of more insight this presentation uses detailed equivalent circuits and parameter the engineer in realty used either a characterized transistor or a foundry for the design.
- While the transistor models are quite mature the real problem lies in the quality of the parameter extraction or likewise in the accuracy of the physics based models.
- For the purpose of this presentation some easy to understand and simplified models are used, the refined models do not make the accuracy infinitely better

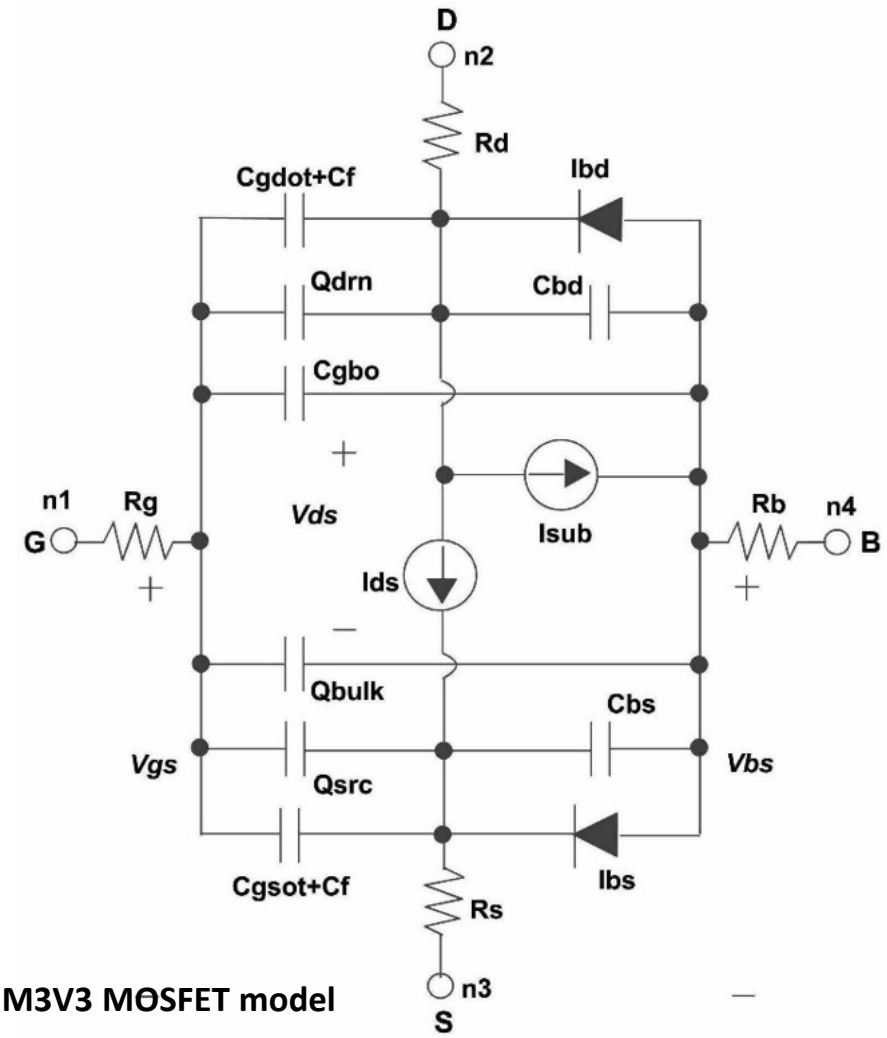

FET-BSIM3V3 MOSFET model

NMOS Mosfet – Noise Model

Let Δf be the bandwidth (normalized to 1Hz). The noise generators introduced in the intrinsic device are shown below, and have mean-square values of:

$$\left\langle i_{dn}^2 \right\rangle = \left\langle i_{dn}^2 \right\rangle_f + \left\langle i_{dn}^2 \right\rangle_{th}$$

$$\left\langle i_{Rgn}^2 \right\rangle = 4\frac{kT}{R_g}\Delta f$$

$$\left\langle i_{Rdn}^2 \right\rangle = 4\frac{kT}{R_d}\Delta f$$

$$\left\langle i_{Rsn}^2 \right\rangle = 4\frac{kT}{R_s}\Delta f$$

$$\left\langle i_{Rbn}^2 \right\rangle = 4\frac{kT}{R_b}\Delta f$$

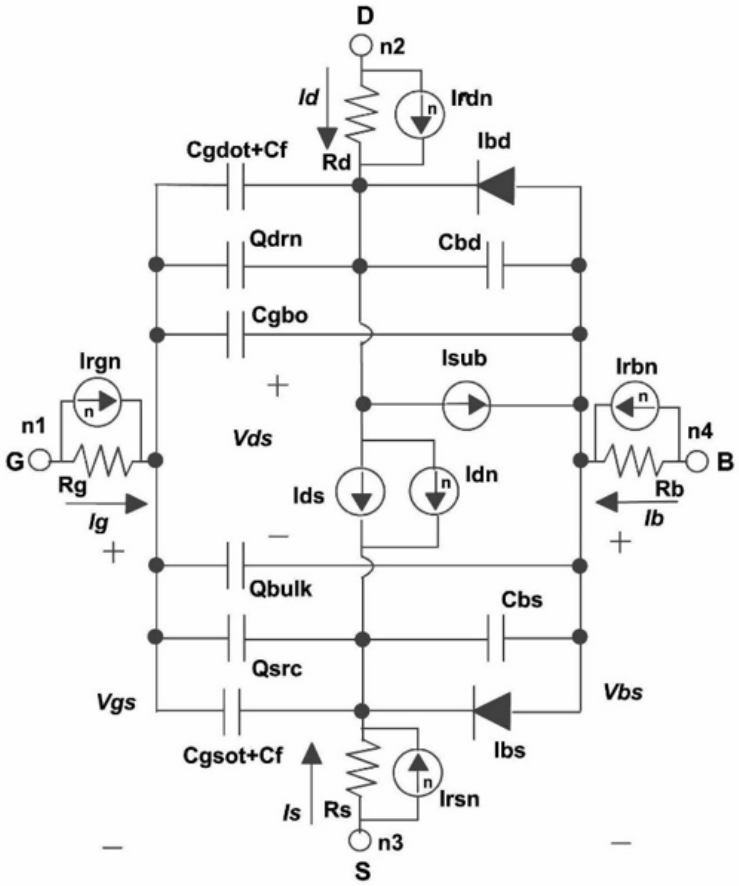

Linear Approach to the Calculation of Oscillator Phase Noise

- In transmitters, oscillator noise can result in adjacent-channel interference and modulation errors; in receivers, oscillator noise can result in demodulation errors, and degraded sensitivity and dynamic range.
- The specification, calculation and reduction of oscillator noise is therefore of great importance in wireless system design

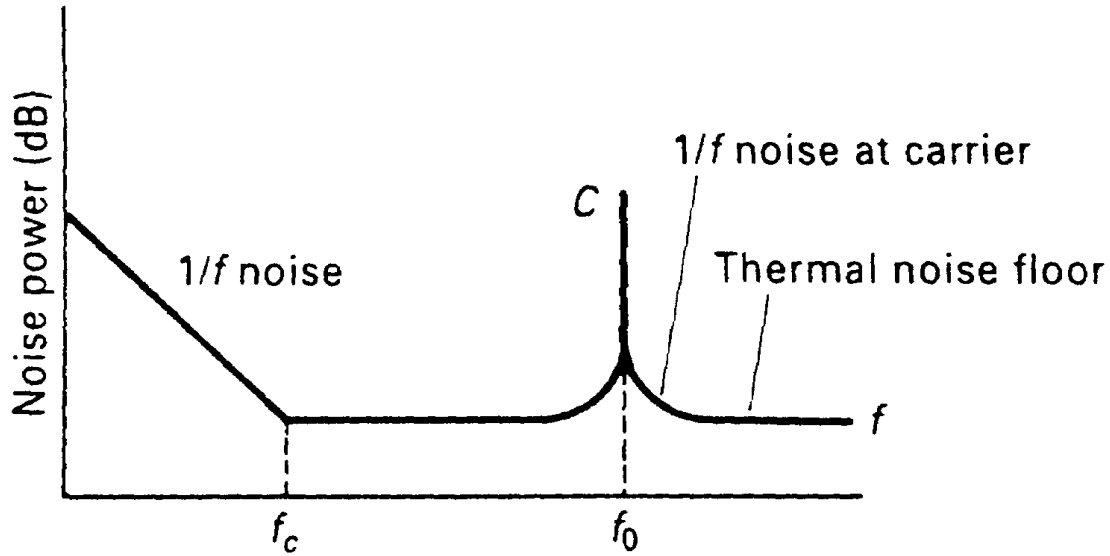

- Noise power versus frequency of a transistor amplifier with an input signal applied.

- The definition of phase noise was first given by E. J. Baghdady, R. N. Lincoln and B. D. Nelin, "Short-term Frequency Stability: Characterization Theory, and Measurement," in Short-Term Frequency Stability, NASA SP-80, 1965, pp. 65-87

Linear Approach to the Calculation of Oscillator Phase Noise

- Since an oscillator can be viewed as an amplifier with feedback, it is helpful to examine the phase noise added to an amplifier that has a noise figure F. With F defined as

$$F = \frac{(S/N)_{\text{in}}}{(S/N)_{\text{out}}} = \frac{N_{\text{out}}}{N_{\text{in}}G} = \frac{N_{\text{out}}}{GkTB}$$

$$N_{\text{out}} = FGkTB$$

$$N_{\text{in}} = kTB$$

- where N_{in} is the total input noise power to a noise-free amplifier. The input phase noise in a 1-Hz bandwidth at any frequency f0 + fm from the carrier produces a phase deviation given by (Figure 5-67)

$$\Delta\theta_{\text{peak}} = \frac{V_{\text{nRMS1}}}{V_{\text{avsRMS}}} = \sqrt{\frac{fKT}{P_{\text{avs}}}}$$

$$\Delta\theta_{\text{1RMS}} = \frac{1}{\sqrt{2}}\sqrt{\frac{FkT}{P_{\text{avs}}}}$$

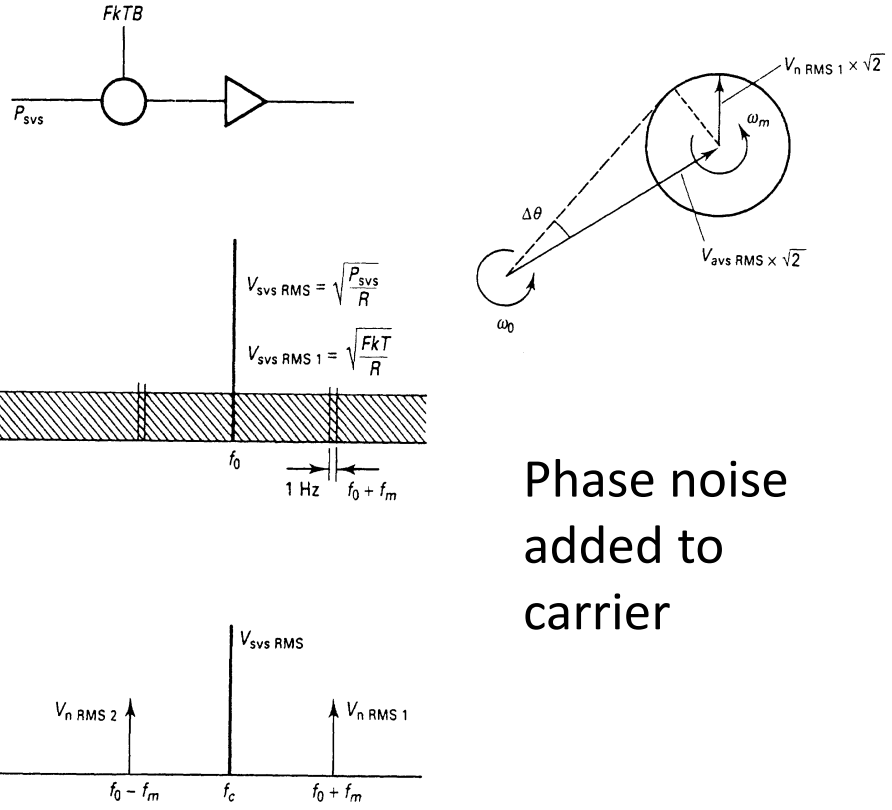

Phase noise added to carrier

Linear Approach to the Calculation of Oscillator Phase Noise

- Since a correlated random phase-noise relation exists at f0 - fm, the total phase deviation becomes

$$\Delta\theta_{\text{RMStotal}} = \sqrt{FkT / P_{\text{avs}}}$$

- The spectral density of phase noise becomes

$$S_\theta(f_m) = \Delta\theta^2_{\text{RMS}} = FkTB / P_{\text{avs}}$$ → where B = 1 for a 1-Hz bandwidth. Using $kTB = -174\,\text{dBm/Hz}$

- allows a calculation of the spectral density of phase noise that is far removed from the carrier (that is, at large values of fm). This noise is the theoretical noise floor of the amplifier. For example, an amplifier with +10 dBm power at the input and a noise figure of 6 dB gives

$$S_\theta(f_m > f_c) = -174\,\text{dBm} + 6\,\text{dB} - 10\,\text{dBm} = -178\,\text{dBm}$$

Linear Approach to the Calculation of Oscillator Phase Noise

- Only if POUT is > 0 dBm can we expect $\mathcal{L}$ (signal-to-noise ratio) to be greater than 174 dBc/Hz (1-Hz bandwidth.)
- For a modulation frequency close to the carrier, S_θ (fm) shows a flicker or 1/f component, which is empirically described by the corner frequency fc.
- The phase noise can be modeled by a noise-free amplifier and a phase modulator at the input as shown in this Figure.

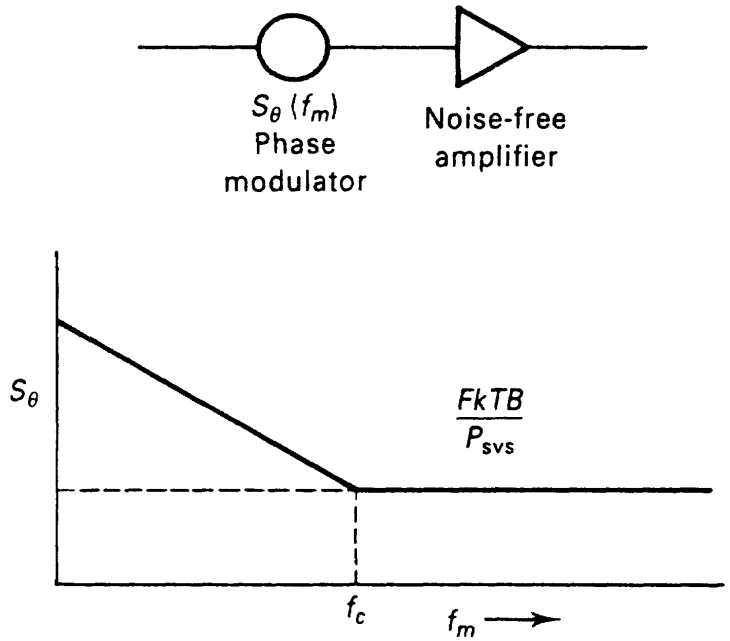

Phase noise modeled by a noise-free amplifier and phase modulator

Linear Approach to the Calculation of Oscillator Phase Noise

- The purity of the signal is degraded by the flicker noise at frequencies close to the carrier. The spectral phase noise can be described by

$$S_\theta(f_m) = \frac{FkTB}{P_{\text{avs}}}\left(1+\frac{f_c}{f_m}\right) \qquad (B = 1)$$

- No AM-to-PM conversion is considered in this equation. The oscillator may be modeled as an amplifier with feedback as shown in Figure 5-69. The phase noise at the input of the amplifier is affected by the bandwidth of the resonator in the oscillator circuit in the following way. The tank circuit or bandpass resonator has a low-pass transfer function

$$L(\omega_m) = \frac{1}{1+j(2Q_L\omega_m/\omega_0)} \qquad \text{where} \qquad \omega_0/2Q_L = B/2$$

- is the half-bandwidth of the resonator. These equations describe the amplitude response of the bandpass resonator; the phase noise is transferred attenuated through the resonator up to the half-bandwidth

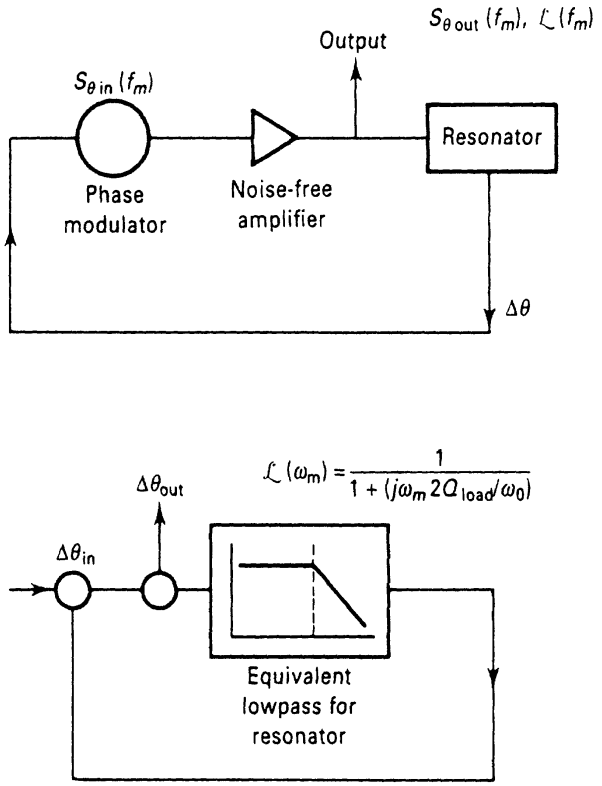

Equivalent feedback models of oscillator phase noise

Linear Approach to the Calculation of Oscillator Phase Noise

- The closed-loop response of the phase feedback loop is given by

$$\Delta\theta_{\text{out}}(f_m) = \left(1 + \frac{\omega_0}{j2Q_L\omega_m}\right)\Delta\theta_{\text{in}}(f_m)$$

- The power transfer becomes the phase spectral density

$$S_{\theta\text{out}}(f_m) = \left[1 + \frac{1}{f_m^2}\left(\frac{f_0}{2Q_L}\right)^2\right]S_{\theta\text{in}}(f_m) \qquad \text{where } S_{\theta\text{in}} \textit{ was given by}$$

$$S_\theta(f_m) = \frac{FkTB}{P_{\text{avs}}}\left(1 + \frac{f_c}{f_m}\right) \qquad (B = 1)$$

Finally, $\mathcal{L}(f_m)$ is $\mathcal{L}(f_m) = \frac{1}{2}\left[1 + \frac{1}{f_m^2}\left(\frac{f_0}{2Q_L}\right)^2\right]S_{\theta\text{in}}(f_m)$

- This equation describes the phase noise at the output of the amplifier (flicker corner frequency and AM-to-PM conversion are not considered). The phase perturbation Sθin at the input of the amplifier is enhanced by the positive phase feedback within the half-bandwidth of the resonator, f0/2QL.

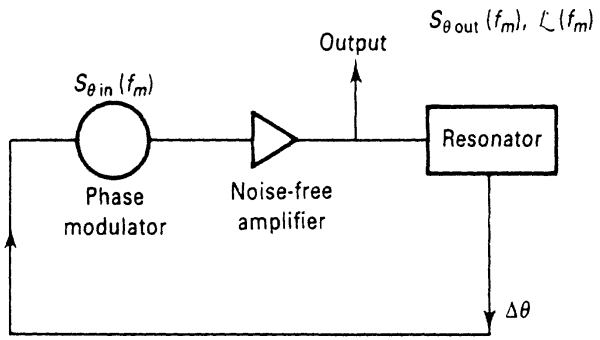

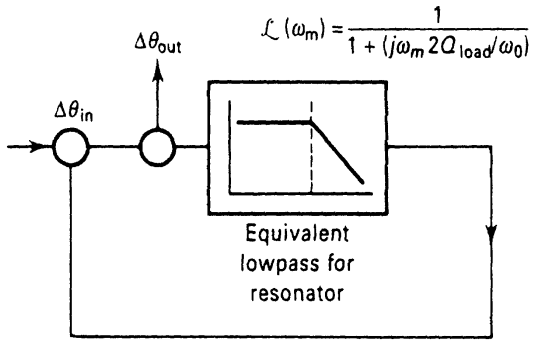

Equivalent feedback models of oscillator phase noise

Linear Approach to the Calculation of Oscillator Phase Noise

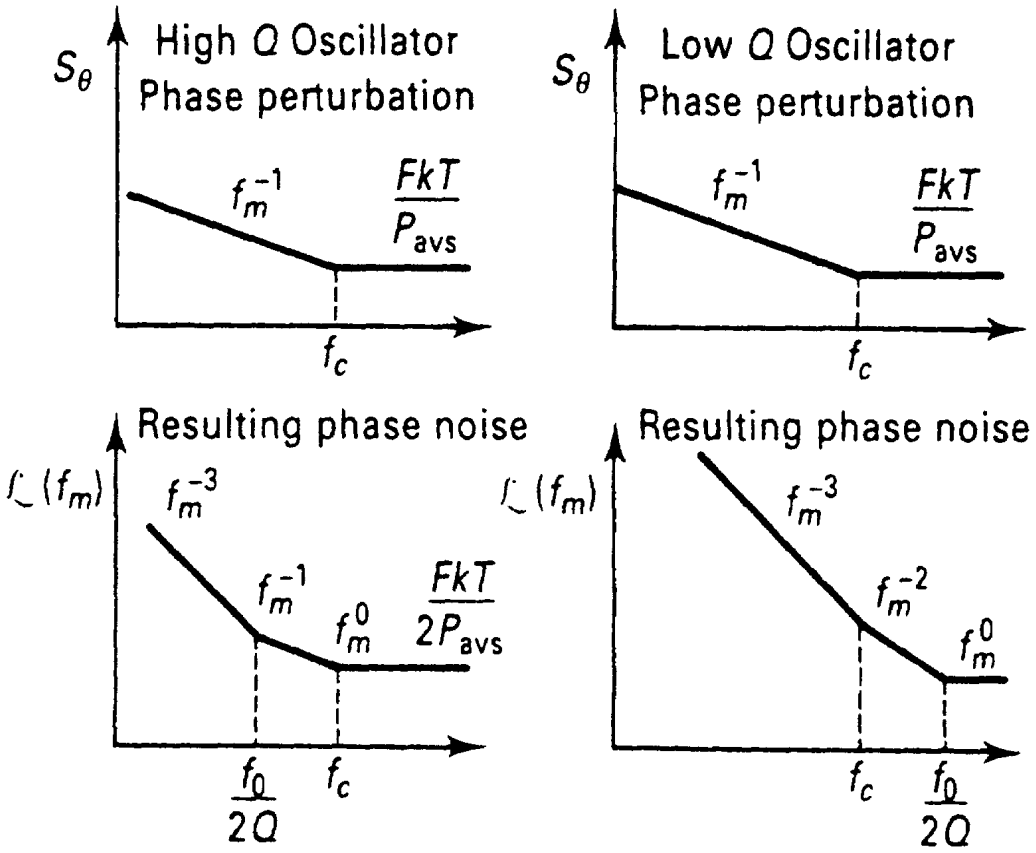

Equivalent feedback models of oscillator phase noise.

Linear Approach to the Calculation of Oscillator Phase Noise

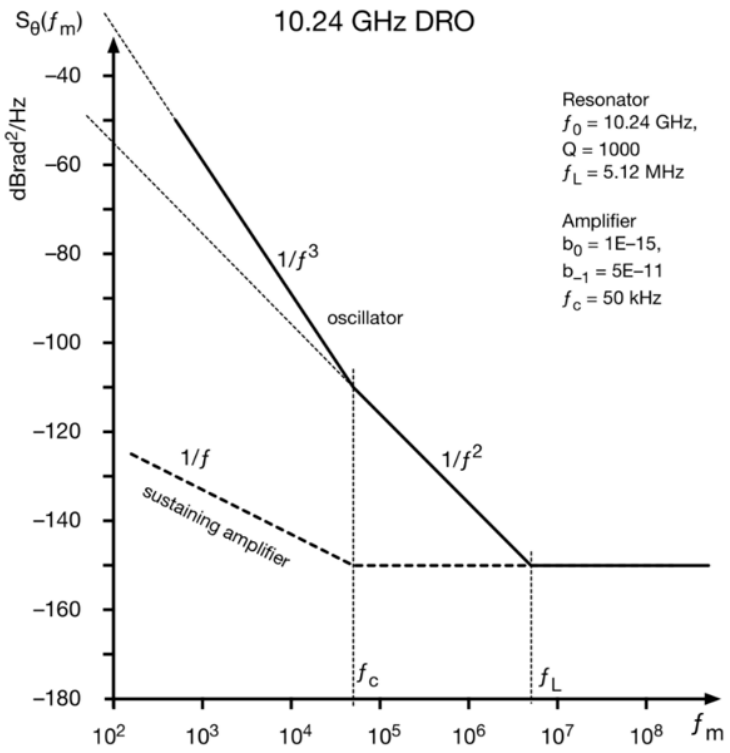

Phase Noise PSD of the 10.24 GHz DRO discussed in the example

Depending on the relation between f_c and $f_0/2Q_L$, there are two cases of interest, as shown in the two figures beore. For the low-Q case, the spectral phase noise is unaffected by the Q of the resonator, but the

$\mathcal{L}(f_m)$ spectral density will show a $1/f^3$ and $1/f^2$ dependence close to the carrier.

For the high-Q case, a region of $1/f^3$ and $1/f$ should be observed near the carrier.

The overall noise can be modelled as:

$$\mathcal{L}(f_m) = \frac{1}{2}\left[1+\frac{1}{f_m^2}\left(\frac{f}{2Q_L}\right)^2\right]\frac{FkT}{P_{\text{avs}}}\left(1+\frac{f_c}{f_m}\right)$$

$$= \frac{FkTB}{2P_{\text{avs}}}\left[\frac{1}{f_m^3}\frac{f^2 f_c}{4Q_L^2}+\frac{1}{f_m^2}\left(\frac{f}{2Q_L}\right)^2+\left(1+\frac{f_c}{f_m}\right)\right] \text{ dBc/Hz} \qquad (5\text{-}112)$$

Linear Approach to the Calculation of Oscillator Phase Noise

$$\mathcal{L}(f_m) = \frac{1}{2}\left[1 + \frac{1}{f_m^2}\left(\frac{f}{2Q_L}\right)^2\right]\frac{FkT}{P_{\text{avs}}}\left(1 + \frac{f_c}{f_m}\right)$$

$$= \frac{FkTB}{2P_{\text{avs}}}\left[\frac{1}{f_m^3}\frac{f^2 f_c}{4Q_L^2} + \frac{1}{f_m^2}\left(\frac{f}{2Q_L}\right)^2 + \left(1 + \frac{f_c}{f_m}\right)\right] \text{ dBc/Hz} \qquad \textbf{(5-112)}$$

Examining Eq. (5-112) gives the four major causes of oscillator noise: the up-converted 1/f noise or flicker FM noise, the thermal FM noise, the flicker phase noise, and the thermal noise floor, respectively.

QL (loaded Q) can be expressed as

$$Q_L = \frac{\omega_o W_e}{P_{\text{diss,total}}} = \frac{\omega_o W_e}{P_{\text{in}} + P_{\text{res}} + P_{\text{sig}}} = \frac{\text{reactive power}}{\text{total dissipated power}}$$

where We is the reactive energy stored in L and C,

$$W_e = \tfrac{1}{2}CV^2 \qquad P_{\text{res}} = \frac{\omega_o W_e}{Q_{\text{unl}}}$$

$$\mathcal{L}(f_m) = \frac{1}{2}\left[1 + \frac{\omega_o^2}{4\omega_m^2}\left(\frac{P_{\text{in}}}{\omega_o W_e} + \frac{1}{Q_{\text{unl}}} + \frac{P_{\text{sig}}}{\omega_o W_e}\right)^2\right]\left(1 + \frac{\omega_c}{\omega_m}\right)\frac{FkT_o}{P_{\text{sav}}}$$

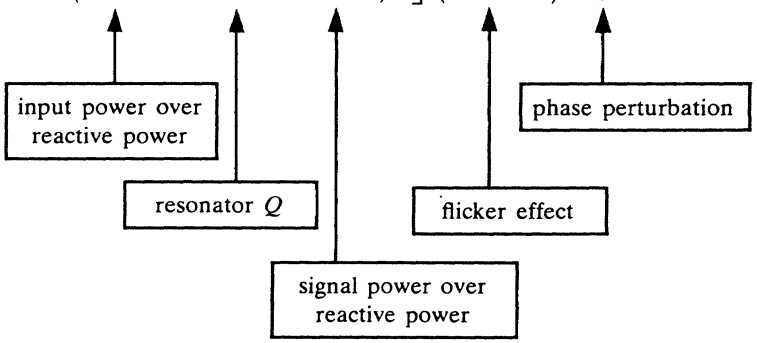

Linear Approach to the Calculation of Oscillator Phase Noise

For bipolar transistors only

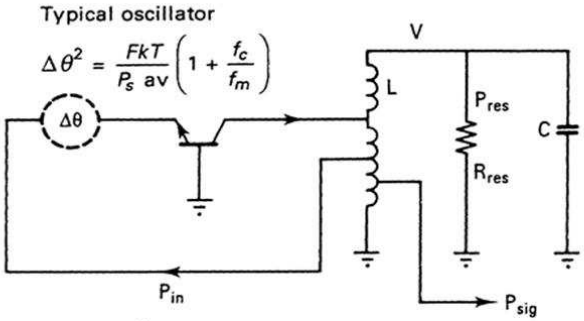

For $f_m < \frac{f_o}{2Q_{load}}$

$$\mathcal{L}(f_m) = \frac{1}{2}\frac{1}{\omega_m^2}\left(\frac{\omega_o}{2Q_{load}}\right)^2 \frac{FkT}{P_{s\ av}}\left(1 + \frac{f_c}{f_m}\right)$$

$$Q_{load} = \frac{\omega_o W_e}{P_{diss,\ total}} = \frac{\omega_o W_e}{P_{in} + P_{res} + P_{sig}}$$

$$= \frac{\text{Reactive power}}{\text{Total dissipated power}}$$

Maximum energy in C or L : $W_e = \frac{1}{2} C V^2$

$$\mathcal{L}(\omega_m) = \frac{1}{8}\frac{FkT}{P_{s\ av}}\frac{\omega_o^2}{\omega_m^2}\left(\frac{P_{in}}{\omega_o W_e} + \frac{1}{Q_{unl}} + \frac{P_{sig}}{\omega_o W_e}\right)^2\left(1 + \frac{\omega_c}{\omega_m}\right)$$

Phase Perturbation — Resonator Q — Flicker Effect

Input power over — Signal power over

Figure 5-19--Diagram for a feedback oscillator illustrating the principles involved, and showing the key components considered in the phase noise calculation and its contribution.

This equation is extremely significant because it covers most of the causes of phase noise in oscillators.

Linear Approach to the Calculation of Oscillator Phase Noise

The basic equation (Scherer, Rohde's Modified Leeson's Equation) needed to calculate the phase noise is found in ***The Design of Modern Microwave Oscillators for Wireless Applications: Theory and Optimization***

$$\mathscr{L}(f_m) = 10\log\left\{\left[1+\frac{f_0^2}{(2f_mQ_L)^2(1-(Q_L/Q_0))^2}\right]\left(1+\frac{f_c}{f_m}\right)\frac{FkT}{2P_{sav}}+\frac{2kTRK_0^2}{f_m^2}\right\}$$

$\mathscr{L}(f_m)$ = SSB noise power spectral density defined as the ratio of sideband power in a 1 Hz bandwidth at f_m to total power in dB; the unit is dBc/Hz

f_m = frequency offset

f_0 = center frequency

f_c = flicker frequency—the region between $1/f^3$ and $1/f^2$

Q_L = loaded Q of the tuned circuit

Q_0 = unloaded Q of the tuned circuit

F = noise of the oscillator

$kT = 4.1 \times 10^{-21}$ at 300 K_0 (room temperature)

P_{sav} = average power at oscillator output

R = equivalent noise resistance of the tuning diode

K_0 = oscillator voltage gain

The last term of Leeson's phase noise equation is responsible for the modulation noise.

Linear Approach to the Calculation of Oscillator Phase Noise

The basic equation (Scherer, Rohde's Modified Leeson's Equation) needed to calculate the phase noise is found in The Design of Modern Microwave Oscillators for Wireless Applications: Theory and Optimization

$$\mathscr{L}(f_m) = 10\log\left\{\left[1+\frac{f_0^2}{(2f_mQ_L)^2(1-(Q_L/Q_0))^2}\right]\left(1+\frac{f_c}{f_m}\right)\frac{FkT}{2P_{sav}}+\frac{2kTRK_0^2}{f_m^2}\right\}$$

The minimum phase noise can be found by differentiating this Equation and equating to zero as $\frac{\partial}{\partial m}[\pounds(f_m)]_{m=m_{\text{opt}}} = 0$

$$\pounds(f_m) = \frac{d}{dm}\left\{10\log\left\{\left[1+\frac{f_0^2}{[2f_mQ_0m(1-m)]^2}\right]\left(1+\frac{f_c}{f_m}\right)\frac{FkT}{2P_0}+\frac{2kTRK_0^2}{f_m^2}\right\}\right\}_{m\neq 1} = 0$$

$$\rightarrow m_{opt} \cong 0.5$$

Linear Approach to the Calculation of Oscillator Phase Noise

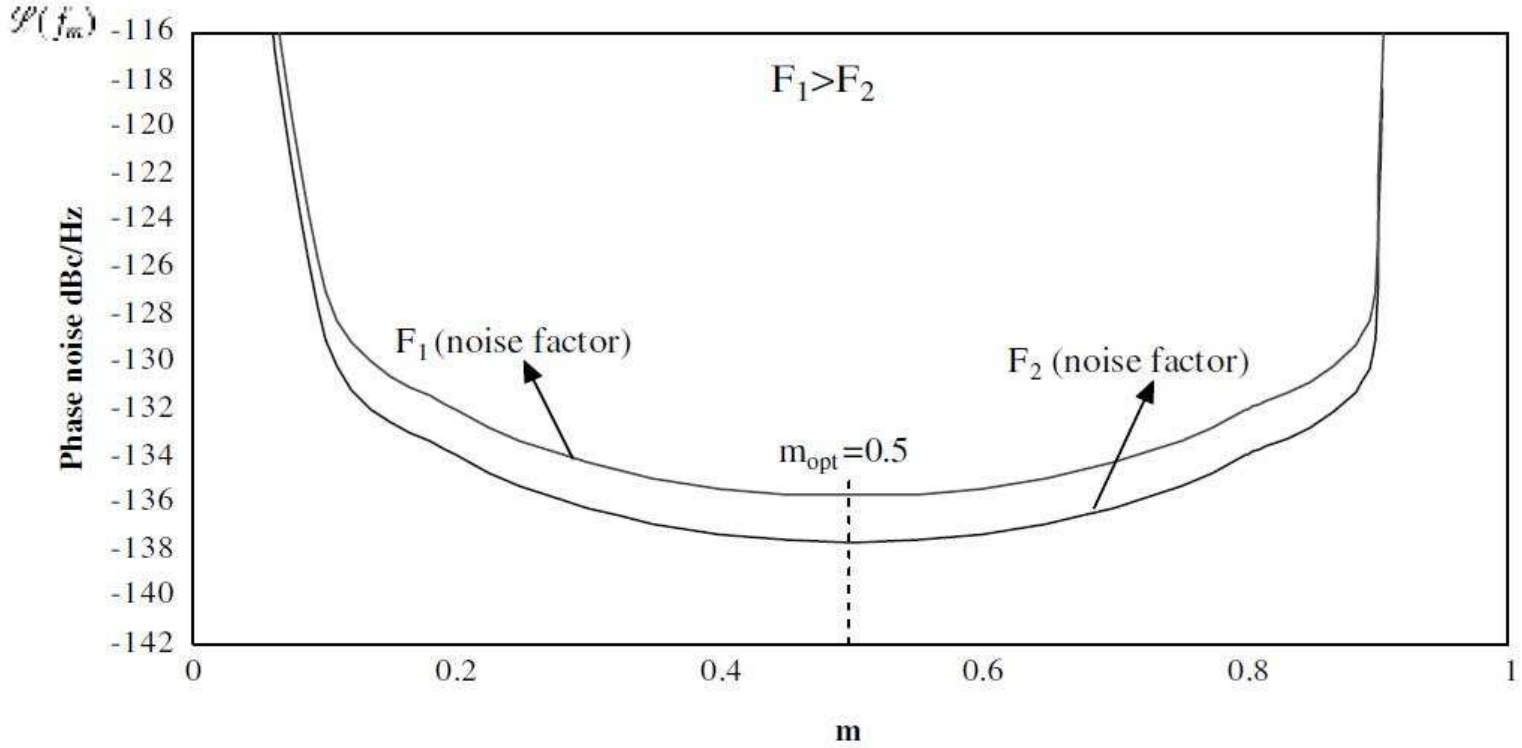

Relative phase noise of the typical oscillator versus the ratio of loaded and unloaded Q of the resonator for noise factor F_1 and $F_2, (F_1 > F_2)$

Some practical parameters

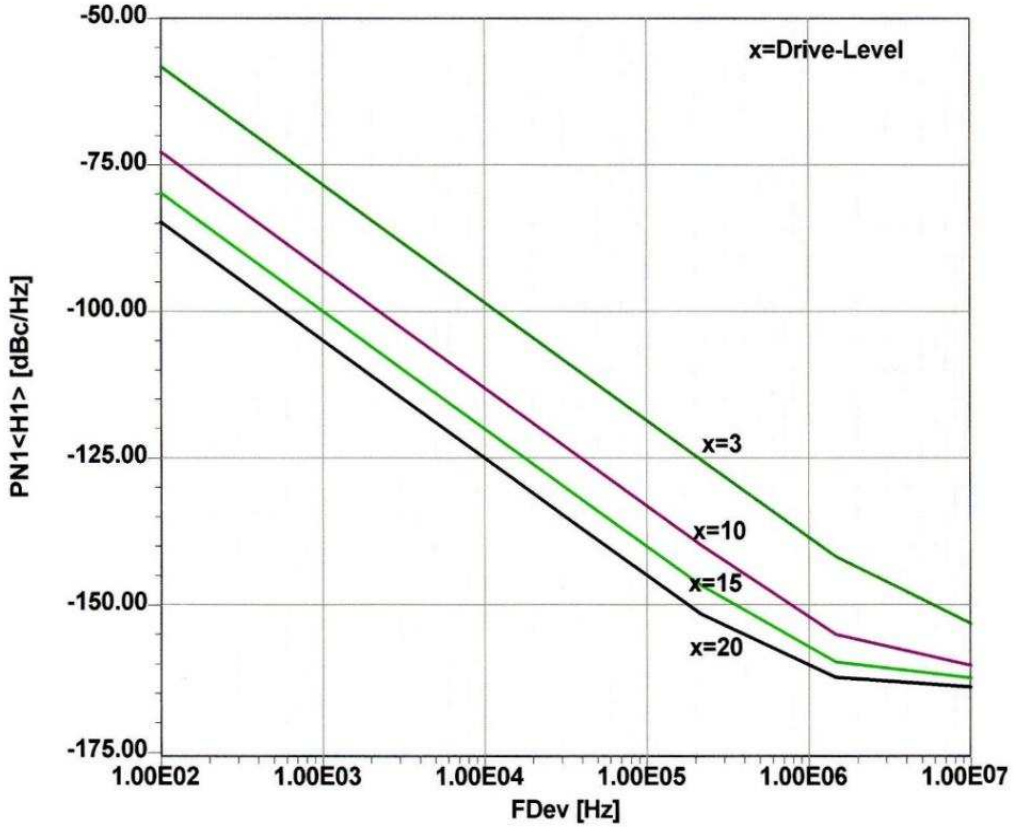

Single sideband phase noise as a function of the normalized drive level x.

The theory behind „X“ will be explained in a few moments

Some practical parameters

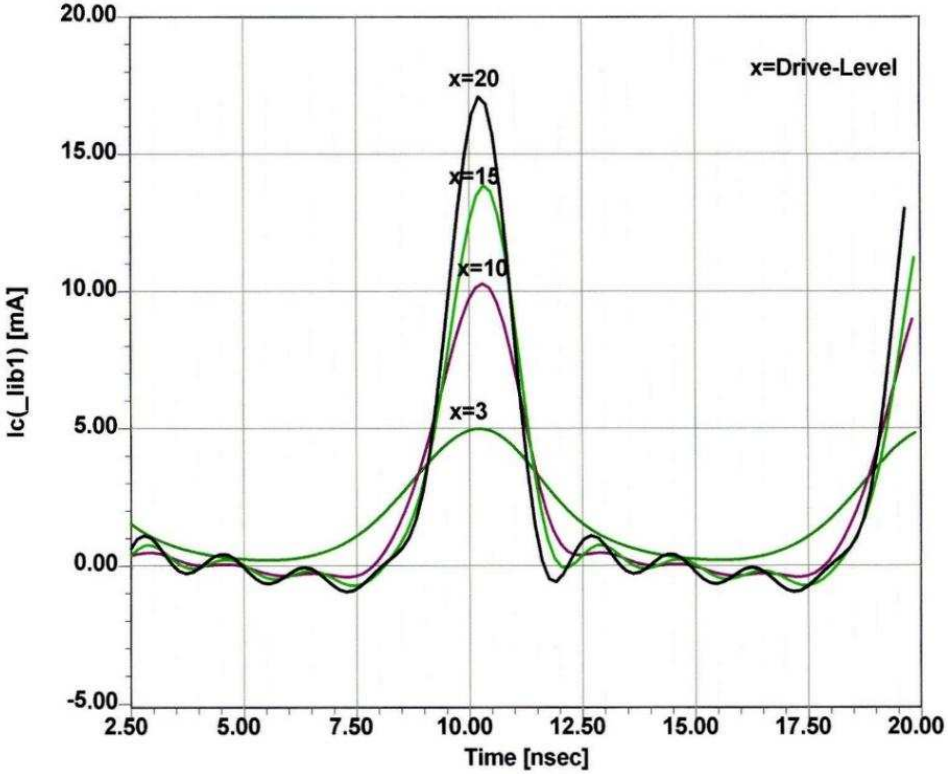

collector current pulses of the oscillator

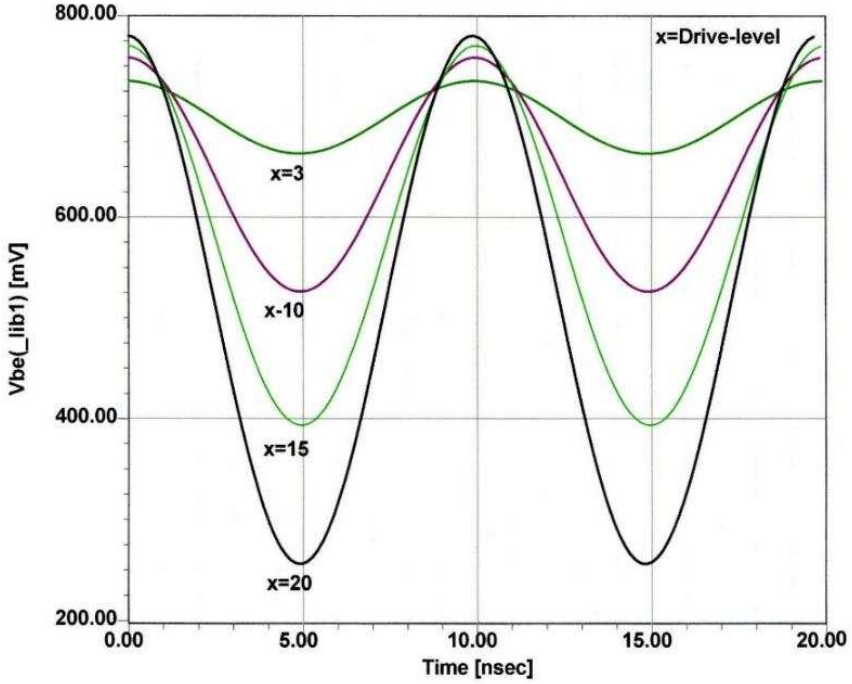

RF voltage Vbe across the base-emitter junction as a function of the normalized drive level x.

Some practical parameters

- Here is a brief introduction to the definition of X, in a way the duty cycle.
- The voltage across the base-emitter junction consists of a DC component and a driven signal voltage .
- It can be expressed as

$$v(t) = V_{dc} + V_1 \cos(wt)$$

- As the driven voltage increases and develops enough amplitude across the base-emitter junction, the resulting current is a periodic series of pulses whose amplitude depends on the nonlinear characteristics of the device and is given as

$$i_e(t) = I_s e^{\frac{qv(t)}{kT}}$$

$$i_e(t) = I_s e^{\frac{qV_{dc}}{kT}} e^{\frac{qV_1 \cos(wt)}{kT}}$$

$$i_e(t) = I_s e^{\frac{qV_{dc}}{kT}} e^{x\cos(wt)}$$

- assuming Ic ≈ Ie (β>10)

$$x = \frac{V_1}{(kT/q)} = \frac{qV_1}{kT}$$

$i_e(t)$ is the emitter current and x is the drive level which is normalized to kT/q.

Some practical parameters

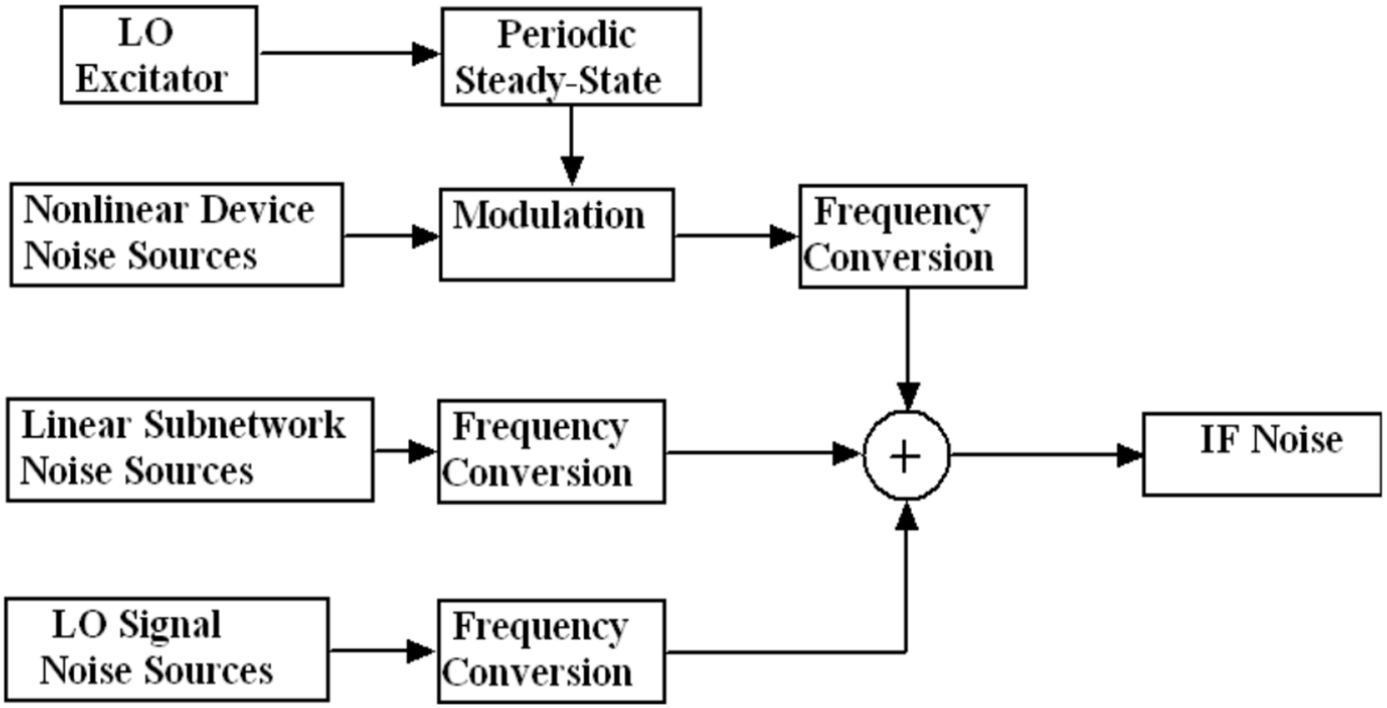

Noise sources of oscillators being mixed on the carrier, amazing to see all the relevant contributions

Oscillator Phase Noise

- This equation does not take into consideration the conducting angle, because it is in the linear domain
- The Leeson phase noise equation is modified to accommodate the tuning diode noise contribution

$$\pounds(f_m) = 10 \log \left\{ \left[1 + \frac{{f_0}^2}{(2 f_m Q_0)^2 m^2 (1-m)^2} \right] \left(1 + \frac{f_c}{f_m} \right) \frac{FkT}{2P_0} + \frac{2\,kTRK_0^2}{f_m^2} \right\}$$

- The Equation above explain the phase noise degradation (as compared to the fixed frequency LC oscillator due to the oscillator voltage gain K0 associated with the tuning diode network as described by Rohde).
- The reason for noise degradation is due to the increased tuning sensitivity of the varactor diode tuning network

Oscillator Phase Noise

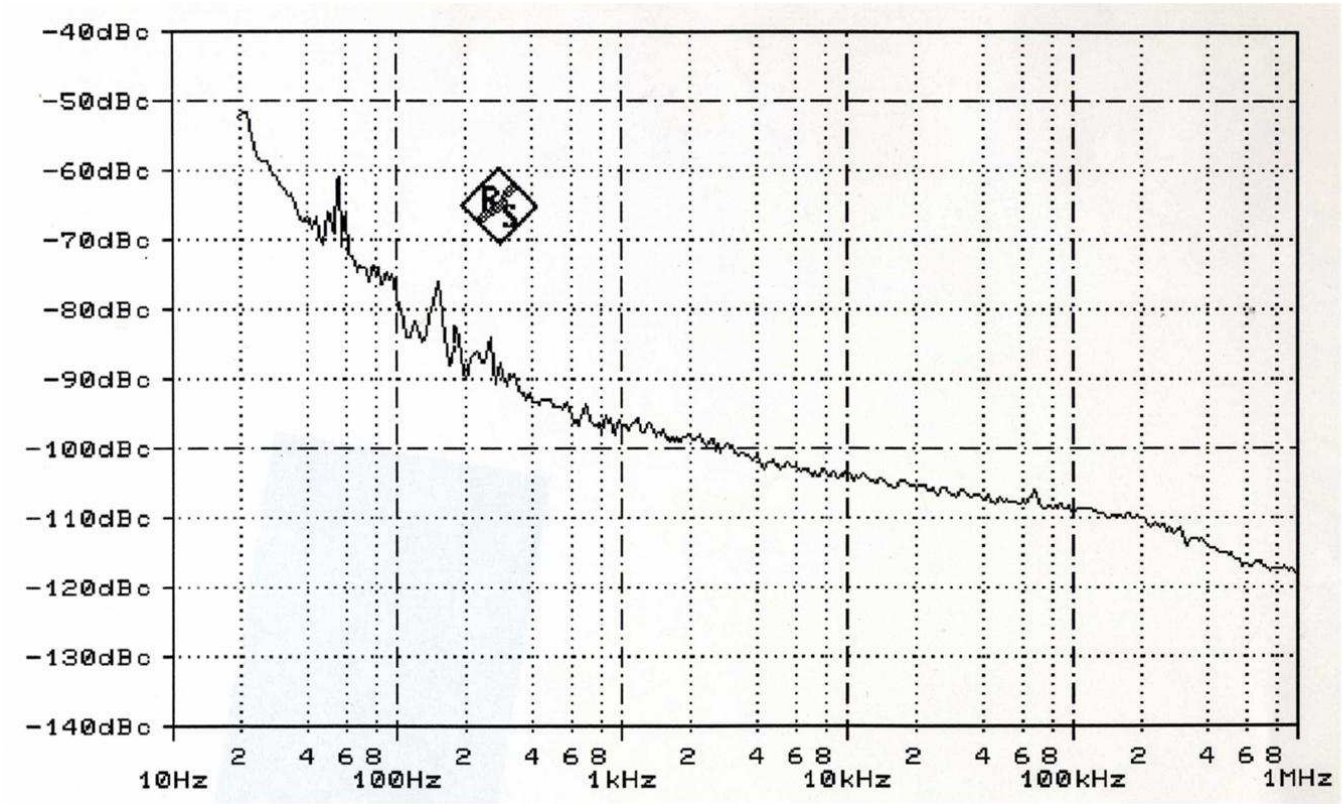

Typical phase noise of a PLL 50 GHz PLL synthesizer

Oscillator Phase Noise - References

https://www.researchgate.net/profile/Mehran-Mossammaparast/publication/4135164_A_review_of_sapphire_whispering_gallery-mode_oscillators_including_technical_progress_and_future_potential_of_the_technology/links/56187e1f08ae044edbad246c/A-review-of-sapphire-whispering-gallery-mode-oscillators-including-technical-progress-and-future-potential-of-the-technology.pdf

A REVIEW OF SAPPHIRE WHISPERING GALLERY-MODE OSCILLATORS INCLUDING TECHNICAL PROGRESS AND FUTURE POTENTIAL OF THE TECHNOLOGY

C. McNeilage, J. H. Searls, E. N. Ivanov*, P. R. Stockwell, D. M. Green, M. Mossammaparast

Poseidon Scientific Instruments Pty Ltd,

1/95 Queen Victoria St, Fremantle WA 6160, Australia

***School of Physics, The University of Western Australia, 35 Stirling Hwy, Crawley WA 6009, Australia**

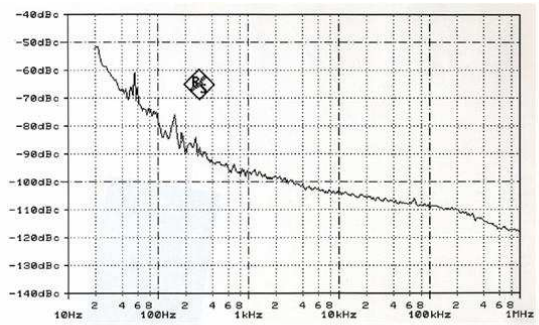

Typical phase noise of a PLL 50 GHz PLL synthesizer

Oscillator Phase Noise – recent Results at PSI

- The PSI 'SBO' series are compact, sapphire oscillators operating near room temperature, while the 'SLCO' is a 19" rack instrument. Since the first SLCOs were produced in 1996, the application-demanded requirements for temperature range, phase and amplitude noise performance, vibration sensitivity, and reliability have become more stringent.

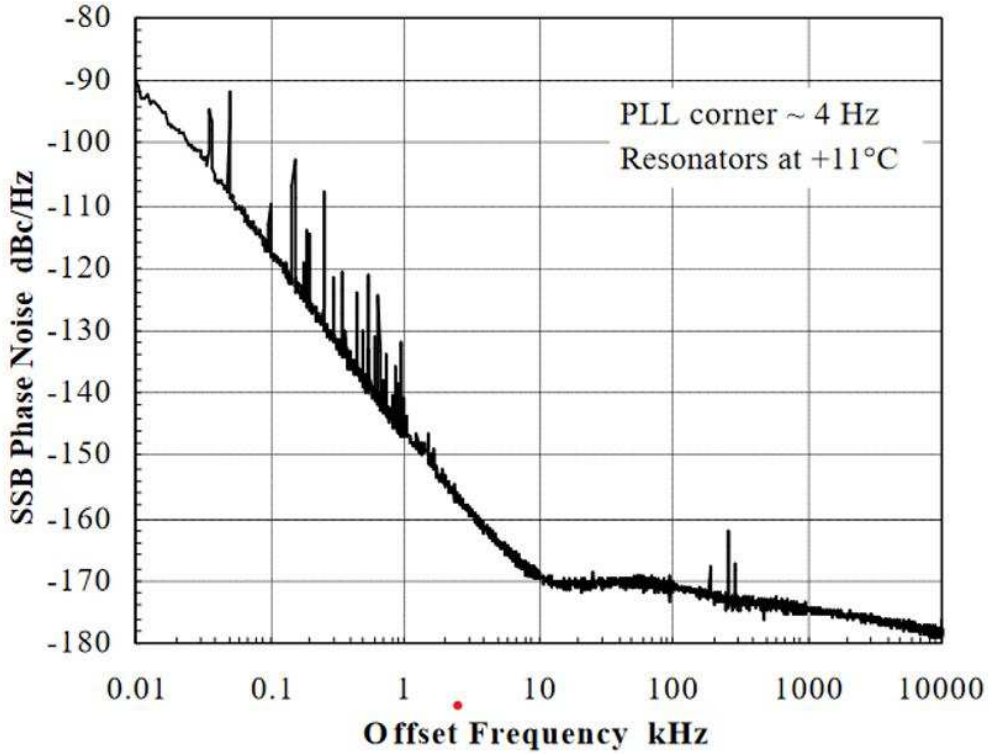

Measured phase noise of PSI room temperature SLCO at 10.24 GHz (August 2003).

Oscillator Phase Noise – Amplitude Noise Results

- With phase noise at these low levels, amplitude (AM) noise can no longer be ignored. In fact, poor AM noise can readily degrade phase noise performance, particularly as temperature varies (an oscillator tuned for minimum AM-to-PM conversion at room temperature may well suffer at operating temperature extremes). At PSI, we have tested various amplifier designs and developed low noise power supplies to minimize oscillator AM noise, and Figure 13 shows the current 'SBO' performance

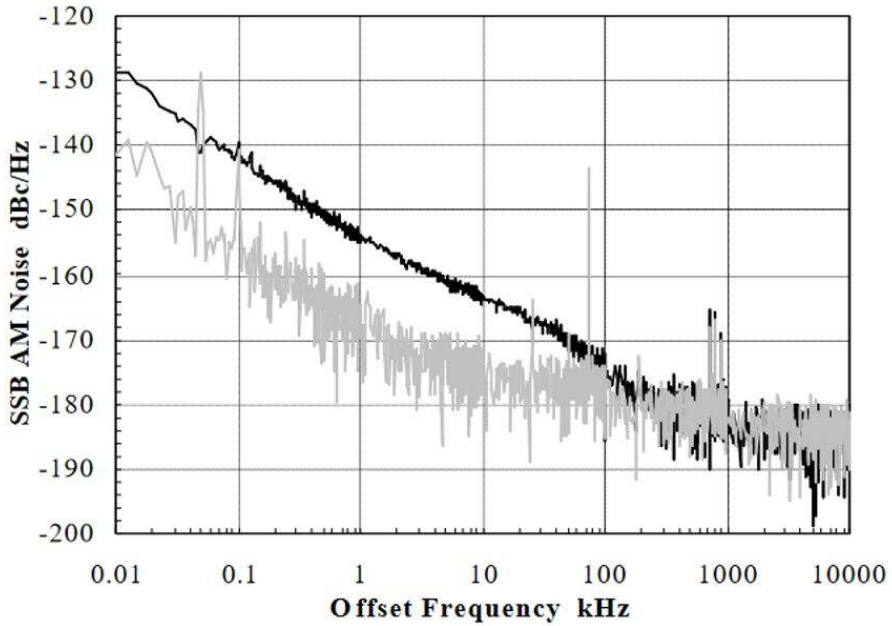

Measured phase noise of PSI room temperature SLCO at 10.24 GHz (August 2004).

- AM noise is $-154\mathrm{dBc/Hz}$ at 1 kHz offset, with a $1/f$ characteristic through to 50 kHz , where the effect of resonator filtering is visible. The measurement was done using cross correlation of the signals from two AM-sensitive mixers, to achieve a low measurement noise floor. The apparent steps in the data are due to limited averaging in the cross-correlation method (a higher number of averages was taken at higher frequencies).

Typical Microwave Oscillators

- Most high performance oscillators are actually based on the Emitter Follower using the Colpitts oscillator circuit

A typical linear oscillator phase noise model (block diagram) Leeson Model

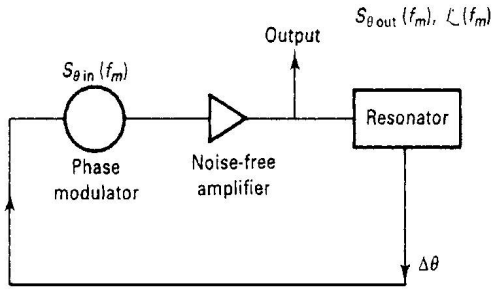

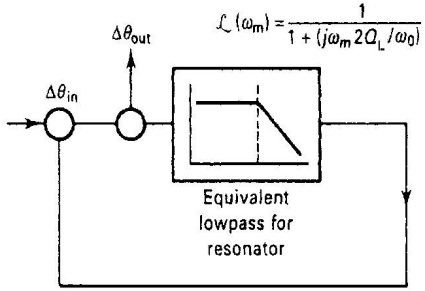

The resulting phase noise in linear terms can be calculated as

$$\mathcal{L}(f_m) = \frac{1}{2}\left[1 + \frac{\omega_o^2}{4\omega_m^2}\left(\frac{P_{in}}{\omega_o W_e} + \frac{1}{Q_{unl}} + \frac{P_{sig}}{\omega_o W_e}\right)^2\right]\left(1 + \frac{\omega_c}{\omega_m}\right)\frac{FkT_o}{P_{sav}}$$

input power over reactive power

resonator Q

signal power over reactive power

flicker effect

phase perturbation

- This equation is the linear Leeson equation, with the pushing effect omitted and the flicker term added by Dieter Scherer (Hewlett Packard, about 1975).
- Phase noise is a dimensionless number, and expressed in dBc/Hz, measured at an offset of Δf (fm) from the carrier relative to the RF output power. At 0 dBm output, the ideal phase noise level far off the carrier is -174dB (T0= 300 Kelvin)

der Bundeswehr Universität München

Designing an Oscillator

- Microwave oscillators are based on the negative resistance principle to compensate for the losses.
- Maximum frequency of oscillation can be determined from linear analysis for start-up conditions, but not necessarily for sustaining oscillation (large signal condition will reduce the gain and shift the frequency).
- Linear analysis is unreliable to determine resonance frequency and other dynamic parameters, beware of parasitics.

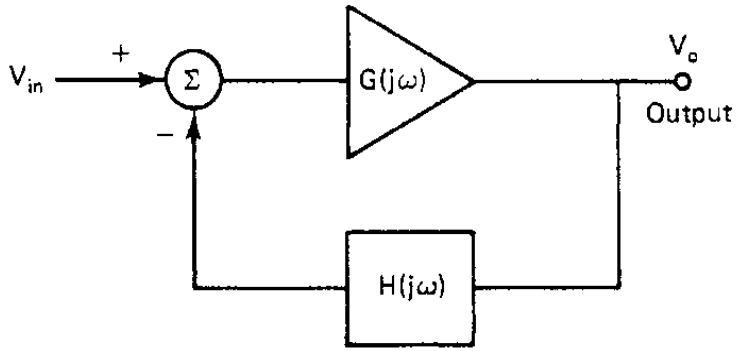

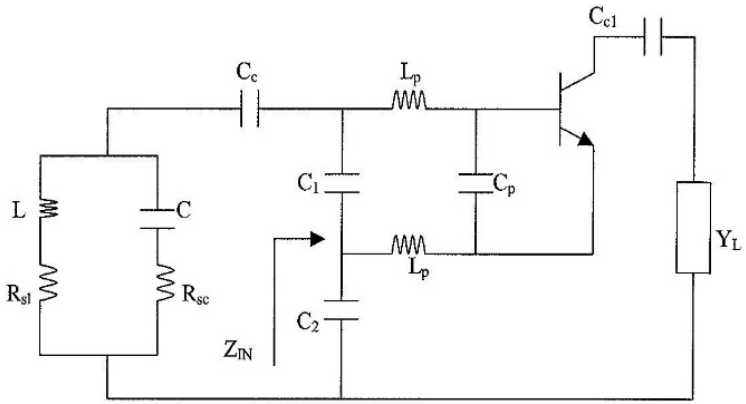

Oscillator as a feedback model and as a one port producing a loss compensation with the electronically generated negative impedance

The Calculation of the Oscillating Condition Considering Parasitics of the Colpitts oscillator

- In the practical case, the device parasitics and loss resistance of the resonator will play an important role in the oscillator design. Figure 6-2 incorporates the base lead-inductance Lp and the package-capacitance Cp.
- It must be noted that part of the intrinsic transistor the Base-Collector capacitance is responsible for the Miller effect, and the Collector Emitter

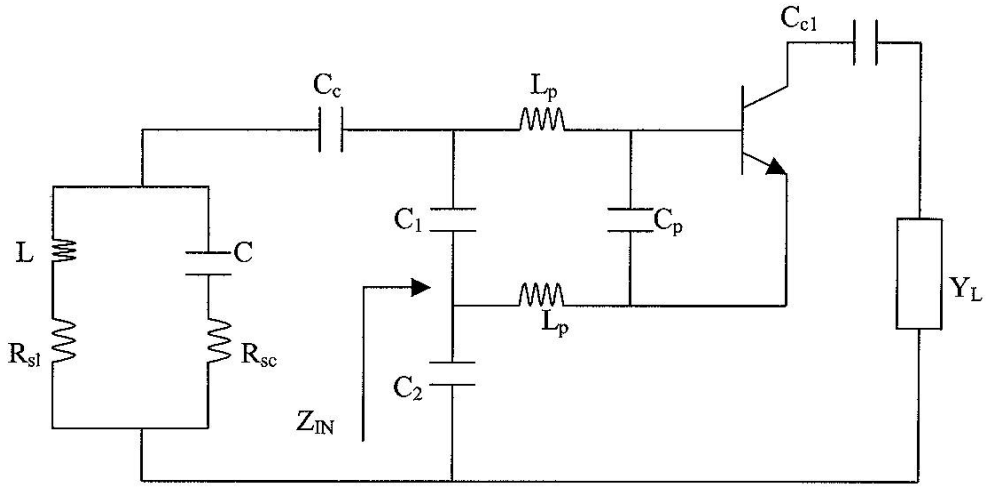

Figure 6-2 Colpitts oscillator with base-lead inductances and package capacitance.
C_C is neglected.

The Calculation of the Oscillating Condition Considering Parasitics of the Colpitts oscillator

- The input impedance is

$$Z_{IN}\Big|_{pacakage} = -\left[\frac{Y_{21}}{\omega^2(C_1+C_p)C_2}\frac{1}{(1+\omega^2 Y_{21}^2 L_p^2)}\right] - j\left[\frac{(C_1+C_P+C_2)}{\omega(C_1+C_P)C_2} - \frac{\omega Y_{21} L_P}{(1+\omega^2 Y_{21}^2 L_p^2)}\frac{Y_{21}}{\omega(C_1+C_P)C_2}\right]$$

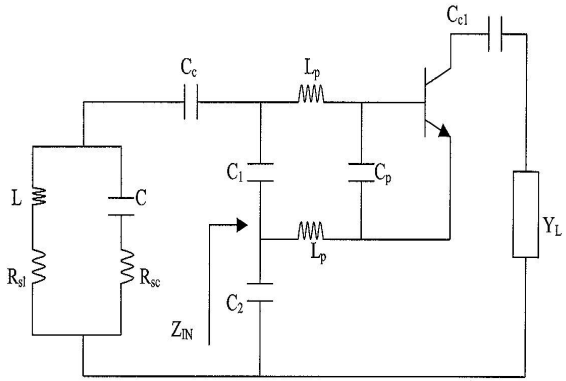

$$Z_{IN}\Big|_{without-pacakage} = -\left[\frac{Y_{21}}{\omega^2 C_1 C_2}\right] - j\left[\frac{(C_1+C_2)}{\omega C_1 C_2}\right]$$

- where Lp is the base-lead inductance of the bipolar transistor and Cp is base-emitter package capacitance. All further circuits are based on this model.

The Calculation of the Oscillating Condition Considering Parasitics of the Colpitts oscillator

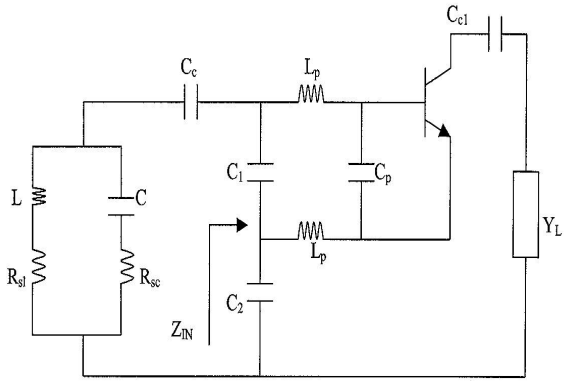

- From the expression of the slide before, it is obvious that the base lead-inductance makes the input capacitance appear larger and the negative resistance appear smaller. The equivalent negative resistance and capacitance can be defined as

$$R_{NEQ} = \frac{R_N}{(1+\omega^2 Y_{21}^2 L_p^2)}$$

$$\frac{1}{C_{EQ}} = \left\{ \left[\frac{1}{\frac{(C_1+C_P)C_2}{(C_1+C_2+C_P)}} \right] - \left[\frac{\omega^2 Y_{21} L_P}{(1+\omega^2 Y_{21}^2 L_P^2)} \right] \left[\frac{Y_{21}}{\omega(C_1+C_P)C_2} \right] \right\}$$

$$R_N = -\frac{Y_{21}}{\omega^2 C_1 C_2}$$

R_N Noisy negative resistance without lead inductance and package capacitance

R_{NEQ} Negative resistance with base-lead inductance and package capacitance.

C_{EQ} Equivalent capacitance with base-lead inductance and package capacitance.

The Calculation of the Oscillating Condition Considering Parasitics of the Colpitts oscillator

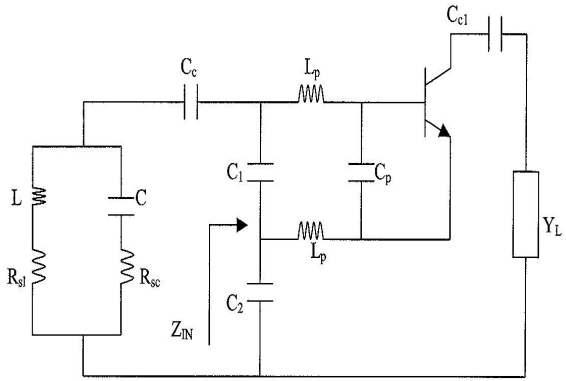

- At resonance:

$$j\left[\frac{\omega L}{1-\omega^2 LC}-\frac{1}{\omega C_C}\right]-j\left[\frac{(C_1+C_P+C_2)}{\omega(C_1+C_P)C_2}-\frac{\omega Y_{21}L_P}{(1+\omega^2 Y_{21}^2 L_p^2)}\frac{Y_{21}}{\omega(C_1+C_P)C_2}\right]=0$$

$$\Rightarrow\left[\frac{\omega L}{1-\omega^2 LC}-\frac{1}{wC_C}\right]=\left[\frac{(C_1+C_P+C_2)}{\omega(C_1+C_P)C_2}-\frac{Y_{21}}{\omega(C_1+C_P)C_2}\frac{\omega Y_{21}L_P}{(1+\omega^2 Y_{21}^2 L_p^2)}\right]$$

$$\Rightarrow\left[\frac{\omega^2 LC_C-(1-\omega^2 LC)}{\omega C_C(1-\omega^2 LC)}\right]=\left[\frac{(1+\omega^2 Y_{21}^2 L_p^2)(C_1+C_P+C_2)-\omega L_P Y_{21}^2}{\omega(C_1+C_P)C_2(1+\omega^2 Y_{21}^2 L_p^2)}\right]$$

The expression at the left can be rewritten in terms of a determinant as:

$$\text{Det}\begin{vmatrix}[\omega^2 LC_C-(1-\omega^2 LC)] & [(1+\omega^2 Y_{21}^2 L_p^2)(C_1+C_P+C_2)-\omega L_P Y_{21}^2] \\ [\omega C_C(1-\omega^2 LC)] & [\omega(C_1+C_P)C_2(1+\omega^2 Y_{21}^2 L_p^2)]\end{vmatrix}$$

The Calculation of the Oscillating Condition Considering Parasitics of the Colpitts oscillator

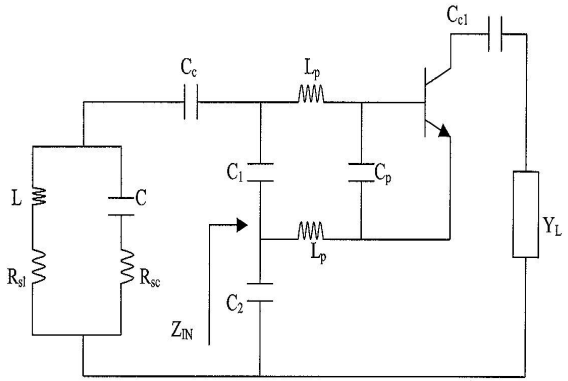

- For Lp → 0

$$\omega_0 = \sqrt{\frac{[C_2C_1 + C_1C_C + C_2C_C]}{L[C_1C_2C_C + C_1C_2C + C_1CC_C + C_2CC_C]}}$$

$$\omega_0 = \sqrt{\frac{1}{L\left[C + \frac{C_1C_2C_C}{C_1C_2 + C_1C_C + C_2C_C}\right]}}$$

- CC is a coupling capacitor used for separating the bias circuit, and its value is normally small, but similar to C1 and C2, typically 0.2pF to 2pF.
- Rewriting the polynomial equation as (CC $\rightarrow \infty$)

$$\omega_0 = \sqrt{\frac{1}{L\left[\frac{C_1C_2}{C_1 + C_2} + C\right]}}$$

The Calculation of the Oscillating Condition Considering Parasitics of the Colpitts oscillator

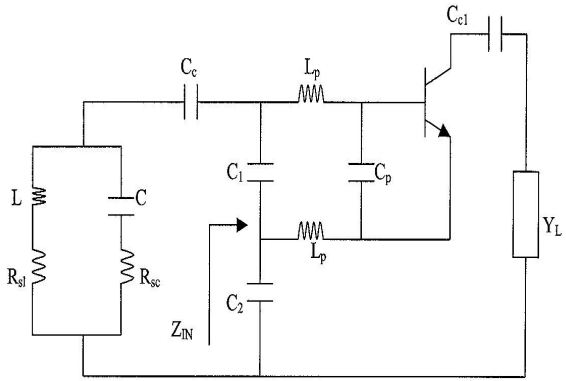

For steady oscillation the following condition has to be satisfied:

$$R_{Loss} < G_i \left[\frac{(1 + \frac{Y_{21}}{G_i})}{\omega^2 C_1 C_2} - \frac{L_3}{C_1} \right]$$

Since $\frac{Y_{21}}{G_i}$ is the frequency dependent current gain β:

$$R_{Loss} < \left| real\left(Y_{11} \left[\frac{(1+\beta)}{\omega^2 C_1 C_2} - \frac{L_3}{C_1} \right] \right) \right|$$

Tuning Diode Noise Contribution

- The practical oscillator will experience a frequency shift when the supply voltage is changed.
- This is due to the voltage and current dependent capacitances of the transistor.
- To calculate this effect, we can assume that the fixed tuning capacitor of the oscillator is a semiconductor junction, which is reverse biased.
- This capacitor becomes a tuning diode
- This tuning diode itself generates a noise voltage and modulates its capacitance by a slight amount, and therefore modulates the frequency of the oscillator by minute amounts.
- The following calculates the phase noise generated from this mechanism, which needs to be added to the phase noise calculated before
- It is possible to define an equivalent noise Raeq that, inserted in Nyquist's equation

$$V_n = \sqrt{4kT_o R_{aeq} \Delta f}$$

- where kTo = 4.2 x 10-21 at 300 K, R is the equivalent noise resistor, Δf is the bandwidth, and determines an open noise voltage across the tuning diode. Practical values of R_{aeq} for carefully selected tuning diodes are in the vicinity of 100Ω, or higher.
- If we now determine the voltage $V_n = \sqrt{4 \times 4.2 \times 10^{-21} \times 100}$, the resulting voltage value is 1.265 × 10-9 V $\sqrt{\text{Hz.}}$

Tuning Diode Noise Contribution

This noise voltage generated from the tuning diode is now multiplied with the VCO gain, resulting in the rms frequency deviation:

$$(\Delta f_{rms}) = K_o \times (1.265 \times 10^{-9}\text{V}) \quad \text{in a 1 Hz bandwidth} \tag{7-22}$$

In order to translate this into the equivalent peak phase deviation,

$$\theta_d = \frac{K_o\sqrt{2}}{f_m}(1.265 \times 10^{-9}\,\text{rad}) \quad \text{in a 1 Hz bandwidth} \tag{7-23}$$

or for a typical oscillator gain of 10 MHz/V,

$$\theta_d = \frac{0.00179}{f_m} \quad \text{rad in a 1 Hz bandwidth} \tag{7-24}$$

For $f_m = 25$ kHz (typical spacing for adjacent channel measurements for FM mobile radios), $\theta_d = 7.17\times10^{-8}$. This can be converted into the SSB signal-to-noise ratio

$$\begin{aligned}\mathscr{L}(f_m) &= 20\log_{10}\frac{\theta_c}{2} \\ &= -149\,\text{dBc/Hz}\end{aligned} \tag{7-25}$$

Tuning Diode Noise Contribution

- This Figure shows a plot with an oscillator sensitivity of 10 kHz/V, 10 MHz/V, and 100 MHz/V. The center frequency is 2.4 GHz. The lowest curve is the contribution of the Leeson equation. The second curve shows the beginning of the noise contribution from the diode, and the third curve shows that at this tuning sensitivity, the noise from the tuning diode by itself dominates as it modulates the VCO.
- This is valid regardless of the Q. This effect is called *modulation noise* (AM-to-PM conversion), while the Leeson equation deals with the conversion noise.

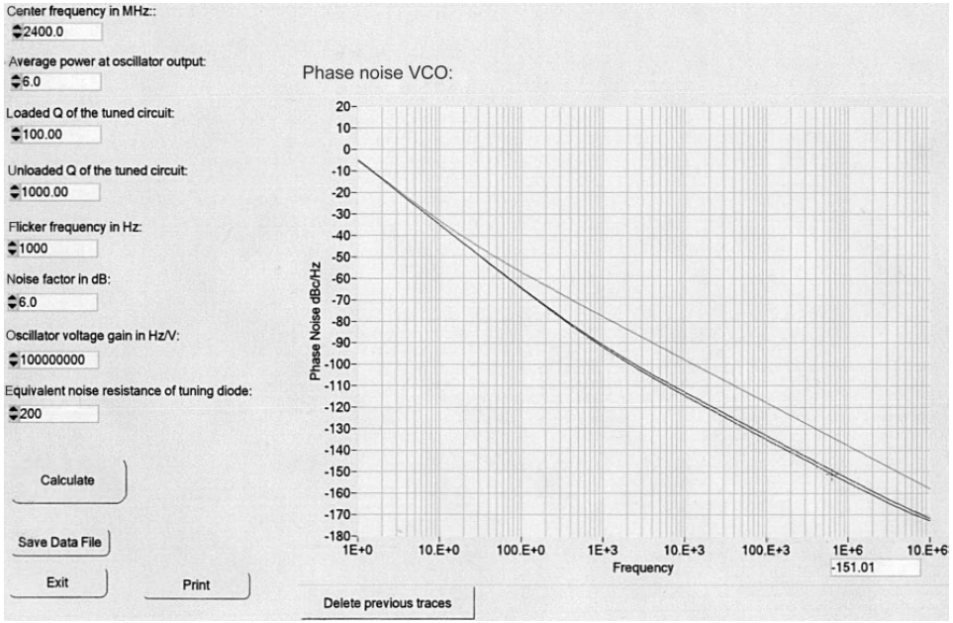

Simulated phase noise following the following Equation

$$\mathscr{L}(f_m) = 10\log\left\{\left[1+\frac{f_0^2}{(2f_mQ_L)^2}\right]\left(1+\frac{f_c}{f_m}\right)\frac{FkT}{2P_{sav}}+\frac{2kTRK_0^2}{f_m^2}\right\}$$

$\mathscr{L}(f_m)$ = ratio of sideband power in a 1 Hz bandwidth at f_m to total power in dB
f_m = frequency offset
f_0 = center frequency
f_c = flicker frequency
Q_L = loaded Q of the tuned circuit
F = noise factor
$kT = 4.1\times10^{-21}$ at 300 K_0 (room temperature)
P_{sav} = average power at oscillator output
R = equivalent noise resistance of the tuning diode (typically 50 Ω – 10 kΩ)
K_0 = oscillator voltage gain

Tuning Diode Noise Contribution

$$\mathcal{L}(f_m) = 10\log\left\{\left[1+\frac{f_0^2}{(2f_mQ_L)^2}\right]\left(1+\frac{f_c}{f_m}\right)\frac{FkT}{2P_{sav}}+\frac{2kTRK_0^2}{f_m^2}\right\}$$

- The limitation of this equation is that the loaded Q in most cases has to be estimated and the same applies to the noise factor.
- The microwave harmonic-balance simulator, which is based on the noise modulation theory (published by Rizzoli), automatically calculates the loaded Q and the resulting noise figure as well as the output power.
- The following equations, based on this equivalent circuit, are the exact values for Psav, QL, and F which are needed for the Leeson equation. This approach shown here is novel.
- The factor of 1000 is needed since the result is expressed in dBm and a function of n and C1.

$$[P_o(n,C_1]_{dBm} = 10Log\left\{\left[\frac{(V_{ce}=-0.7)^2}{4(\omega_0 L)^2}\right]\left[\frac{Q_L^2\left[C_1^2\left(\frac{C_1}{n-1}\right)^2\omega_0^4L^2\right]}{Q_L^2\left(C_1+\frac{C_1}{n-1}\right)^2+\omega_0^4L^2C_1^2\left(\frac{C_1}{n-1}\right)^2}\right]R_L*1000\right\}$$

0.7 = high current saturation voltage,

Vce collector emitter voltage <Vcc

To calculate the loaded QL, we have to consider the unloaded Q0 and the loading effect of the transistor. There we have to consider the influence of Y21+. The inverse of this is responsible for the loading and reduction of the Q

$$Q_L = \frac{Q_0\times Q^*}{Q_0+Q^*};\ Q^* = \frac{\omega_0\times\left|\frac{1}{Y_{21}^+}\right|(C_1+C_2)}{1-\omega_0^2\,C_1\,L(Q=Q_0)}$$

Designing an Oscillator based on Linear S-Parameters

- It may be interesting for readers to see how an oscillator can be analyzed using S-parameters.
- It should be noted that this method is based on linear approximations and works for practically all microwave oscillator designs
- The equivalent criteria of the negative resistance can be calculated in the form of S-parameters.
- This negative resistance will cause oscillations if the following conditions are satisfied.
- Assume that the oscillation condition is satisfied at port 1 of a two port device and is given by

$$\frac{1}{S_{11}} = \Gamma_G \quad (6)$$

$$S'_{11} = S_{11} + \frac{S_{12}S_{21}\Gamma_L}{1 - S_{22}\Gamma_L} = \frac{S_{11} - D\Gamma_L}{1 - S_{22}\Gamma_L} \quad (7)$$

$$\frac{1}{S'_{11}} = \frac{1 - S_{22}\Gamma_L}{S_{11} - D\Gamma_L} = \Gamma_G \quad (8)$$

From expanding (7) we get

$$\Gamma_G S_{11} - D\Gamma_L\Gamma_G = 1 - S_{22}\Gamma_L \quad (9)$$

$$\Gamma_L\left(S_{22} - D\Gamma_G\right) = 1 - S_{11}\Gamma_G \quad (10)$$

$$\Gamma_L = \frac{1 - S_{11}\Gamma_G}{S_{22} - D\Gamma_G} \quad (11)$$

$$S'_{22} = S_{22} + \frac{S_{12}S_{21}\Gamma_G}{1 - S_{11}\Gamma_G} = \frac{S_{22} - D\Gamma_G}{1 - S_{11}\Gamma_G} \quad (12)$$

$$\frac{1}{S'_{22}} = \frac{1 - S_{11}\Gamma_G}{S_{22} - D\Gamma_G} \quad (13)$$

Comparing equations (9) and (12), we find that

$$\frac{1}{S'_{22}} = \Gamma_G \quad (14)$$

where, S11 and S22 are the input and output reflection coefficients, respectively

Designing an Oscillator based on Linear S-Parameters

- The discussion above means that the oscillation condition is also satisfied at port 2; which proves the simultaneous oscillation condition at both ports. Thus, if either port is oscillating the other port must be oscillating as well. A load may appear at either or both ports, but normally the load is in , the output termination.
- It is helpful to use the common-source based amplifier to compute the oscillator output power.
- For oscillators, the objective is to maximize of the amplifier, which is the useful power to the load. An empirical expression for the common-source amplifier output power found by Johnson is:

$$P_{out} = P_{sat}\left(1 - \exp\frac{-GP_{in}}{P_{sat}}\right)$$

where Psat is the saturated output power of the amplifier and G is the tuned small-signal common-source transducer gain of the amplifier, which is identical to $|S_{21}|^2$

Since the objective is to maximize $\left(P_{out} - P_{in}\right)$, where Pout and Pin are the output and input power of the amplifier

$$d\left(P_{out} - P_{in}\right) = 0 \quad (16) \qquad \frac{\partial P_{out}}{\partial P_{in}} = 1 \quad (17) \qquad \frac{\partial P_{out}}{\partial P_{in}} = G_{exp} - \frac{GP_{in}}{P_{sat}} = 1 \quad (18) \qquad \exp\frac{GP_{in}}{P_{sat}} = G \quad (19) \qquad \frac{P_{in}}{P_{sat}} = \frac{\ln G}{G} \quad (20)$$

Designing an Oscillator based on Linear S-Parameters

At the maximum value of $\left(P_{\text{out}} - P_{\text{in}}\right)$, the amplifier output is $P_{\text{out}} = P_{\text{sat}}\left(1 - \frac{1}{G}\right)$ (21)

and the maximum oscillator output power is $P_{\text{osc}} = \left(P_{\text{out}} - P_{\text{in}}\right)$ (22) $= P_{sat}\left(1 - \frac{1}{G} - \frac{\ln G}{G}\right)$ (23)

- Thus, the maximum oscillator output power can be predicted from the common-source amplifier saturated output power and the small signal common source transducer gain G.
- For high oscillator output power, high (loop) gain is of importance. Another definition of gain that is useful for large-signal amplifier or oscillator design is the maximum efficient gain, defined by

$$G_{\text{ME}} = \frac{P_{\text{out}} - P_{\text{in}}}{P_{\text{in}}} \quad (24)$$

- For maximum oscillator power the maximum efficient gain from (20) and (21) is $G_{\text{MEmax}} = \frac{G-1}{\ln G}$ (25)

- Designing oscillators based on S-parameters in a linear mode has been quoted by many authors using first approximation for large signals. The problem with this published approach is that it uses a GaAs FET, where only the transconductance g_m has a major influence. S_{11} changes very little under large signal conditions, as does S_{22}. Reliable large signal S-parameters for bipolar transistors and FETs are difficult to get. Under steady state condition Y_{21}* is approximately $\text{Re}(Y_{21})/\pi$.

Conditions for Oscillations

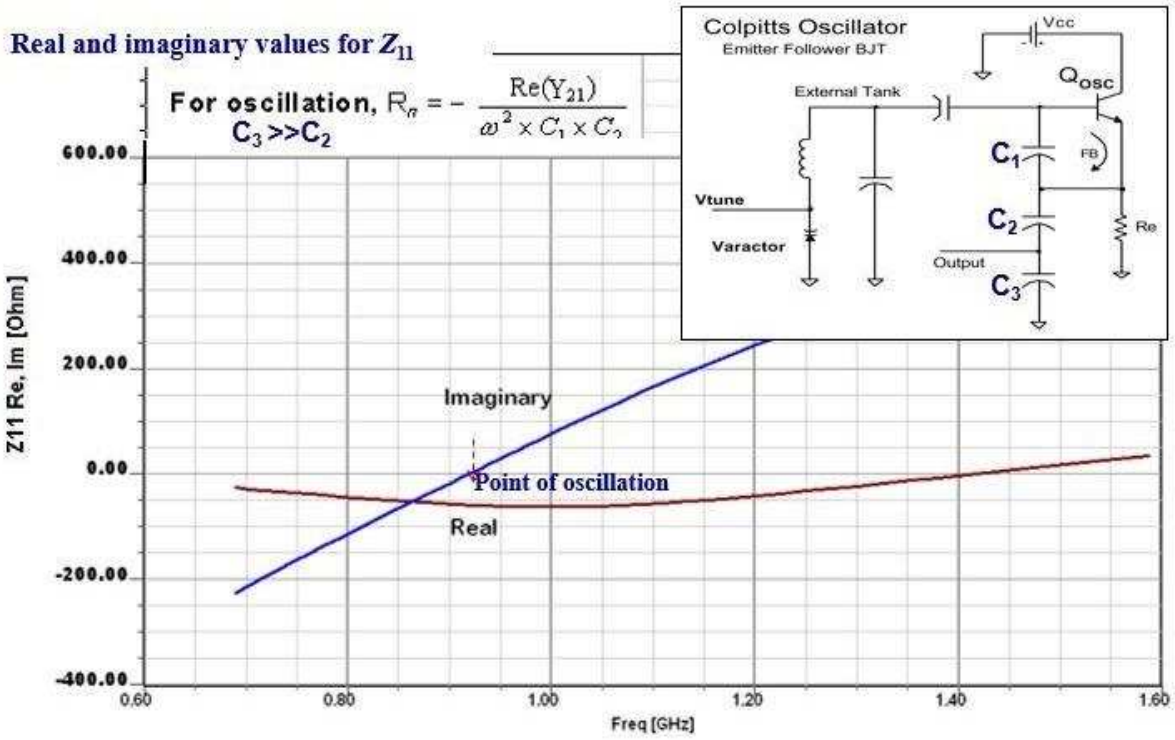

- Real (Z_{11}) must be slightly more negative than the loss resistance in the circuit for oscillation to start. The resulting dc shift in the transistor will then provide the amplitude stabilization as gm will be reduced
- Next we need to look at the large signal condition which will affect Y_{11} and Y_{21}. The best way to get the data is to measure the parameters. At microwave frequencies it is convenient to do so in a 50 Ohm system and then convert them to Y parameter

Large signal Operation of Oscillators

- Definition: RF voltages/currents are of similar magnitude as the DC values.
- Test points were Vc = 2V, Ic = 20mA.
- The transistor behaves differently under large signal conditions.
- Large signal parameters can be obtained from simulation using SPICE parameters, calculating the Bessel functions of the currents of the intrinsic transistor and adding the parasitics and measurements.
- This Figure shows the R&S VNA and the test fixture for the transistor of choice

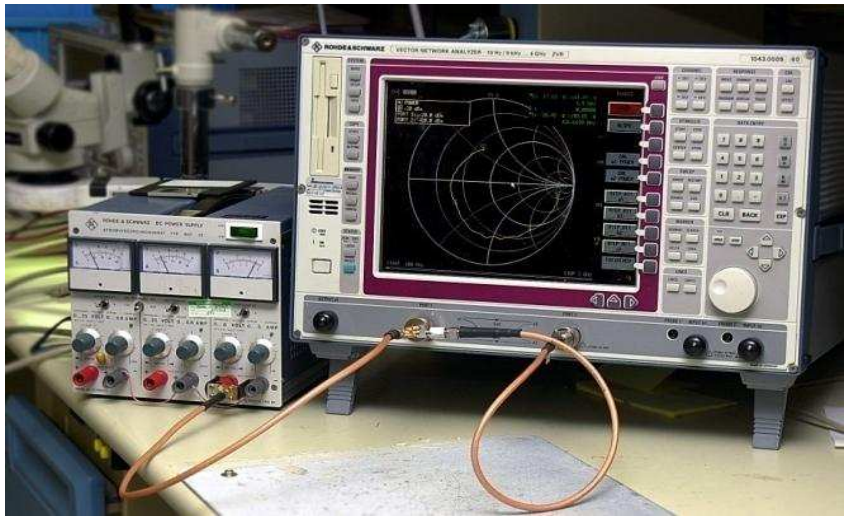

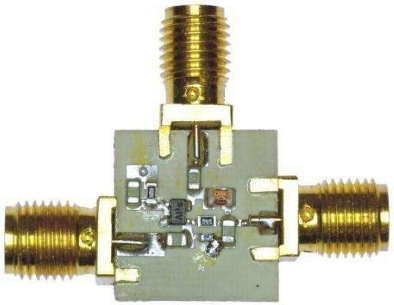

- Typical measurement setup for evaluation of large signal parameters (R&S vector analyzer and the test fixture for the transistor of choice), Agilent now calls this X Parameters
- The bias, drive level, and frequency dependent S parameters are then obtained for practical use

Some Test Results – D.U.T: BFP520

Measured large-signal S_{11}

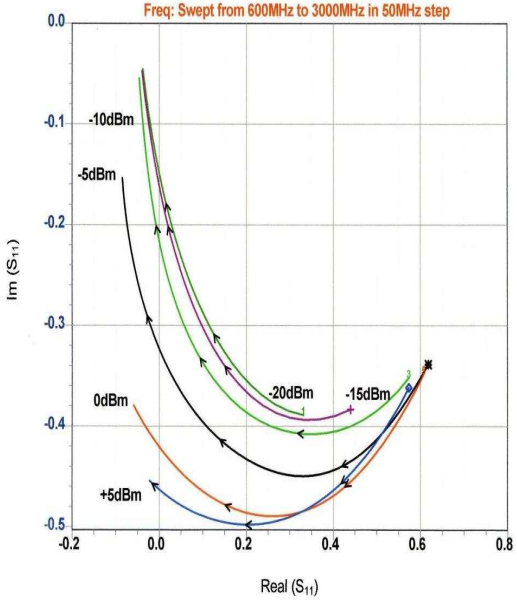

Measured large-signal S_{12}

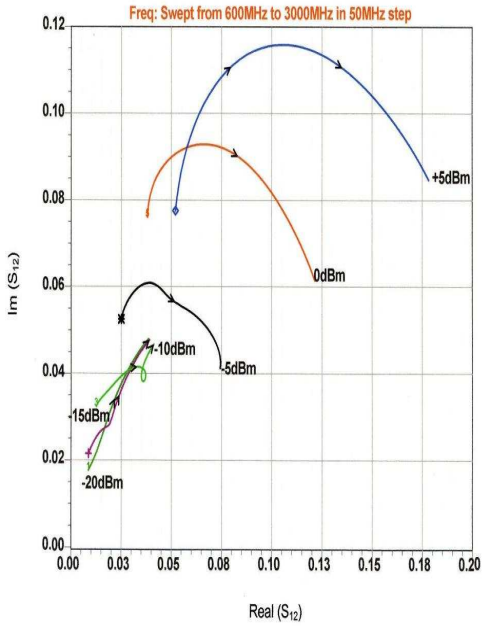

Measured large-signal S_{21}

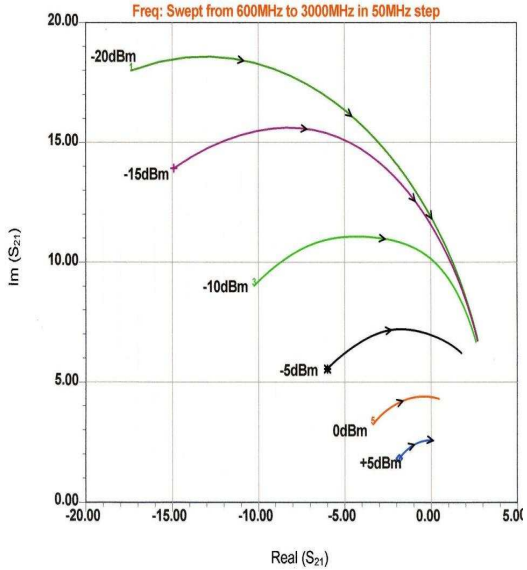

Measured large-signal S_{22}

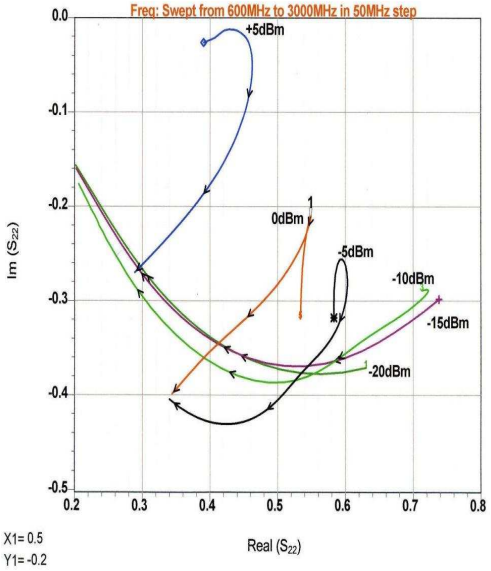

Oscillator Design Based on the Measured Large-Signal S-parameters

A) Parallel Resonant (Colpitts Oscillator)

- This Figure shows the standard Colpitts oscillator using large-signal S-parameters.
- This example is of particular interest because it requires an inductor instead of the familiar capacitor, C2, between base and emitter

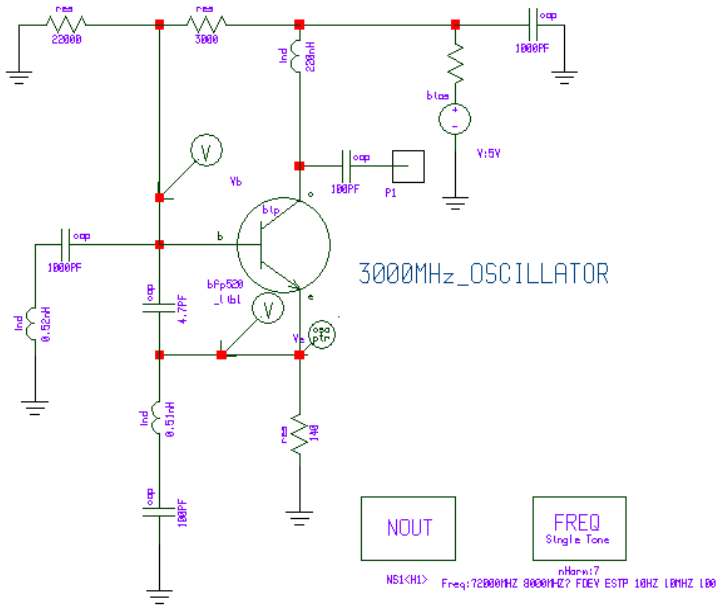

A 3000 MHz oscillator using a BFP520 transistor operating at 2V and 20mA. In this case, the capacitor C2 needs to be replaced by an inductor L3 which tunes out the collector emitter capacitance to achieve the optimum value. The 1nF on the left is a DC separation capacitor. This case is optimized for output power

Oscillator Design Based on the Measured Large-Signal S-parameters

- The measured large-signal Y-parameter data (Ic=20mA, Vce=2V), see above, @ 3000MHz are:

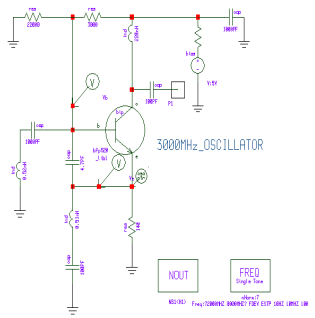

$$Y_{11} = G_{11} + jB_{11} = (11.42 + j8.96)\ mS \qquad \text{(A-1)}$$

$$Y_{21} = G_{21} + jB_{21} = (4.35 - j196.64)\ mS \qquad \text{(A-2)}$$

$$Y_{12} = G_{12} + jB_{12} = (-433.09 - j1.5643\ mS \qquad \text{(A-3)}$$

$$Y_{22} = G_{22} + jB_{22} = (4.41 + j9.10)\ mS \qquad \text{(A-4)}$$

- The optimum values of feedback element are calculated from the given expression of B_1^* and B_2^* are

Oscillator Design Based on the Measured Large-Signal S-parameters

- The optimum values of feedback element are calculated from the given expression of B_1^* and B_2^* are

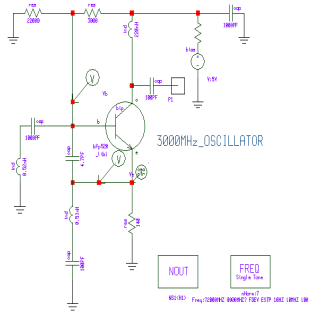

$$B_1^* = -\left\{B_{11} + \left[\frac{B_{12}+B_{21}}{2}\right] + \left[\frac{G_{21}-G_{12}}{B_{21}-B_{12}}\right]\left[\frac{G_{12}+G_{21}}{2} + G_{11}\right]\right\} \quad \text{(A-5)}$$

$$jB_1^* = 89.8E-3 \quad \text{(A-6)}$$

$$jB_1^* = j\omega C_1 \quad \text{(A-7)}$$

$$C_1 = \frac{89.8E-3}{2\pi f} = 4.77\,pF \quad \text{(A-8)}$$

$$B_2^* = \left[\frac{B_{12}+B_{21}}{2}\right] + \left[\frac{(G_{12}+G_{21})(G_{21}-G_{12})}{2(B_{21}-B_{12})}\right] \quad \text{(A-9)}$$

$$jB_2^* = -103.5E-3 \quad \text{(A-10)}$$

$$jB_2^* = \frac{1}{j\omega L_2} \quad \text{(A-11)}$$

$$L_2 = \frac{1}{(2\pi f)\times 103.5E-3 L_2}\,0.515\,nH \quad \text{(A-12)}$$

Oscillator Design Based on the Measured Large-Signal S-parameters

- The optimum values of the real and imaginary part of the output admittance are

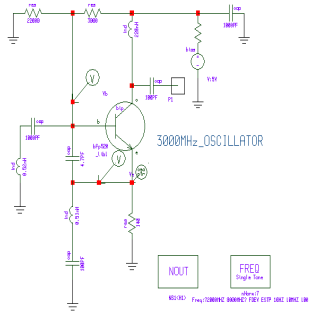

$$Y_{out}^{*} = [G_{out}^{*} + jB_{out}^{*}] \quad \text{(A-13)}$$

where G_{out}^{*} and B_{out}^{*} is given as

$$G_{out}^{*} = G_{22} - \left[\frac{(G_{12}+G_{21})^2 (B_{21}-B_{12})^2}{4G_{11}}\right] \quad \text{(A-14)}$$

$$G_{out}^{*} = -823.53E-3 \quad \text{(A-15)}$$

$$B_{out}^{*} = B_{22} + \left[\frac{G_{21}-G_{12}}{B_{21}-B_{12}}\right] - \left[\frac{(G_{12}+G_{21})}{2} + G_{22} - G_{out}^{*}\right] + \left[\frac{B_{21}+B_{12}}{2}\right] \quad \text{(A-16)}$$

$$B_{out}^{*} = -105.63E-3 \quad \text{(A-17)}$$

$$jB_{out}^{*} = \frac{1}{j\omega L_3} \quad \text{(A-18)}$$

$$L_3 = 0.502nH \quad \text{(A-19)}$$

Oscillator Design Based on the Measured Large-Signal S-parameters

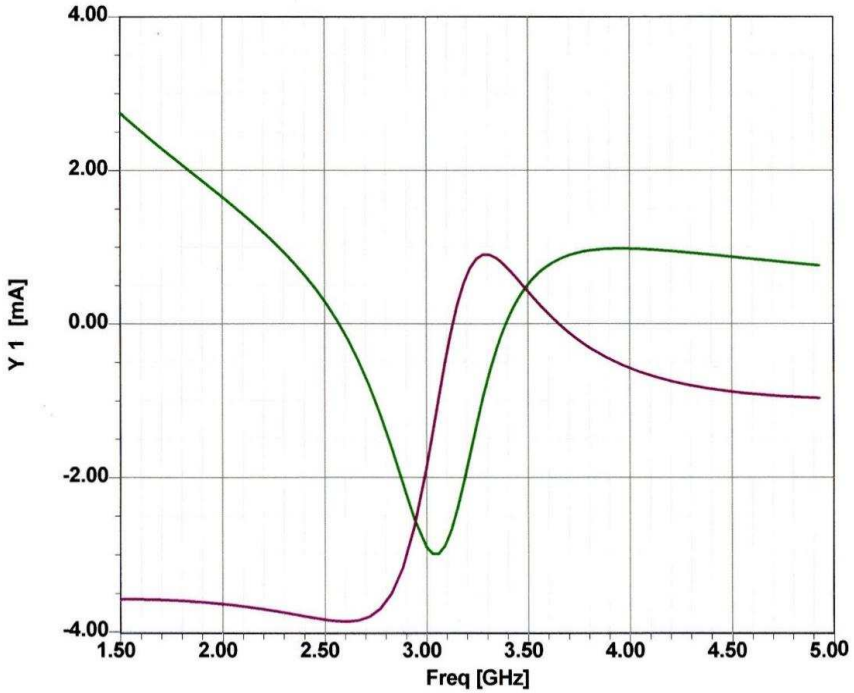

the real and imaginary currents for oscillation. The reactive current crosses the zero line at 3120 MHz. This is close, but not exactly at the point of most negative resistance current. The reason for the shift of 120 MHz is due to the use of small-signal analysis rather than the large-signal analysis.

- This Figure shows the simulated response of the oscillator circuit having resonance at 3120 MHz or 5% error. The little variation in resonant frequency may be due to the frequency dependent packaged parameters, but it is a good starting value for tuning and optimization for the best phase noise and output power.
- The best phase noise at a given power output is basically dependent upon the ratio and absolute value of the feedback capacitors, which in turn depends upon the optimum drive-level.

$$Z_{out}(I,\omega)+Z_L(\omega)=0 \qquad \text{(A-20)}$$

$$Z_L(\omega)\rightarrow Z_3(\omega) \qquad \text{(A-21)}$$

Where I is the load current amplitude and w is the resonance frequency.

Z_{out} is current and frequency dependent output impedance, whereas Z_L is only function of frequency.

Now the Evaluation

- The bias condition of the transistor is:

Voltage	Current
Vp(Vb) = 3.9442 V	Ip(Vb) = 0 A
Vp(Ve) = 3.01649 V	Ip(Ve) = 0 A
Vp() = 3.01649 V	Ip() = 0 A
Vbe(_lib1) = 0.912885 V	Ib(_lib1) = 0.172653 mA
Vce(_lib1) = 1.80815 V	Ic(_lib1) = 21.3737 mA

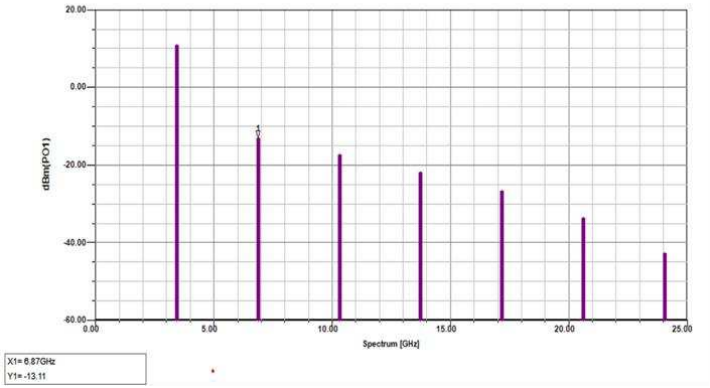

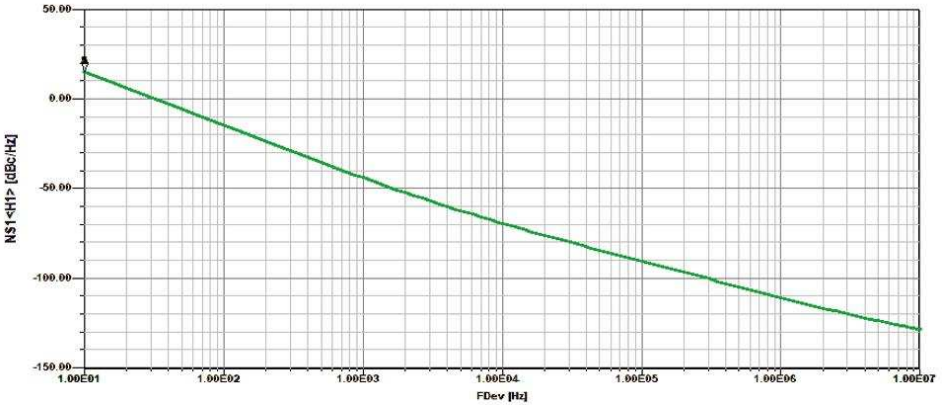

The loaded Q of the printed resonator was 200. Now evaluating the influence of the values of the feedback capacitors gives an interesting result.

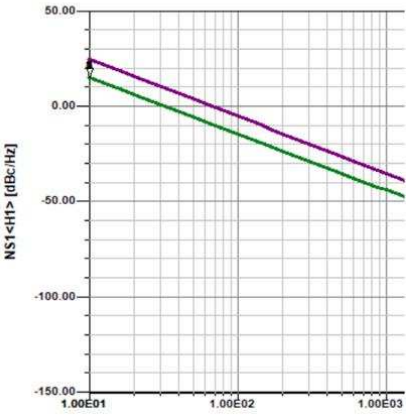

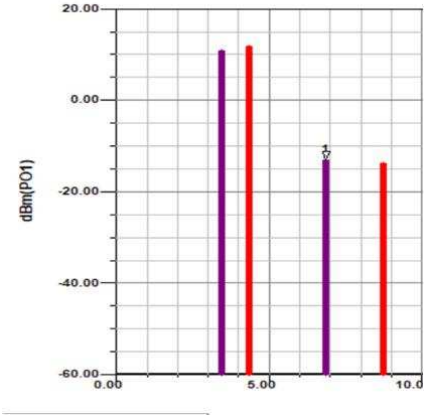

Increasing the output power strongly reduces the phase noise!

Now the Evaluation

- The important message that can be derived from this calculation is the fact that the parasitics now dominate the design.
- The negative resistance which used to be proportional to $1/\omega 2$ now is $1/\omega 4$.
- The rule of thumb is to use a large device for lower frequencies and operate it at medium DC currents.
- This in the millimeter wave area would be fatal. The large device would have excessive parasitic elements such as inductors and capacitors and the optimum design is no longer possible since the parasitics would be larger than the values required for optimum performance.
- These parasitics are the major reason why at millimeter wave and wide tuning ranges the phase noise is not as good as what a narrowband Colpitts oscillator would provide.
- The oscillator operates in a reasonable linear mode so the load line has a minimum surface area
- Modeling the actual complex layout is much more relevant than a standard circuit diagram

Oscillator Design Based on the Measured Large-Signal S-parameters

B) Series Feedback Oscillator: Applicable to YIG Oscillators

- The steady-state oscillation condition for series feedback configuration can be expressed as

$$Z_{out}(I,\omega)+Z_L(\omega)=0 \qquad \text{(A-20)}$$

$$Z_L(\omega)\rightarrow Z_3(\omega) \qquad \text{(A-21)}$$

where I is the load current amplitude and w is the resonance frequency.

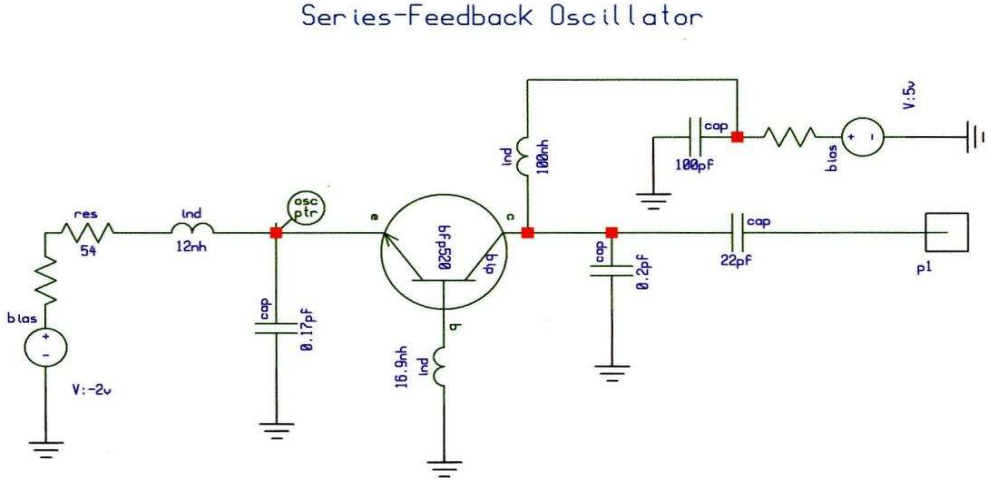

Z_{out} is current and frequency dependent output impedance, where as Z_L is only function of frequency.

$$Z_{out}(I,\omega)=R_{out}(I,\omega)+jX_{out}(I,\omega) \qquad \text{(A-22)}$$

$$Z_L(\omega)=R_L(\omega)+jX_L(\omega) \qquad \text{(A-23)}$$

The expression of output impedance Z_{out}, can be written as

$$Z_{out}=-Z_3 \Rightarrow [Z_{22}+Z_2]-\frac{[Z_{12}+Z_2][Z_{21}+Z_2]}{[Z_{11}+Z_1+Z_2]} \qquad \text{(A-24)}$$

where Z_{ij} (i,j=1,2) is Z-parameters of hybrid transistor model and can be written as

$$Z_{i,j}=[R_{ij}+jX_{ij}]_{i,j=1,2} \qquad \text{(A-25)}$$

Oscillator Design Based on the Measured Large-Signal S-parameters

B) Series Feedback Oscillator: Applicable to YIG Oscillators

- According to optimum criterion, the negative real part of the output impedance Z_{out} has to be maximized and the possible optimal values of feedback reactance under which the negative value R_{out} is maximized by setting

$$\frac{\partial \mathrm{Re}[Z_{out}]}{\partial X_1} = 0 \; and \; \frac{\partial \mathrm{Re}[Z_{out}]}{\partial X_2} = 0 \qquad \text{(A-26)}$$

$$\Rightarrow \frac{\partial [R_{out}]}{\partial X_1} = 0 \; and \; \frac{\partial [R_{out}]}{\partial X_2} = 0 \qquad \text{(A-27)}$$

The optimal values and X_1^* and X_2^*, based on above condition, can be expressed in terms of a 2-port parameter of the active device e.g. BJT/FET

$$X_1^* = -X_{11} + \left[\frac{X_{12}+X_{21}}{2}\right] + \left[\frac{R_{21}-R_{12}}{X_{21}-X_{12}}\right]\left[\frac{R_{12}+R_{21}}{2} - R_{11} - R_1\right] \qquad \text{(A-28)}$$

$$X_2^* = -\left[\frac{X_{12}+X_{21}}{2}\right] - \left[\frac{(R_{21}-R_{12})(2R_2+R_{12}+R_{21})}{2(X_{21}-X_{12})}\right] \qquad \text{(A-29)}$$

$$Z_{out}^* = R_{out}^* + X_{out}^* \qquad \text{(A-30)}$$

$$R_{out}^* = R_2 + R_{22} - \left[\frac{(2R_2+R_{21}+R_{12})^2 + (X_{21}-X_{12})^2}{4(R_{11}+R_2+R_1)}\right] \qquad \text{(A-31)}$$

By substituting values of X_1^* and X_2^* into above equation, the optimal real and imaginary parts of the output impedance Z_{out}^* can be expressed as:

$$X_{out}^* = X_2^* + X_{22} - \left[\frac{R_{21}-R_{12}}{X_{21}-X_{12}}\right]\left[R_{out}^* - R_2 - R_{22}\right] \qquad \text{(A-32)}$$

where

$$X_2^* = -\left[\frac{X_{12}+X_{21}}{2}\right] - \left[\frac{(R_{21}-R_{12})(2R_2+R_{12}+R_{21})}{2(X_{21}-X_{12})}\right] \qquad \text{(A-33)}$$

Oscillator Design Based on the Measured Large-Signal S-parameters

B) Series Feedback Oscillator: Applicable to YIG Oscillators

- thus, in the steady-state operation mode of the oscillator, amplitude and phase balance conditions can be written as:

$$R_{out}^{*} + R_L = 0 \tag{A-34}$$

$$X_{out}^{*} + X_L^{*} = 0 \tag{A-35}$$

The output power of the oscillator can be expressed in terms of load current and load impedance as

$$P_{out} = \frac{1}{2} I^2 \,\mathrm{Re}[Z_L] \tag{A-36}$$

where I and V is the corresponding load current and voltage across the output.

$$I = \left[\frac{Z_{11} + Z_1 + Z_2}{Z_{22}(Z_{11} + Z_1 + Z_2) - Z_{21}(Z_{12} + Z_2)} \right] V \tag{A-37}$$

Oscillator Design Based on the Measured Large-Signal S-parameters

B) Series Feedback Oscillator: Applicable to YIG Oscillators

- The expression of the phase noise for the series feedback oscillator, following the approach for the Colpitts oscillator, is :

$$|\overline{L}|_{SSB}=\left[4KTR+\frac{4qI_c g_m^2(t)}{\omega_0^4\beta^2 C_{ce}^2(C_2+C_{be}-L_1C_2C_{be}\omega_0^2)^2+g_m^2\omega_0^2(C_2+C_{be}-L_1C_2C_{be}\omega_0^2)^2}\right]*$$

$$\left[\frac{\omega_0^2}{4(\Delta\omega)^2V_{cc}^2}\right]\left[\frac{1}{Q_L^2}+\left(1-\left(\frac{1}{\omega_0^2L_1}\right)\left(\frac{[(C_2+C_{be}-L_1C_2C_{be}\omega_0^2)+C_{ce}]}{C_{ce}[(C_2+C_{be}-L_1C_2C_{be}\omega_0^2)]}\right)\right)^2\right] \quad \text{(A-38)}$$

For large value of Q_L,

$$|\overline{L}|_{SSB}=\left[4KTR+\frac{4qI_c g_m^2(t)}{\omega_0^4\beta^2 C_{ce}^2(C_2+C_{be}-L_1C_2C_{be}\omega_0^2)^2+g_m^2\omega_0^2(C_2+C_{be}-L_1C_2C_{be}\omega_0^2)^2}\right]*$$

$$\left[\frac{\omega_0^2}{4(\omega)^2V_{cc}^2}\right]\frac{1}{\omega_0^4L_1^2}\left(\frac{[(C_2+C_{be}-L_1C_2C_{be}\omega_0^2)+C_{ce}]}{C_{ce}[(C_2+C_{be}-L_1C_2C_{be}\omega_0^2)]}\right) \quad \text{(A-39)}$$

- The important message that can be derived from this calculation is the fact that the parasitics now dominate the design. The negative resistance which used to be proportional to 1/ω2 now is 1/ω4. The rule of thumb is to use a large device for lower frequencies and operate it at medium DC currents. This in the millimeterwave area would be fatal. The large device would have excessive parasitic elements such as inductors and capacitors and the optimum design is no longer possible since the parasitics would be larger than the values required for optimum performance. These parasitics are the major reason why at millimeterwave and wide tuning ranges the phase noise is not as good as what a narrowband Colpitts oscillator would provide.

Example: 3000 MHz YIG Oscillator

- A 3000MHz oscillator is designed based on the above shown analytical series feedback approach and is also validated with the simulated results. Figure A-3 shows the series feedback oscillator.

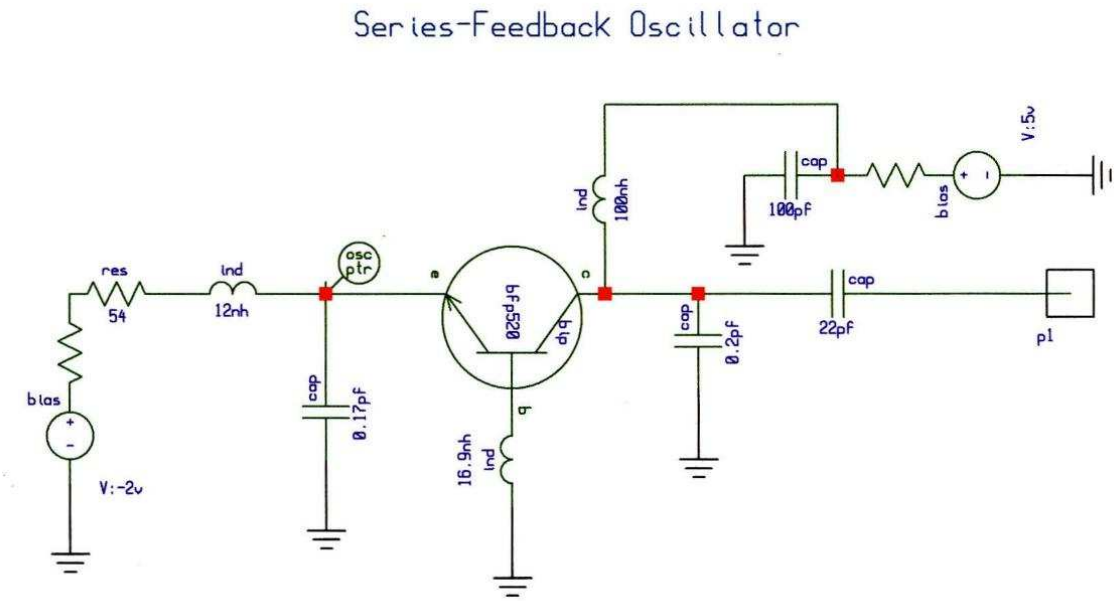

A series feedback oscillator. For oscillation condition, the base to ground inductance and the emitter to ground capacitance is required. The 12nH inductor acts a choke. The output is tuned and terminated into 50Ω.

Example: 3000 MHz YIG Oscillator

- Large signal Z-parameters measured data (Ic=20mA, Vce=2V) @ 3000 MHz are given as:

$$Z_{11} = R_{11} + jX_{11} = (22.96 + j27.30)\Omega \quad \text{(A-40)}$$

$$Z_{21} = R_{21} + jX_{21} = (140 + j670)\Omega \quad \text{(A-41)}$$

$$Z_{12} = R_{12} + jX_{12} = (2.72 + j4.99)\Omega \quad \text{(A-42)}$$

$$Z_{22} = R_{22} + jX_{22} = (46.04 + j21.45)\Omega \quad \text{(A-43)}$$

$$X_1^* = -X_{11} + \left[\frac{X_{12} + X_{21}}{2}\right] + \left[\frac{R_{21} - R_{12}}{X_{21} - X_{12}}\right]\left[\frac{R_{12} + R_{21}}{2} - R_{11} - R_1\right] \quad \text{(A-44)}$$

$$X_1^* = 319.9654\Omega \Rightarrow L_1 = 16.9nH \quad \text{(A-45)}$$

$$X_2^* = -\left[\frac{X_{12} + X_{21}}{2}\right] - \left[\frac{(R_{21} - R_{12})(2R_2 + R_{12} + R_{21})}{2(X_{21} - X_{12})}\right] \quad \text{(A-46)}$$

$$\left|X_2^* = -311.67084 \Rightarrow C_2 = 0.17\,pF\right. \quad \text{(A-47)}$$

$$X_{out}^* = X_2^* + X_{22} - \left[\frac{R_{21} - R_{12}}{X_{21} - X_{12}}\right]\left[R_{out}^* - R_2 - R_{22}\right] \quad \text{(A-48)}$$

$$\left|X_{out}^* = -259.31176 \Rightarrow C_3 = 0.2\,pF\right. \quad \text{(A-49)}$$

- The simulated response of the oscillator circuit, having resonance at 2980MHz or 1% error, is a good starting value for tuning and optimization for optimum phase noise and output power.
- The best phase noise at a given power output is basically dependent upon the ratio and absolute value of the feedback capacitor, which in turn depends upon the optimum drive-level.
- The detailed analysis for designing the best phase noise, based on a unified approach, is discussed in the next section.

Example: 3000 MHz YIG Oscillator

- This figure shows the real and imaginary currents for oscillating conditions for optimum output power.
- In this case, the operating Q is very low, as can be seen from the shallow curve at which the imaginary current crosses the zero line, while the real current is still negative.
- To optimize this circuit for phase noise, the imaginary curve should go through the zero line at the point of steepest ascent, while maintaining a negative real current.
- The low Q resonator guarantees that the most output power is available, and the resonator is heavily loaded.

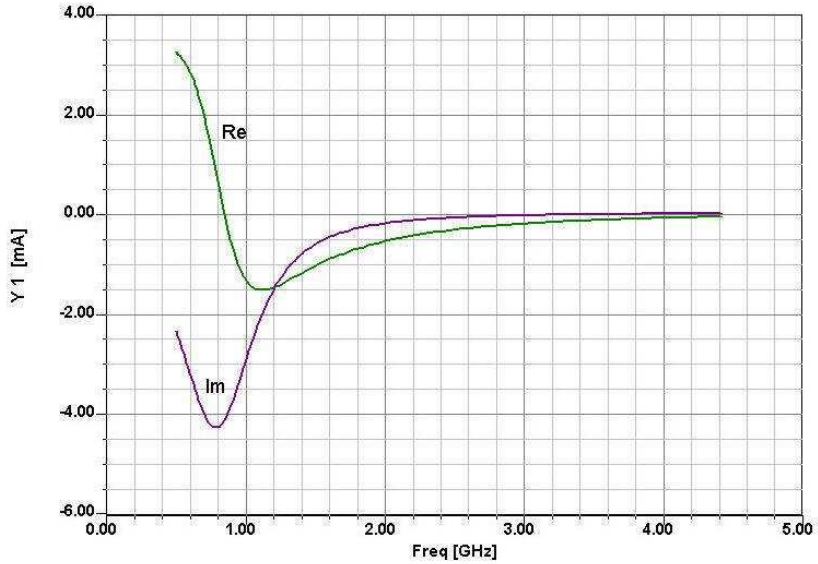

This figure the real and imaginary currents of the 3 GHz series-type oscillator. The very shallow curve should be noted.

Classical Linear Two-Port Oscillator Design

- In many cases in old publications and even today a first approximation is made for two port oscillators using the published small signal S parameters. This may be good for getting oscillation started but may not be correct for predicting sustaining oscillation
- This older, unreliable but frequently common method for designing oscillators is to resonate the input port with a passive high-Q circuit at the desired frequency of resonance. This only works if the transistor has access gain! It will be shown that if this is achieved with a load connected on the output port, the transistor is oscillating at both ports and is thus delivering power to the load port.
- The oscillator may be considered a two-port structure, where M3 is the lossless resonating port and M4 provides lossless matching such that all of the external RF power is delivered to the load. The resonating network has been described. Nominally, only parasitic resistance is present at the resonating port, since a high-Q resonance is desirable for minimizing oscillator noise. It is possible to have loads at both the input and the output ports if such an application occurs, since the oscillator is oscillating at both ports simultaneously.
- Note: Using the hopefully high Q tuned circuit also as a filter gives better far out phase noise than the more common method taking like the energy from the collector if the circuit is based on the Colpitts design.

Classical Linear Two-Port Oscillator Design

- The simultaneous oscillation condition is proved as follows. Assume that the oscillation condition is satisfied at port 1:

$$1/S_{11}^{'} = \Gamma_G \tag{4-218}$$

Thus,

$$S_{11}^{'} = S_{11} + \frac{S_{12}S_{21}\Gamma_L}{1-S_{22}\Gamma_L} = \frac{S_{11}-D\Gamma_L}{1-S_{22}\Gamma_L} \tag{4-219}$$

$$\frac{1}{S_{11}^{'}} = \frac{1-S_{22}\Gamma_L}{S_{11}-D\Gamma_L} = \Gamma_G \tag{4-220}$$

By expanding Eq. (4-220), we find

$$\begin{aligned} \Gamma_G S_{11} - D\Gamma_L\Gamma_G &= 1 - S_{22}\Gamma_L \\ \Gamma_L\left(S_{22} - D\Gamma_G\right) &= 1 - S_{11}\Gamma_G \\ \Gamma_L &= \frac{1-S_{11}\Gamma_G}{S_{22}-D\Gamma_G} \end{aligned} \tag{4-221}$$

Thus,

$$S_{22}^{'} = S_{22} + \frac{S_{12}S_{21}\Gamma_G}{1-S_{11}\Gamma_\Gamma} = \frac{S_{22}-D\Gamma_G}{1-S_{11}\Gamma_G} \tag{4-222}$$

$$\frac{1}{S_{22}^{'}} = \frac{1-S_{11}\Gamma_G}{S_{22}-D\Gamma_G} \tag{4-223}$$

Comparing Eqs. (4-221) and (4-223), we find

$$1/S_{22}^{'} = \Gamma_L \tag{4-224}$$

which means that the oscillation condition is also satisfied at port 2; this completes the proof. Thus, if either port is oscillating, the other port must be oscillating as well. A load may appear at either or both ports, but normally the load is in Γ_L, the output termination. This result can be generalized to an n-port oscillator by showing that the oscillator is simultaneously oscillating at each port:

$$\Gamma_1 S_{11}^{'} = \Gamma_2 S_{22}^{'} = \Gamma_3 S_{33}^{'} = \cdots = \Gamma_n S_{nn}^{'} \tag{4-225}$$

Classical Linear Two-Port Oscillator Design

- Before concluding this section on two-port oscillator design, the buffered oscillator shown in Figure 4-166 must be considered. This design approach is used to provide the following:
  - A reduction in loading-pulling, which is the change in oscillator frequency when the load reflection coefficient changes.
  - A load impedance that is more suitable to wideband applications.
  - A higher output power from a working design, although the higher output power can also be achieved by using a larger oscillator transistor.
- Buffered oscillator designs are quite common in wideband YIG applications, where changes in the load impedance must not change the generator frequency.

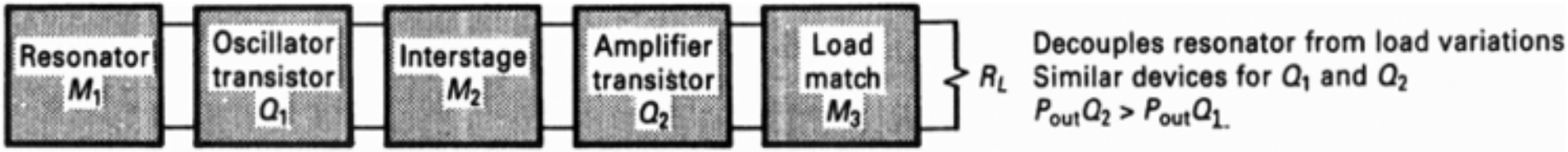

Figure 43: Figure 4-166 Buffered oscillator design.

Classical Linear Two-Port Oscillator Design

- Two-port oscillator design may be summarized as follows:
  - Select a transistor with sufficient gain and output power capability for the frequency of operation. This may be based on oscillator data sheets, amplifier performance, or S-parameter calculation.
  - Select a topology that gives k < 1 at the operating frequency. Add feedback if k < 1 has not been achieved.
  - Select an output load matching circuit that gives $\left|S_{11}^{'}\right|>1$ over the desired frequency range. In the simplest case this could be a 50 Ω load.
  - Resonate the input port with a lossless termination so that $\Gamma_G S_{11}^{'}=1$
  - . The value of $S_{22}^{'}$ greater than unity with the input properly resonated

- In all cases, the transistor delivers power to a load and the input of the transistor. Practical considerations of readability and dc biasing will determine the best design.
- For both bipolar and FET oscillators, a common topology is common-base or common-gate, since a common-lead inductance can be used to raise S22 to a large value, usually greater than unity even with a 50-Ω generator resistor.
- However, it is not necessary for the transistor S_{22} to be greater than unity, since the 50-Ω generator is not present in the oscillator design. The requirement for oscillation is k < 1; then resonating the input with a lossless termination will provide that $\left|S_{11}^{'}\right|>1$

.

Classical Linear Two-Port Oscillator Design

- A simple example will clarify the design procedure. A common-base bipolar transistor (HP2001) was selected to design a fixed-tuned oscillator at 2 GHz. The common-base S parameters and stability factor are given in Table 4-16. Using the load circuit in Figure 4-167, we see that the reflection coefficients are:

$$\Gamma_L = 0.62\angle 30°$$

$$S_{11}' = 1.18\angle 173°$$

Table 4-16 HP2001 bipolar chip common base $(V_{CE} = 15\,\text{V},\ I_c = 25\,\text{mA})$

$L_B = 0$	$L_B = 0.5\,\text{nH}$
$S_{11} = 0.94\angle 174°$	$1.04\angle 173°$
$S_{21} = 1.90\angle -28°$	$2.00\angle -30°$
$S_{12} = 0.013\angle 98°$	$0.043\angle 153°$
$S_{22} = 1.01\angle -17°$	$1.05\angle -18°$
$k = -0.09$	-0.83

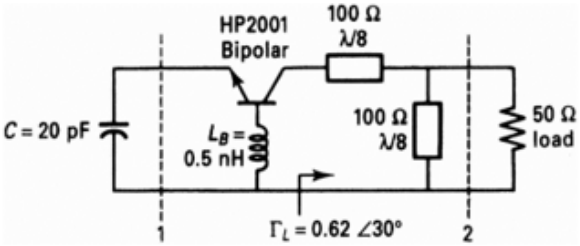

Figure 44: Figure 4-167 Oscillator example at 2 GHz.

Classical Linear Two-Port Oscillator Design

- Another two-port design procedure is to resonate the Γ_G port and calculate $S_{22}^{'}$, until $\left|S_{22}^{'}\right|>1$, than design the load port to satisfy. This design procedure is summarized in Figure 4-168

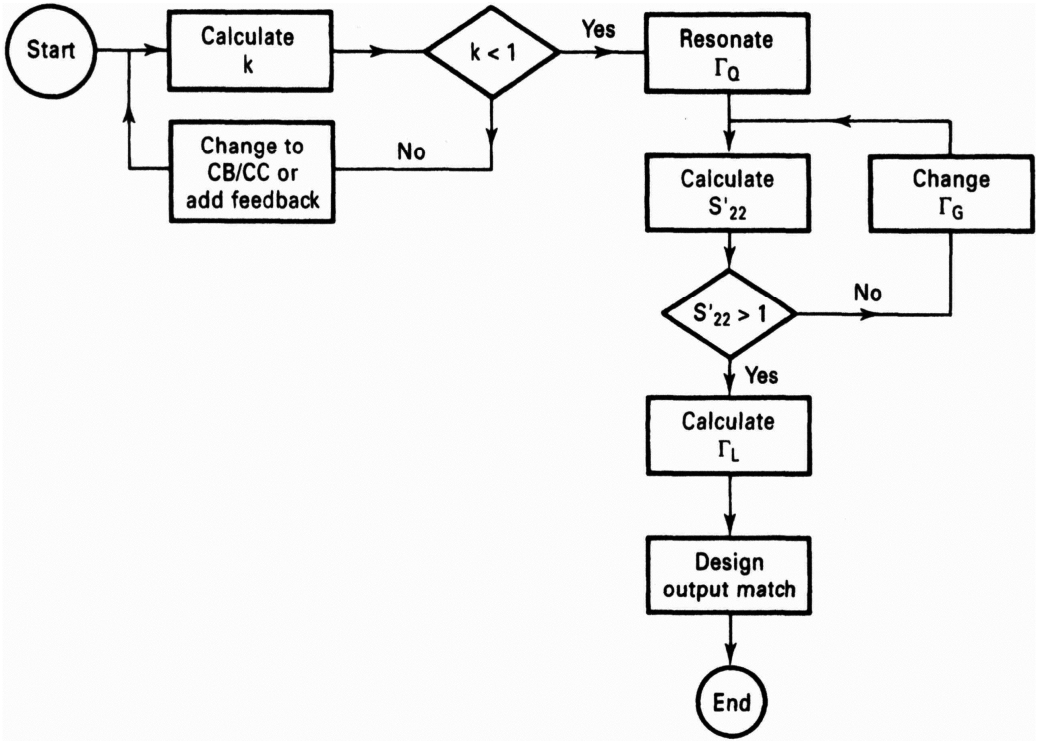

Figure 4-168 Oscillator design flowchart

Classical Linear Two-Port Oscillator Design

- An example using this procedure at 4 GHz is given in Figure 4-169 using an AT 41400 silicon bipolar chip in the common-base configuration with a convenient value of base and emitter inductance of 0.5 nH. The feedback parameter is the base inductance, which can be varied if needed.

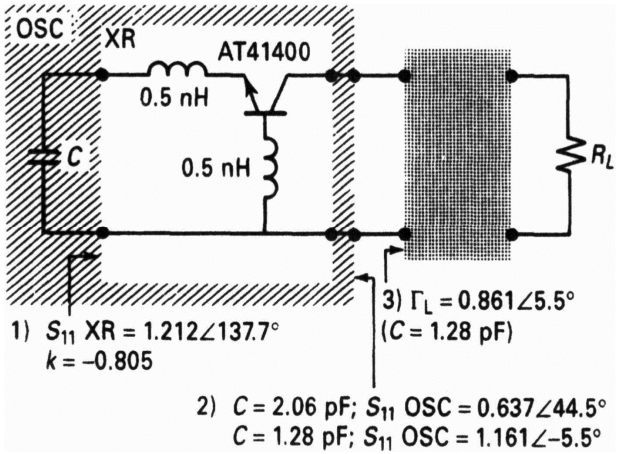

Figure 4-169 A 4-GHz lumped resonator oscillator using AT41400

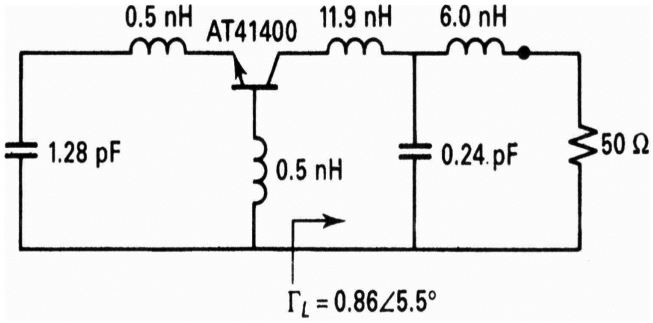

Figure 4-170 Completed lumped resonator oscillator (LRO).

Classical Linear Two-Port Oscillator Design

- Another Example: DRO stabilized Oscillator

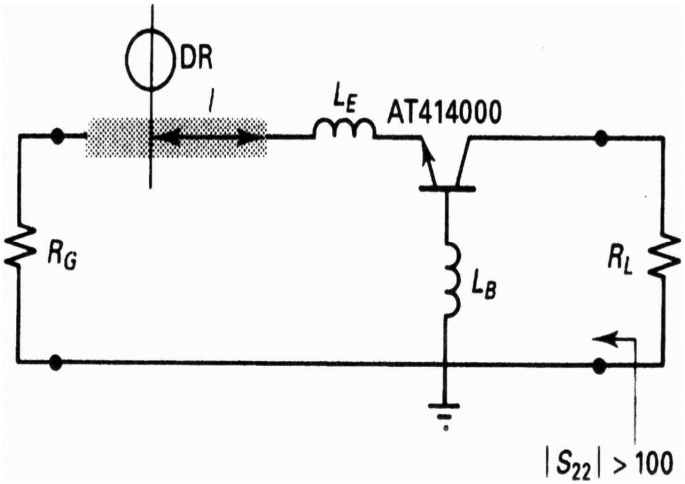

Figure 4-171 Transmission line oscillator with dielectric resonator.

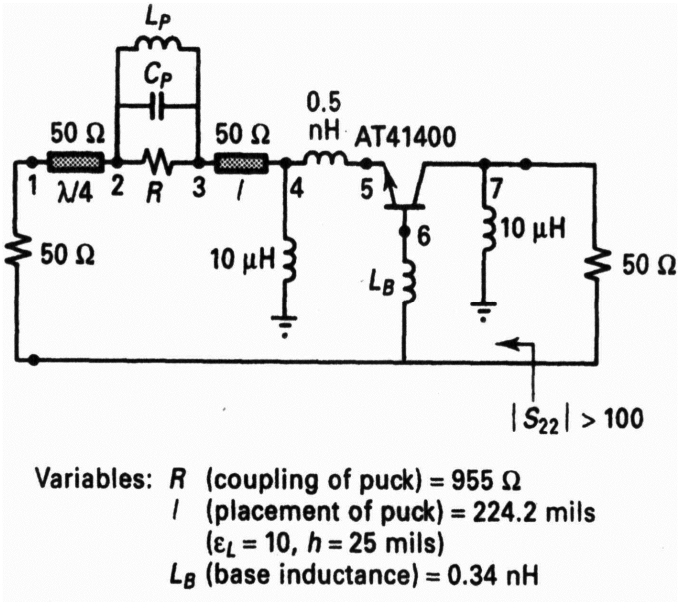

Figure 4-172 Equivalent circuit for dielectric resonator oscillator (DRO).

Classical Linear Two-Port Oscillator Design

- Some practical hints
- For simple oscillators with no isolating stage, one can expect a certain amount of pulling. Figure 4-173 shows the tuning parameters as the load varies from 50 Ω. The load $C_L = R + jX$ influences the required input capacitance C_E and the base inductor L_B. The numbers in the graph are the resonant portion of the load impedance and the ratio X/R determines the Q line. It is obvious that such a circuit is quite interactive. As to the model for the dielectric resonator, the valid relationship is shown in Figure 4-174.

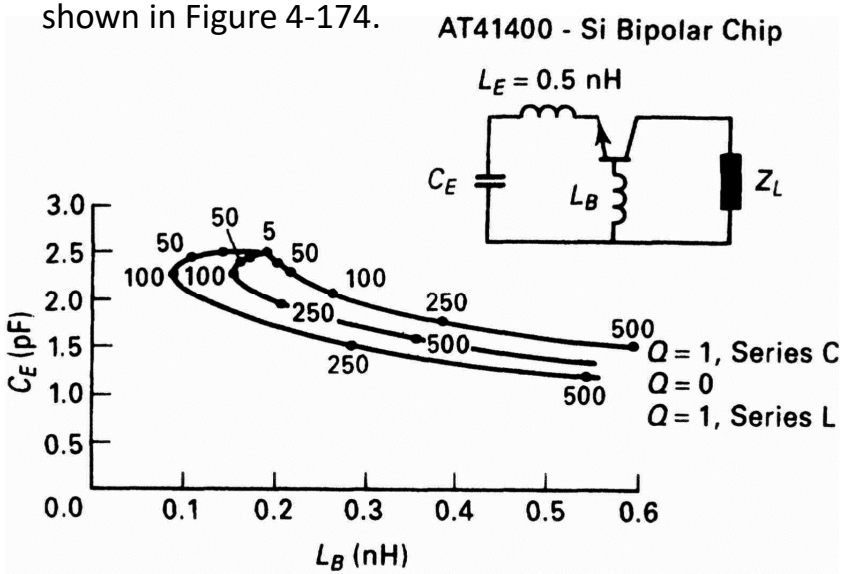

Figure 4-173 Tuning parameters for a 4-GHz oscillator versus load impedance as the load varies from 50 H..

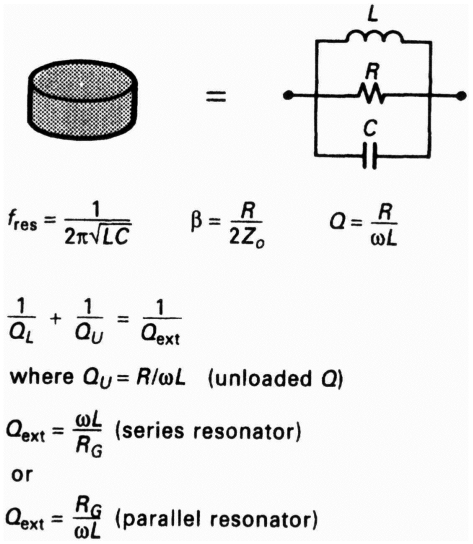

Figure 4-174 Simple equivalent circuit for the dielectric resonator.

Microwave Resonators – SAW Oscillators

- For microwave applications, one is rapidly moving away from lumped to distributed elements. In the previous section, we looked at the case of a transmission line-based oscillator, which by itself has a low Q and was shown only for descriptive and design purposes. In similar fashion, we looked at the simplified description of a dielectric resonator-based oscillator.
- From a practical design point of view, most relevant applications are SAW resonators, dielectric resonators, and YIG oscillators. These are the three types of resonators we will cover in this section.
- **SAW Oscillators**
  - The SAW oscillator has an equivalent circuit similar to a crystal but should be enhanced by adding the appropriate capacitance to ground. Figure 4-175 shows this. SAW oscillators are frequently used in synthesizers and provide a low phase noise, highly stable source, as can be seen in Figure 4-175. The SAW oscillator comes as either a one-port or two-port device.

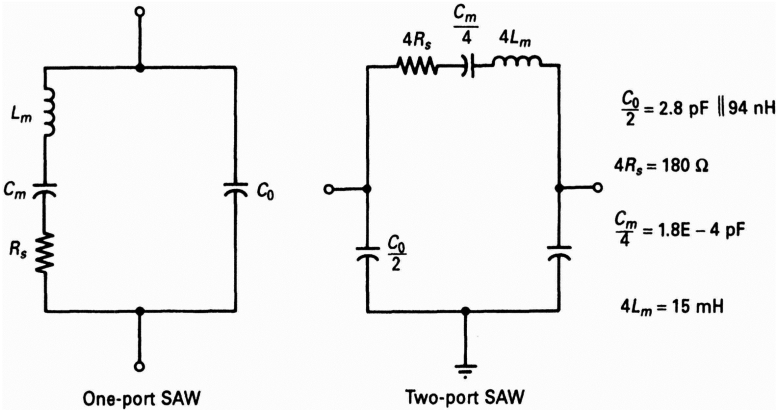

Figure 4-175: Appropriate capacitance to ground for the SAW resonator

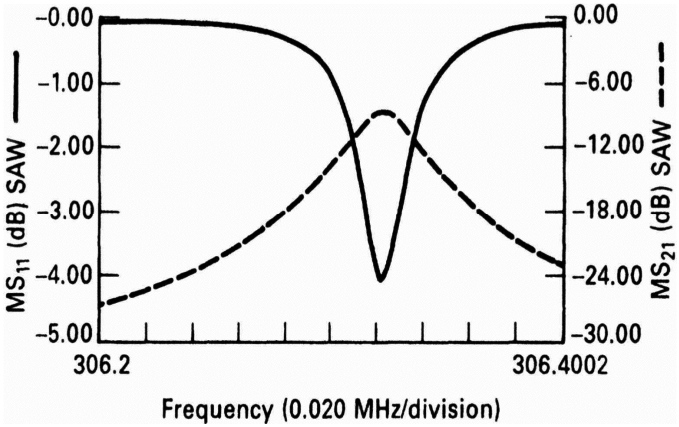

Figure 4-176 Frequency response of a SAW oscillator.

Microwave Resonators – SAW Oscillators

- The SAW resonator has fairly high insertion loss, as can be seen from Figure 4-176 (previous slide). The actual circuit of a high-performance SAW oscillator, as shown in Figure 4-177, consists of a bipolar transistor with a dc stabilizing circuit, SAW oscillator, and a feedback loop, which allows the phase to be adjusted. The SAW oscillator provides very good phase noise. The measured phase noise of such an oscillator is shown in Figure 4-178. The actual measured phase noise agrees quite well with this prediction

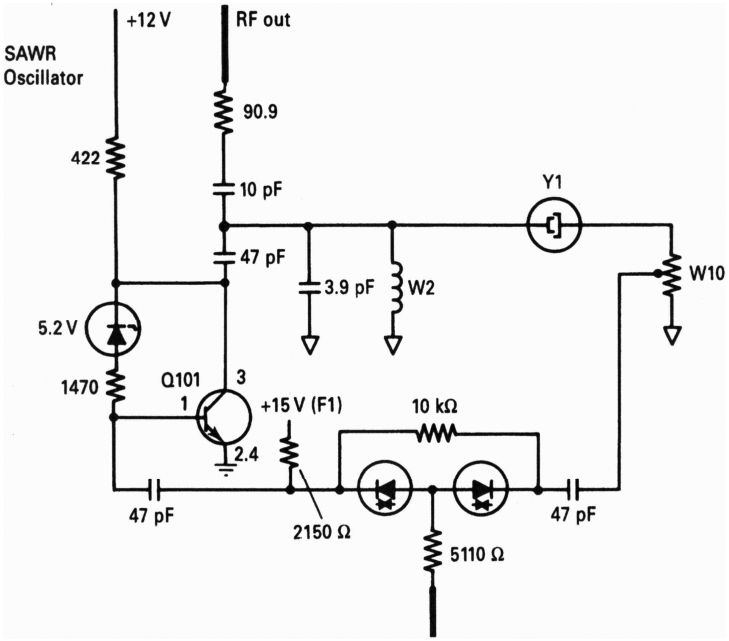

Figure 4-177 Schematic of a SAW oscillator.

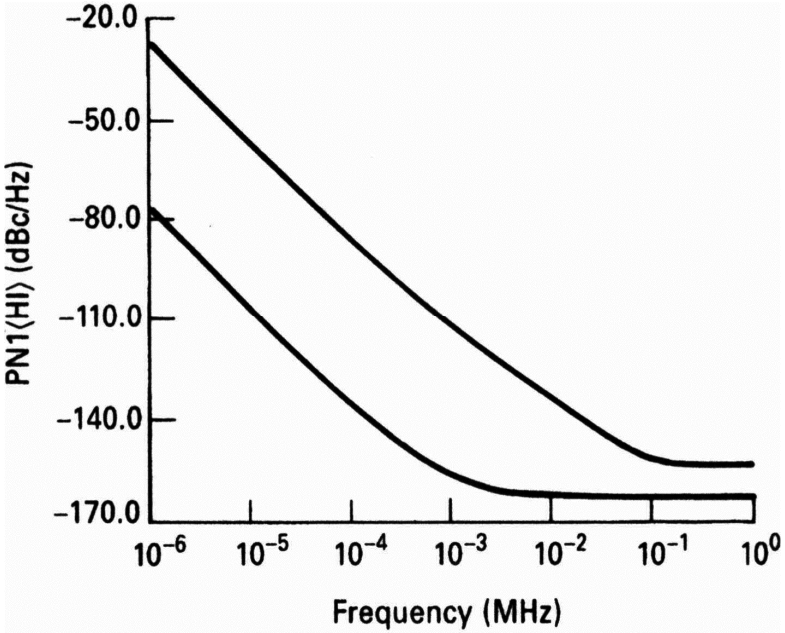

Figure 4-178 Phase noise as determined by the initial start-up values and after optimization.

Microwave Resonators – DRO – Dielectric Resonators Oscillators

- In designing dielectric resonator-based oscillators, several methods of frequency stabilization are available that have been proposed by various authors. Figure 4-179 shows some recommended methods of frequency stabilization for dielectric resonator oscillators. The dielectric resonator consists of some high dielectric material coupled to a transmission line or microstrip structure.

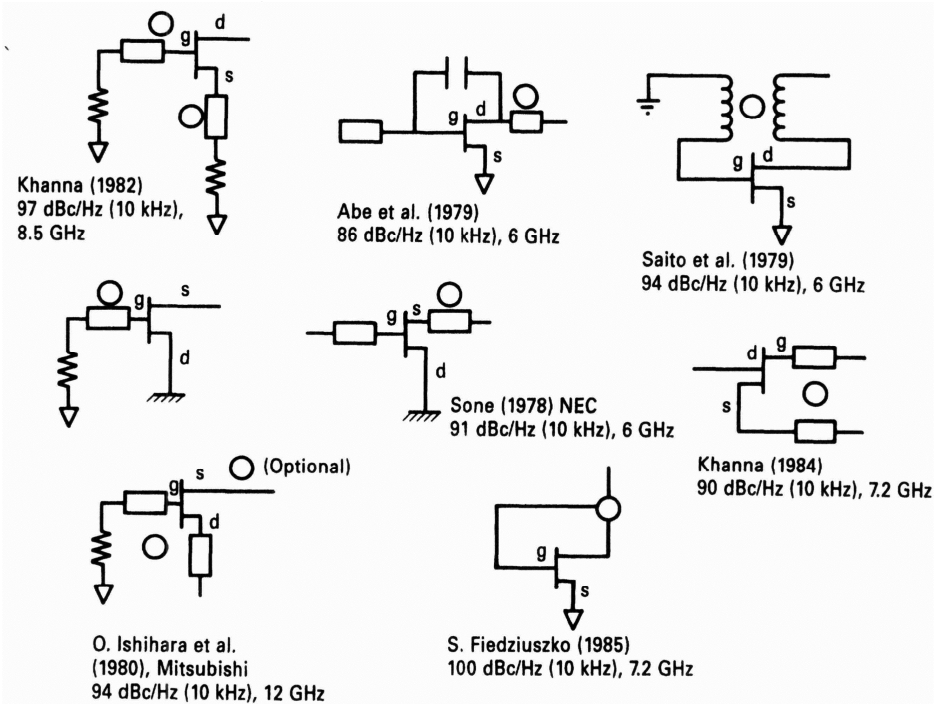

Figure 4-179 Recommended methods of frequency stabilization for DROs

Microwave Resonators – DRO – Dielectric Resonators Oscillators

- Figure 4-180 shows the field distribution and interaction between the microstrip and the dielectric resonator. The two resulting applications, BandStop and BandPass filters, are displayed. Modeling this type of resonator is done by describing the resonator in the form of its physical dimensions.

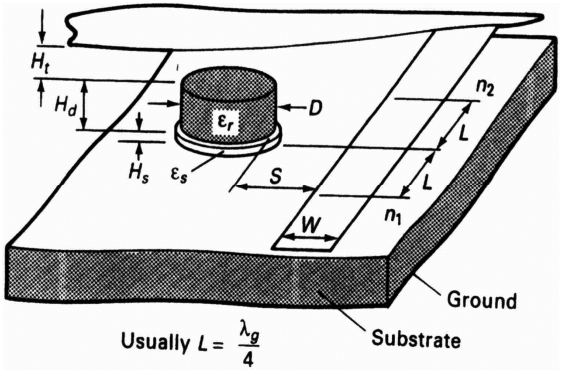

Figure 4-180a DRO on microstrip as BandStop filter.

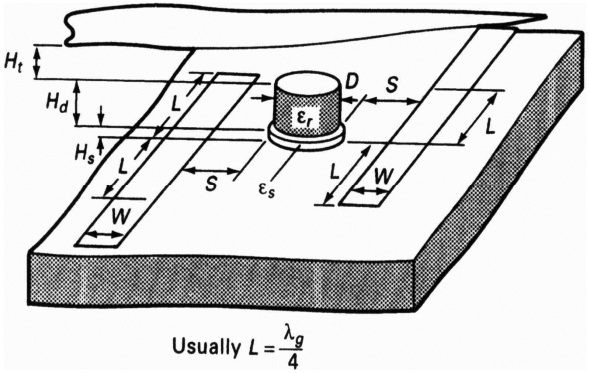

Figure 4-180b DRO on microstrip as BandPass filter..

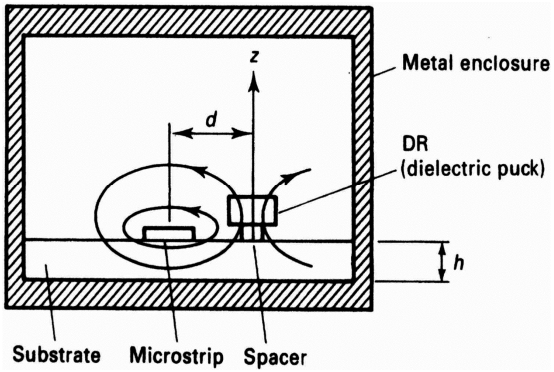

Figure 4-180c Field distribution and interaction between the microstrip and the DRO..

Microwave Resonators – DRO – Dielectric Resonators Oscillators

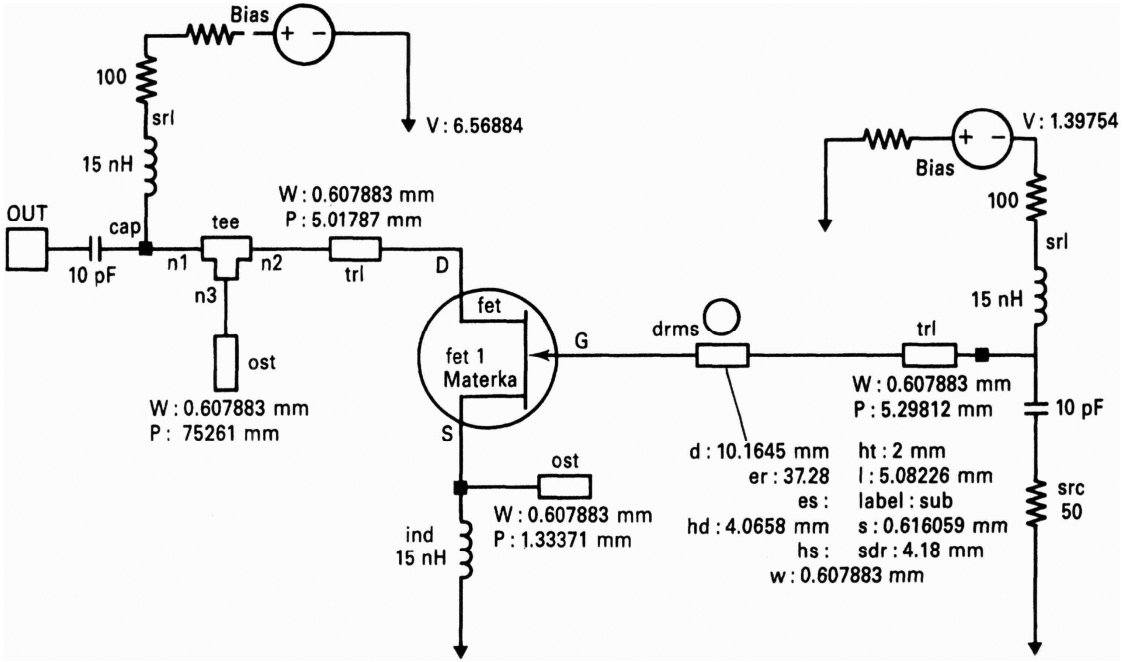

Figure 4-181 Schematic of 6-GHz DRO.

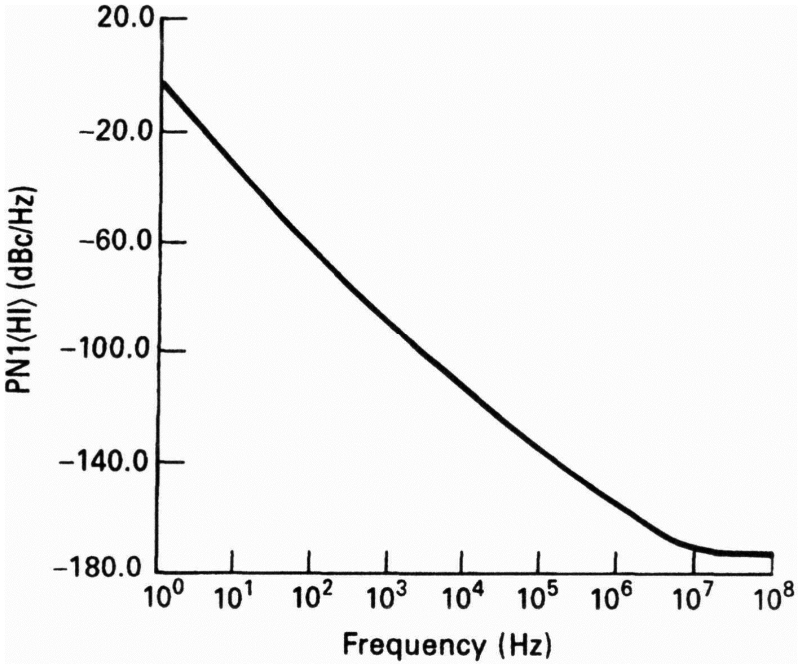

Figure 4-182 Predicted phase noise of the 6-GHz DRO pictured in Figure 4-181.

Microwave Resonators – YIG Oscillators

- For wideband electrically tunable oscillators, we use either a YIG or a varactor resonator. The YIG resonator is a high-Q, ferrite sphere of yttrium ion garnet, Y2Fe2 (FeO4)3, that can be tuned over a wide band by varying the biasing dc magnetic field. Its high performance and convenient size for applications in microwave integrated circuits make it an excellent choice in a large number of applications, such as filters, multipliers, discriminators, limiters, and oscillators. A YIG resonator makes use of the ferrimagnetic resonance, which, depending on the material composition, size, and applied field, can be achieved from 500 MHz to 50 GHz. An unloaded Q greater than 1000 is usually achieved with typical YIG material.
- Figure 4-185 shows the mechanical drawing of a YIG oscillator assembly. The drawing is somewhat simplified and the actual construction is actually more difficult to do. Its actual circuit diagram is shown in Figure 4-186.

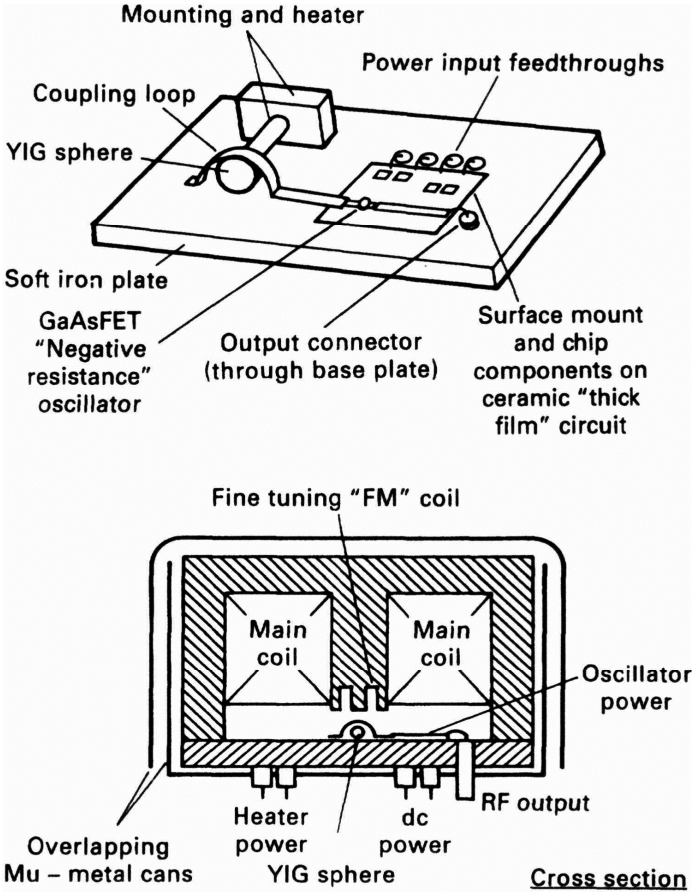

Figure 4-185: The yttrium–iron–garnet (YIG) sphere serves as the resonator in the sweep oscillators used in many spectrum analyzers.

Microwave Resonators – YIG Oscillators

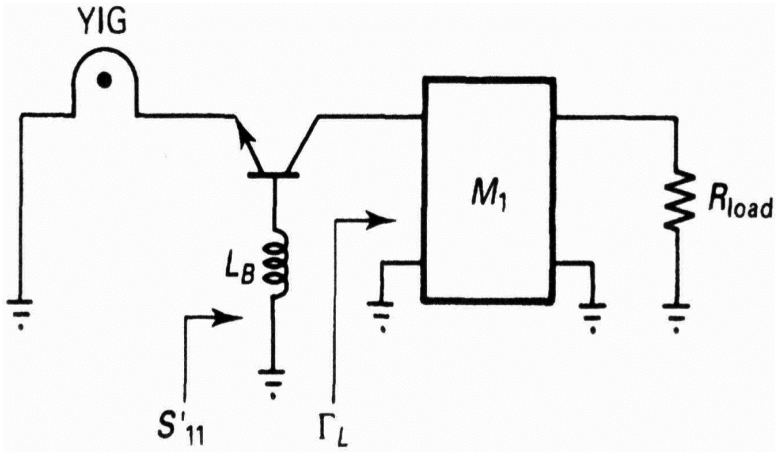

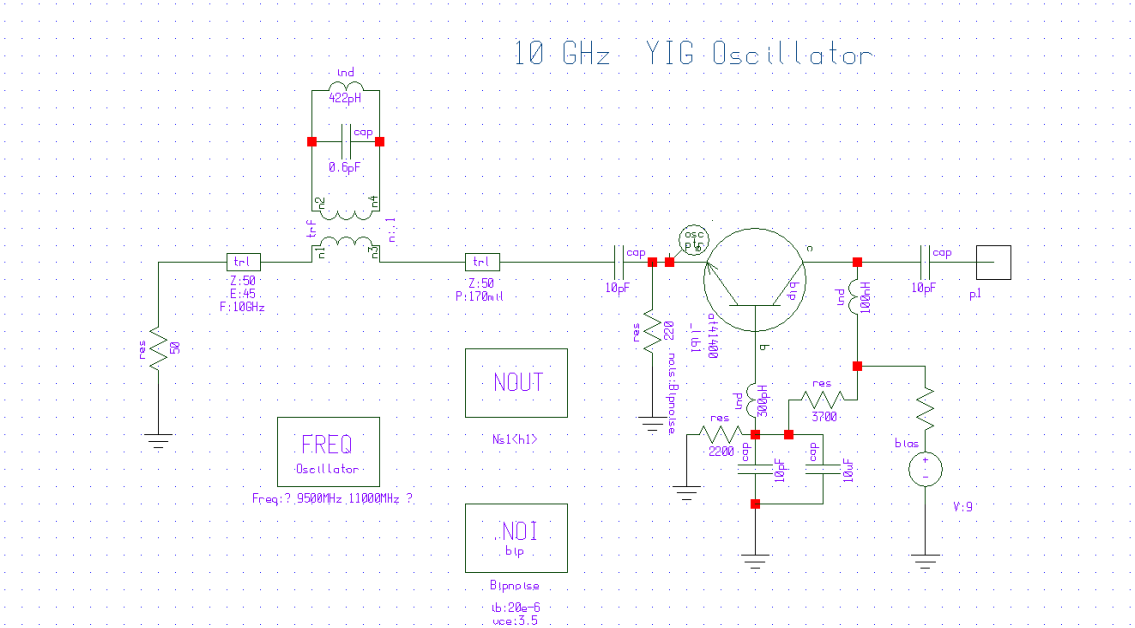

Figure 4-186: Actual circuit diagram for YIG-tuned oscillator depicted in Figure 4-185.

Tuning Diode based Resonators

- The dual of the current-tuned YIG resonator is the voltage-tuned varactor, which is a variable reactance achieved from a low-loss, reverse-biased semiconductor PN junction.
- These diodes are designed to have very low loss and therefore high Q.
- The silicon varactors have the fastest settling time in fast-tuning applications, but the gallium arsenide varactors have higher Q values. The cutoff frequency of the varactor is defined as the frequency where $Q_v = 1$
- . For a simple series RC equivalent circuit, we have

$$Q_v = \frac{1}{\omega R C_v} \qquad (4\text{-}226)$$

$$f_{c0} = \frac{1}{2\pi R C_v} \qquad (4\text{-}227)$$

The tuning range of the varactor will be determined by the capacitance ratio C_{max}/C_{min}, which can be 12 or higher for hyper-abrupt varactors. Since R is a function of bias, the maximum cutoff frequency occurs at a bias near breakdown, where both R and C_v have minimum values. Tuning diodes or GaAs varactors for microwave and millimeter-wave applications are frequently obtained by using a GaAs FET and connecting source and drain together.

Tuning Diode based Resonators

- Figure 4-187 shows the dynamic capacitance and dynamic resistors as a function of tuning voltage. In using a transistor instead of a diode, the parameters become more complicated. Figure 4-188 shows the capacitance, equivalent resistor, and Q, as well as the magnitude of S_{11}, as a function of reverse voltage. This is due to the breakdown effects of the GaAs FET.

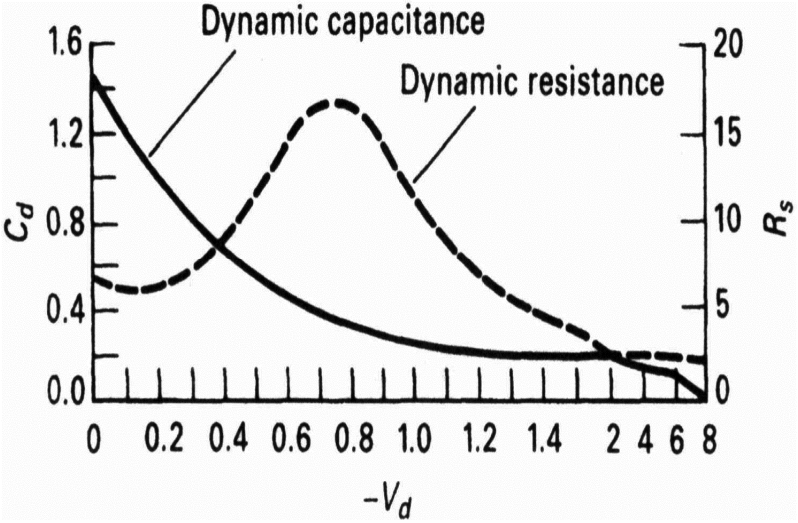

Figure 4-187 Dynamic capacitance and dynamic resistors as a function of tuning voltage for GaAs varactor.

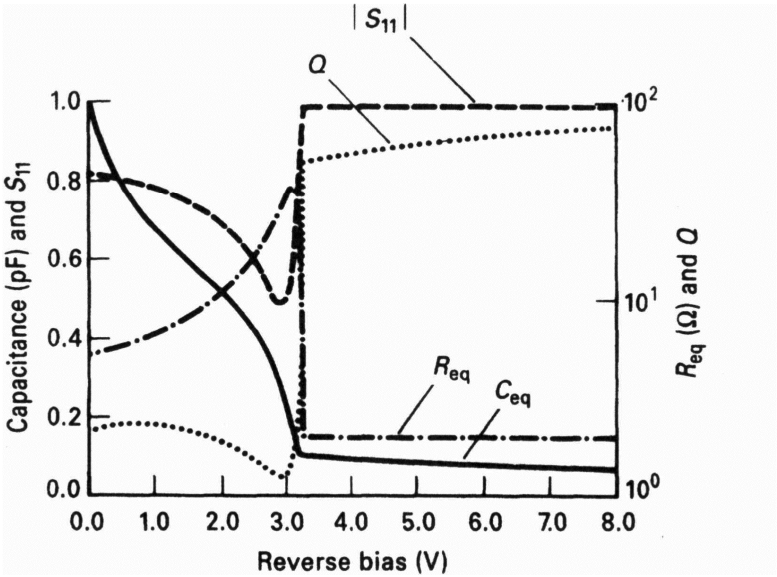

Figure 4-188 Varactor parameters: capacitance, equivalent resistor, and Q, as well as the magnitude of S11, as a function of reverse voltage.

Ceramic Resonators

- An important application for a new class of resonators called ceramic resonators (CRs) has emerged for wireless applications. The CRs are similar to shielded coaxial cable, where the center controller is connected at the end to the outside of the cable.
- These resonators are generally operating in quarter-wavelength mode and their characteristic impedance is approximately 10 Ω.
- Because their coaxial assemblies are made for a high-ε low-loss material with good silver plating throughout, the electromagnetic field is internally contained and therefore provides very little radiation.
- These resonators are therefore ideally suited for high-Q, high-density oscillators.
- The typical application for this resonator is VCOs ranging from not much more than 200 MHz up to about 3 or 4 GHz. At these high frequencies, the mechanical dimensions of the resonator become too tiny to offer any advantage.
- One of the principal requirements is that the physical length is considerably larger than the diameter. If the frequency increases, this can no longer be maintained.

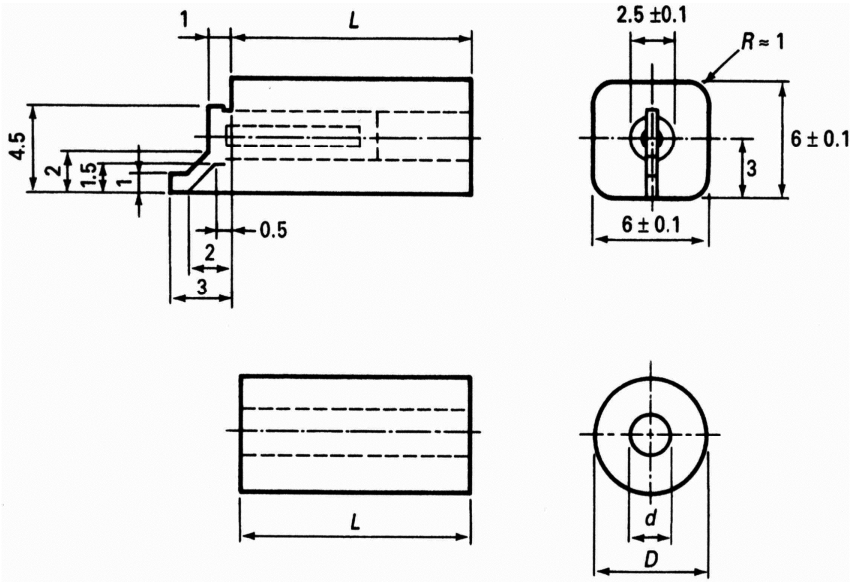

CR with Standard round/square packaging

Calculation of an Equivalent Circuit of the Ceramic Resonator

- The equivalent parallel-resonant circuit has a resistance at resonant frequency of:

$$R_p = \frac{2(Z_0)^2}{R^* l}$$

where Z_0 = characteristic impedance of the resonator
l = mechanical length of the resonator
R^* = equivalent resistor due to metalization and other losses

- As an example, one can calculate:

$$C^* = \frac{2\pi\varepsilon_0\varepsilon_r}{\log_e(D/d)} = 55.61\times10^{-12}\frac{\varepsilon_r}{\log_e(D/d)} \quad \text{and} \quad L^* = \frac{\mu_r\mu_0}{2\pi} = \log_e\left(\frac{D}{d}\right) = 2\times10^{-7}\log_e\left(\frac{D}{d}\right)$$

$$Z_0 = 60\ \Omega\frac{1}{\sqrt{\varepsilon_r}}\log_e\left(\frac{D}{d}\right)$$

- A practical example for $\varepsilon_r = 88$ and 450 MHz is:

$$C_p = \frac{C^* l}{2} = 49.7\ \text{pF} \qquad L_p = 8L^* l = 2.52\ \text{nH} \qquad R_p = 2.5\ \text{k}\Omega$$

Ceramic Resonators – some practical values

- The available material has a dielectric constant of 88 and is recommended for use in the 400- to 1500-MHz range.
- The next higher frequency range (800 MHz to 2.5 GHz) uses ε of 38, while the top range (1 to 4.5 GHz) uses ε of 21.
- Given the fact that ceramic resonators are prefabricated and have standard outside dimensions, the following quick calculation applies:

Relative dielectric constant of resonator material	$\varepsilon_r = 21$	$\varepsilon_r = 38$	$\varepsilon_r = 88$
Resonator length in millimeters	$l = \frac{16.6}{f}$	$l = \frac{12.6}{f}$	$l = \frac{8.2}{f}$
Temperature coefficient (ppm/°C)	10	6.5	8.5
Available temperature coefficients	–3 to +12	–3 to +12	–3 to +12
Typical resonator Q	800	500	400

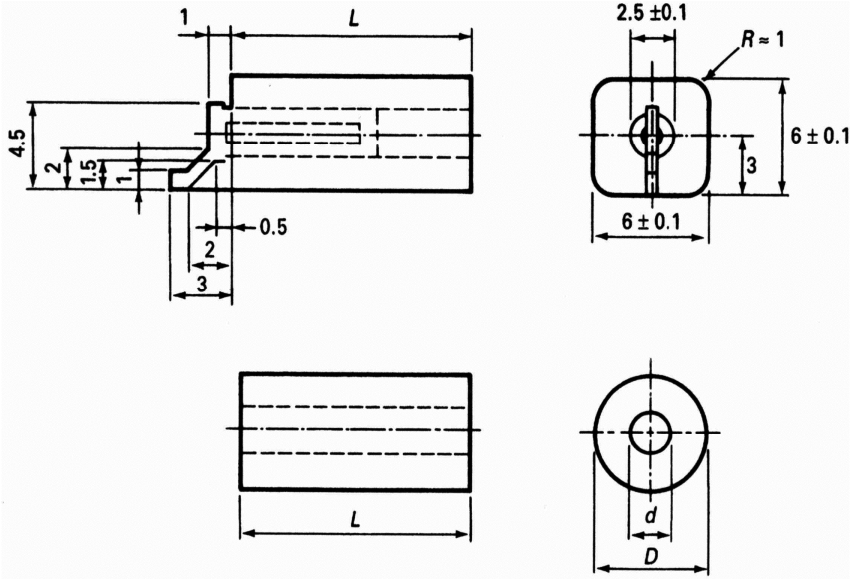

CR with Standard round/square packaging

Oscillators with Ceramic Resonators

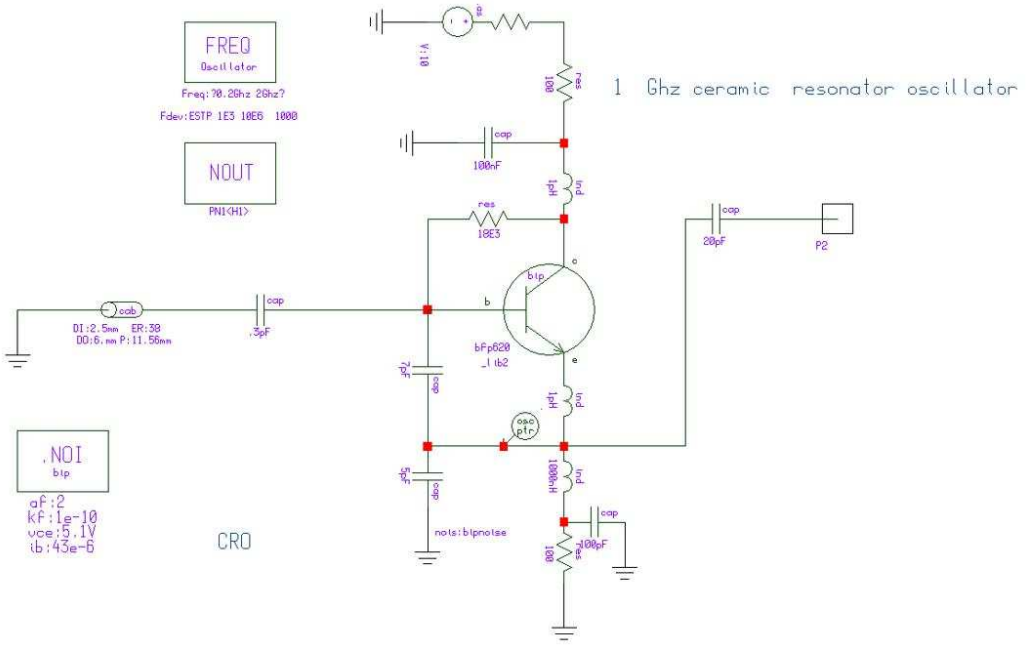

Schematic of a ceramic resonator-based oscillator

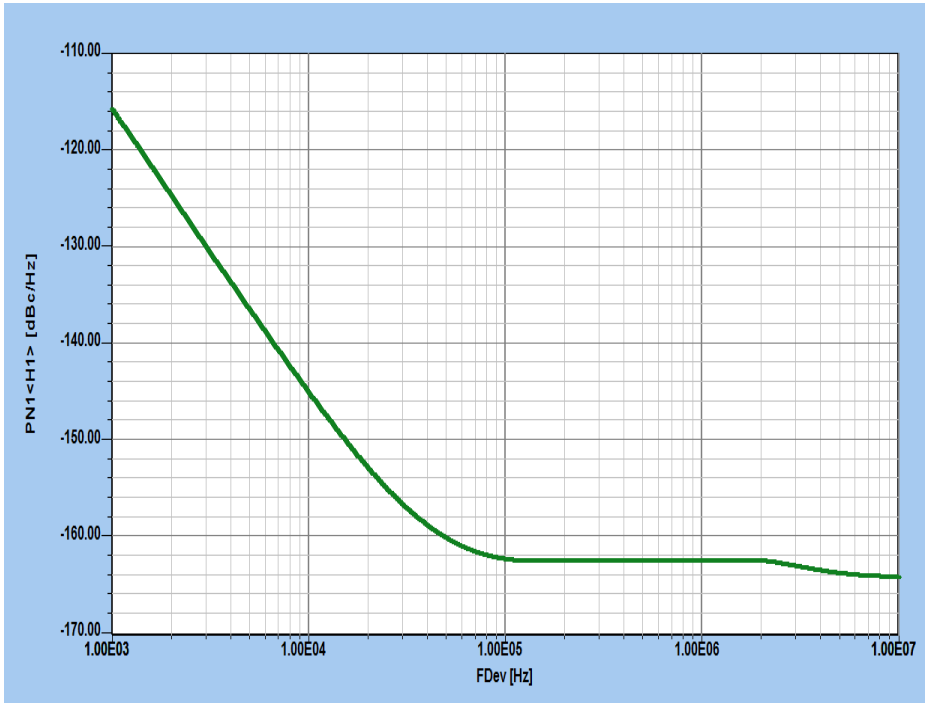

Simulated phase noise of an NPN bipolar 1-GHz ceramic resonator-based oscillator

Oscillators with Ceramic Resonators – an Example

- By using ceramic-resonator-based oscillators in conjunction with miniature synthesizer chips, it is possible to build extremely small phase-locked loop systems for cellular telephone operation.
- This figure shows one of the smallest available PLL-based synthesizers manufactured by Synergy Microwave Corporation.
- Because of the high-Q resonator, these types of oscillators exhibit extremely low phase noise.
- Values of better than 150 dB/Hz, 1 MHz off the carrier, are achievable.
- The ceramic resonator reduces the sensitivity toward microphonic effects and proximity effects caused by other components.

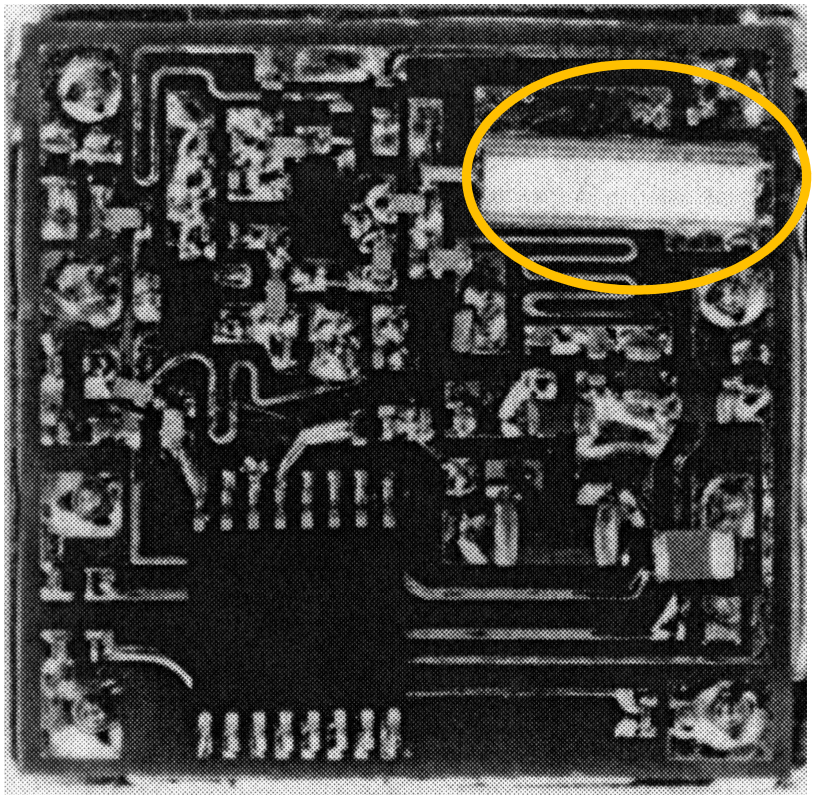

Looking at the resonator of the oscillator

A Novel Tunable Active Spiral Inductor

- All oscillators including the Colpitts Oscillator need both capacitor and inductor and they need to be in resonance at the desired frequency.
- So far we have made no comments about the inductor, but showed some resonators like the ceramic resonators (quarter wave resonator) or DRO (dielectric resonator based oscillator) but in most cases the inductor is a discrete element.
- For the use on printed circuits or in integrated circuits, the inductors are typically rectangular wound devices, as shown in the figure at the right: **(A typical sketch of spiral inductor)**
- The sketch of the spiral inductor shows the mechanical assembly.
- One of the tricks is to connect the input and output of the inductor, for the inner connection, an air-bridge is not uncommon. Of course it adds to the inductor value.
- The real electrical values depend upon the substrate and other manufacturing methods.
- The second figure shows a detailed lumped model of a spiral inductor.

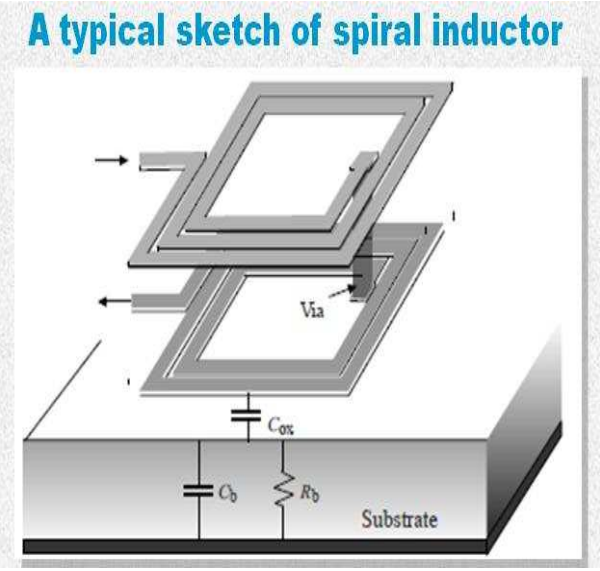

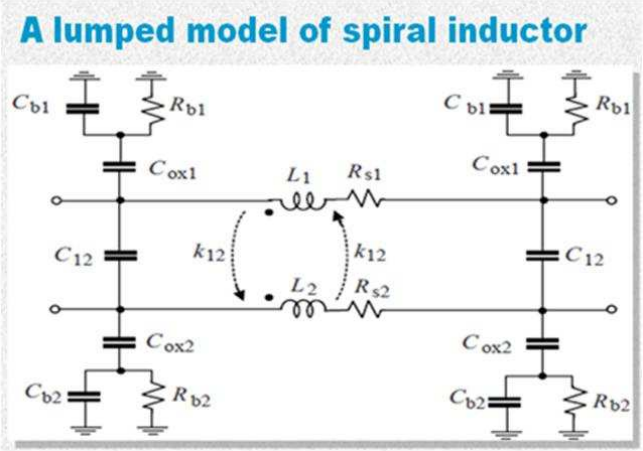

Simulating an Active Spiral Inductor

- Modern simulation tools are able to deliver very good results macthing niceley with mesured values.
- However, the physical size of the chip inductor requires a large die area, thus not a cost-effective solution.

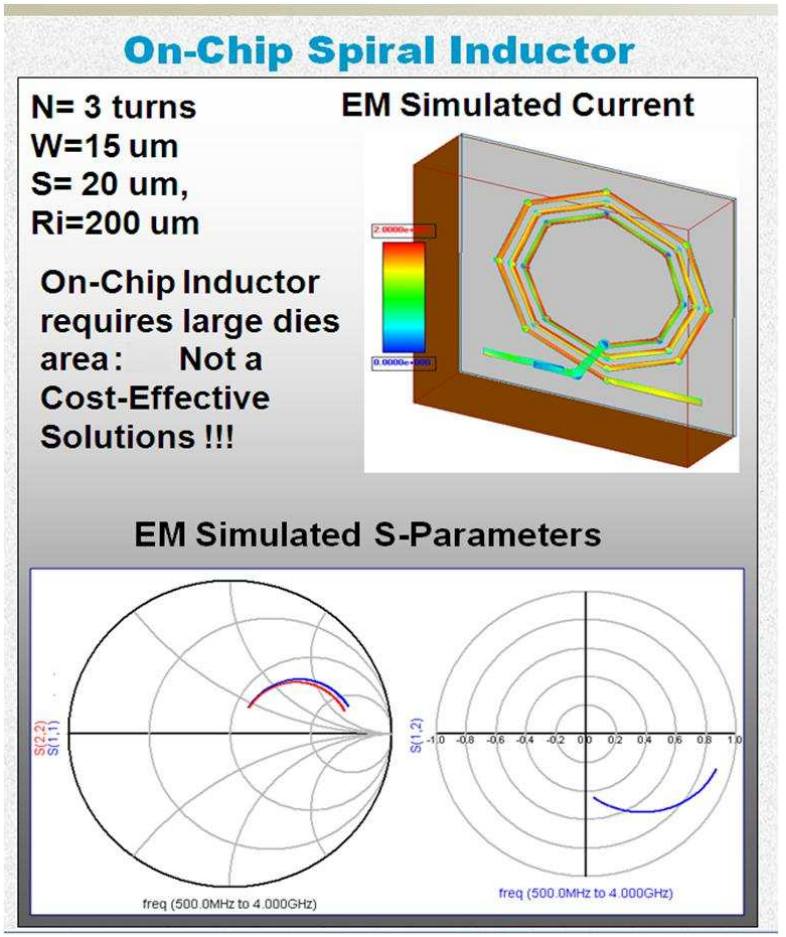

Introducing the Gyrator

- B. D. H. Tellegen of Philips Research Laboratory proposed a new 2-port network element, a Gyrator in 1948, which exhibits an immittance conversion property, needed to generate an synthesized active inductor using transistors.

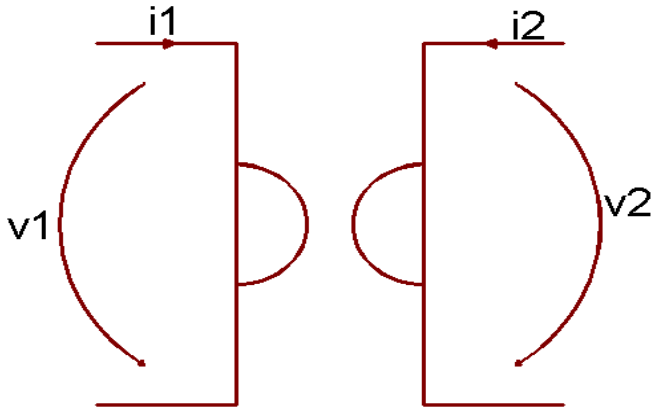

$$\begin{bmatrix} i_1 \\ i_2 \end{bmatrix} = \begin{bmatrix} 0 & g \\ -g & 0 \end{bmatrix} \begin{bmatrix} v_1 \\ v_2 \end{bmatrix}$$

where ‘g’ is called gyration capacitance.

- An admittance Y connected to the secondary terminals is converted to its dual g2/Y, this phenomena is called immittance conversion, C transforms into L, parallel tuned circuit into series tuned circuit
- We have just seen that the inductor requires a lot of space and is difficult to build. So if we resort to the gyrator, invented by a researcher of Phillips Research Lab, in 1948, we can electronically transform a capacitor into an inductor.
- However, we need to ask the question immediately, how about the dynamic range under large signal conditions, the noise contribution of the active circuit and the required DC power? We will get to this soon.

The Active Inductor Using a Gyrator

Tunable Active Inductor (TAI)

- ✓ Integrable and Compact
- ✓ Cost-Effective
- ✓ Power-Efficient Solutions

TAI: Design Challenges

- ✓ High Power Consumption
- ✓ Noise Figure & Instability
- ✓ Low Dynamic Ranges

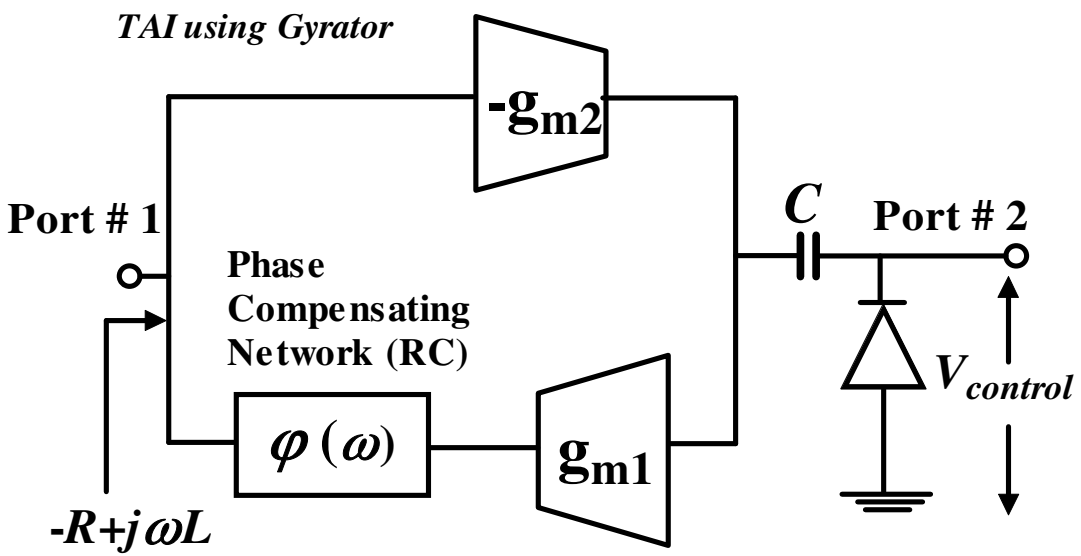

- Phase shift network φ(ω) is required in TAI topology for suppressing the higher order modes and self-oscillation

SYNTHESIZED INDUCTOR BEHAVIOUR

- The impedance plot reveals the inductive behavior of the circuit from 600MHz to 30GHz.
- Care must be taken to avoid the encircling and crossing at 4.3GHz, which limits the applications.
- In the case of a mathematics based time domain related prediction in the nonlinear oscillator system the use of Bessel function is helpful.

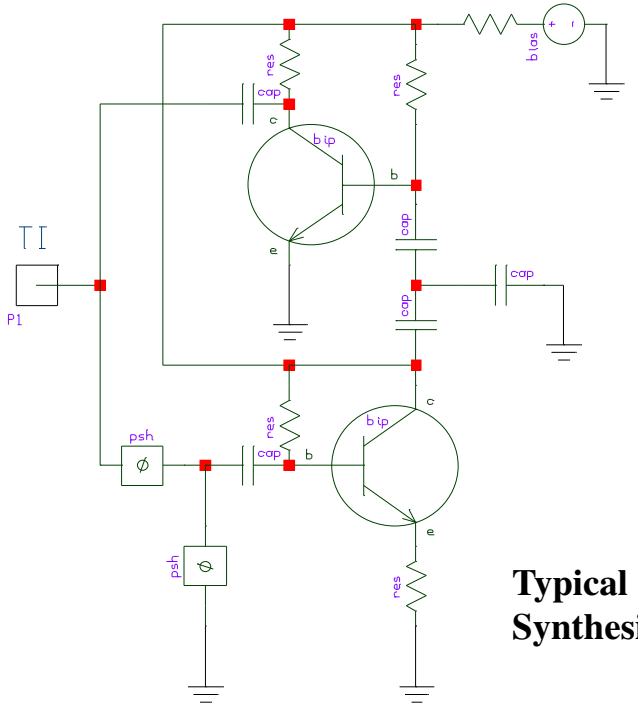

Typical Schematic of a Synthesized Inductor

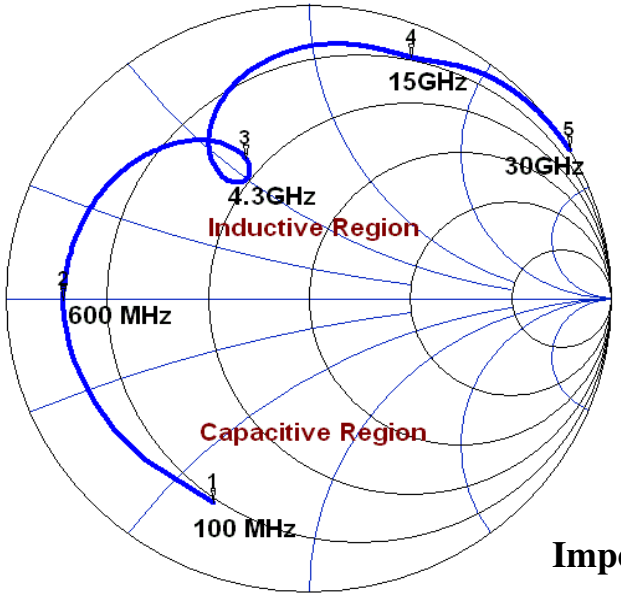

Impedance Plot

LAYOUT OF an OSCILLATOR USING a SPIRAL INDUCTOR

- Why use an Active Inductor instead of a Spiral Inductor?

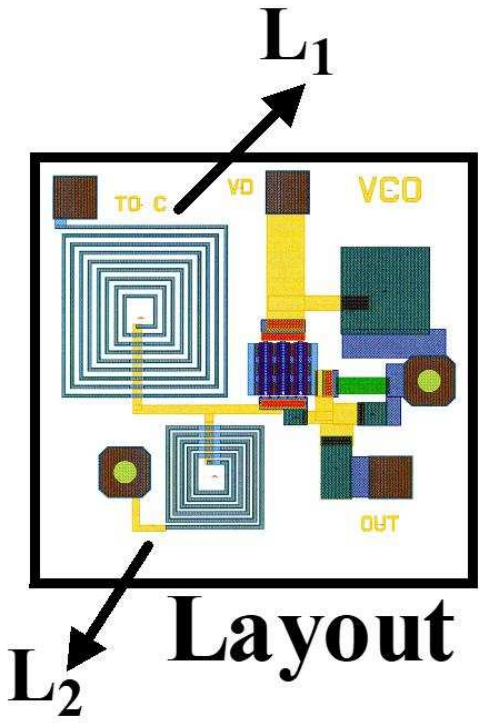

- We avoid the use of on-chip inductors!?

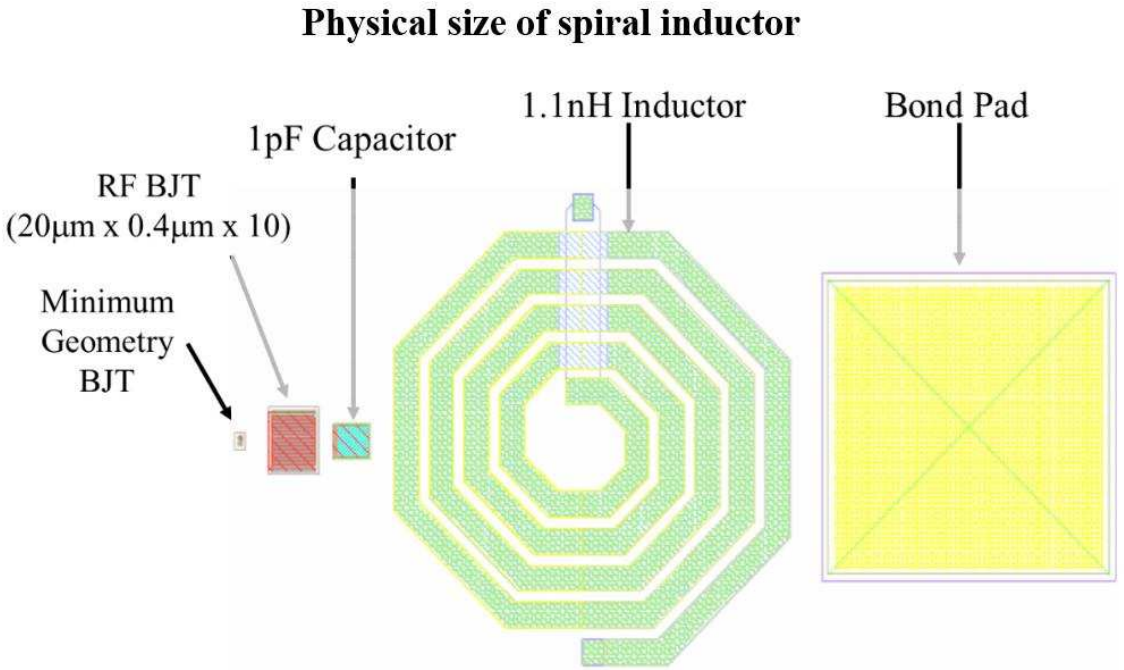

Comparing active Inductors with passive ones

Passive and Active Inductors

Performances	Passive Inductor (Spiral)	Active Inductor (Simulated: Active Device
Q-factor	Low Q: Q-factor can be improved by differential method but added cost	High Q: active inductor offers higher Q than the passive spiral inductor
Tunability	Fixed/Limited	Large tuning range
Die-Area	Large die-area	Small die-area
Power-Consumption	Zero	Significant: consumes power for generating active inductance, resulting to high Q that may offsets the power consumptions
Linearity	Good Linearity	Poor Linearity: driven under large-signal condition, causing shift in operating point, distortions, and impedance fluctuations
Noise	Superior: good phase noise performance	Poor : poor phase noise performance
EMI	Significant: Due to EM coupling in spiral inductors	EMI insensitive
Floor-Planning	Poor: large die- area makes difficult floor-planning	Not required

INTRODUCTION: ACTIVE INDUCTOR OSCILLATOR

- The Figure shows the typical Active Inductor Oscillator (AIO), includes a stable active inductor within a conventional integrated LC oscillator

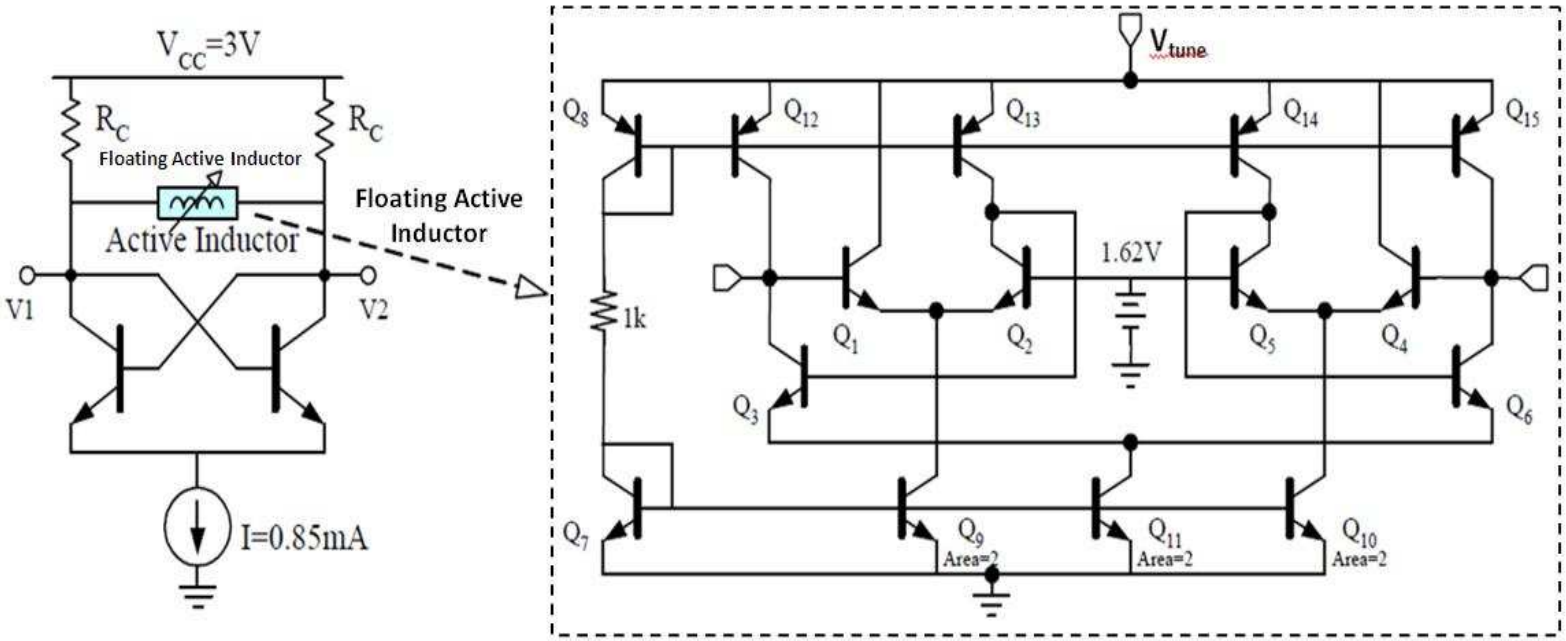

Typical Active Inductor Oscillator (AIO), includes a stable active inductor within a conventional integrated LC oscillator

OSCILLATOR PHASE NOISE BASED ON ACTIVE INDUCTOR

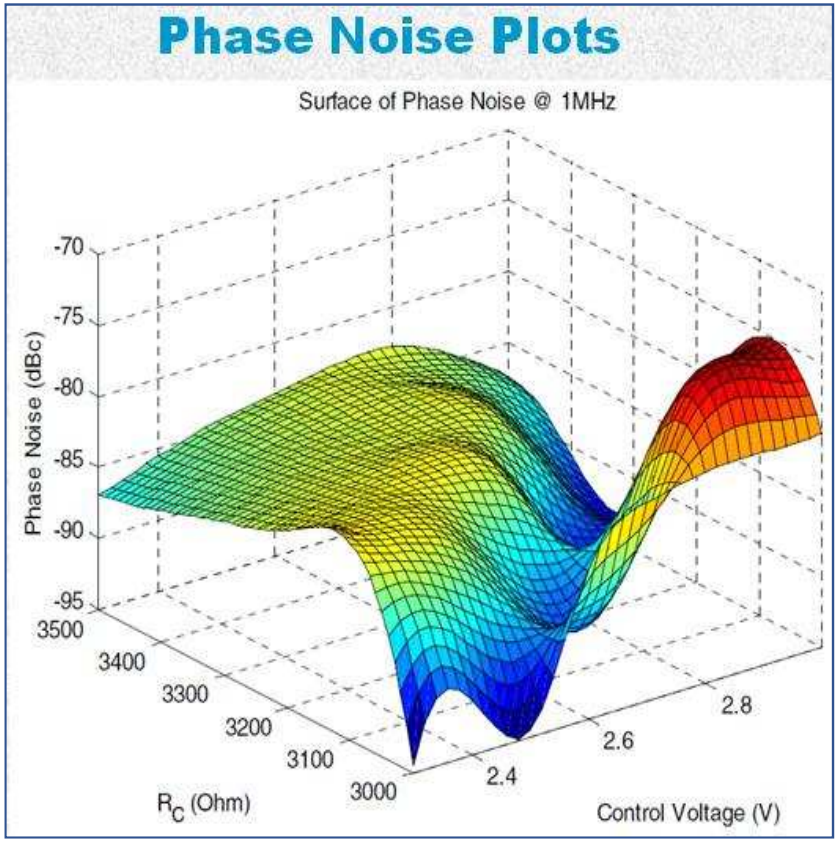

Advantages:

1. Broadband VCO Operation (Tuned L)
2. Multi-Band VCO Operation (Switched L)

Drawbacks:

1. DC Power Consumption
2. Poor Phase Noise Performances
3. Limited Large Signal Performances

SYNTHESIZED INDUCTOR CIRCUITS

- This Figure shows a schematic of a transistorized inductor using SiGe HBT (BFP 620) from Infineon.
- The reason for using a high cut-off frequency (ft=75 GHz) SiGe HBT transistor is to minimize the package parasitic effects and allow comparative evaluations of the 1.9 GHz varactor-tuned and synthesized inductor-tuned LC oscillator using discrete components for experimental validations!

SIMULATED TUNBALE INDUCTOR USING SiGe HBT DEVICE

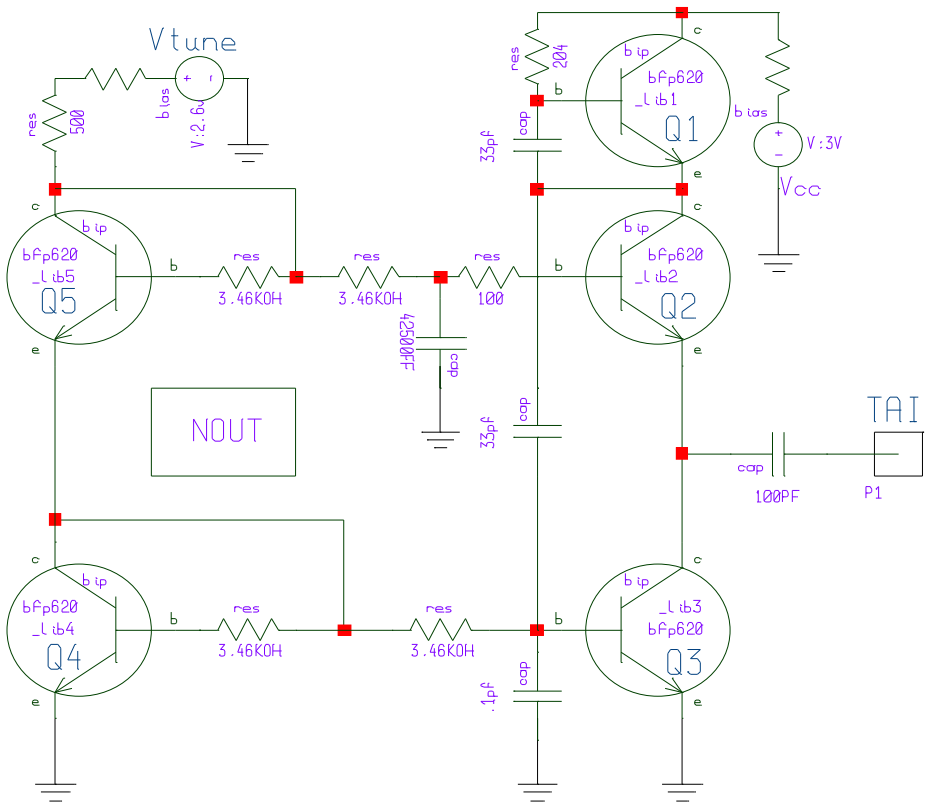

SYNTHESIZED INDUCTOR CIRCUITS

- The graph below shows the typical plot of reactance and equivalent loss resistance of the synthesized inductor using high cut-off frequency (ft=75 GHz) SiGe HBTs.

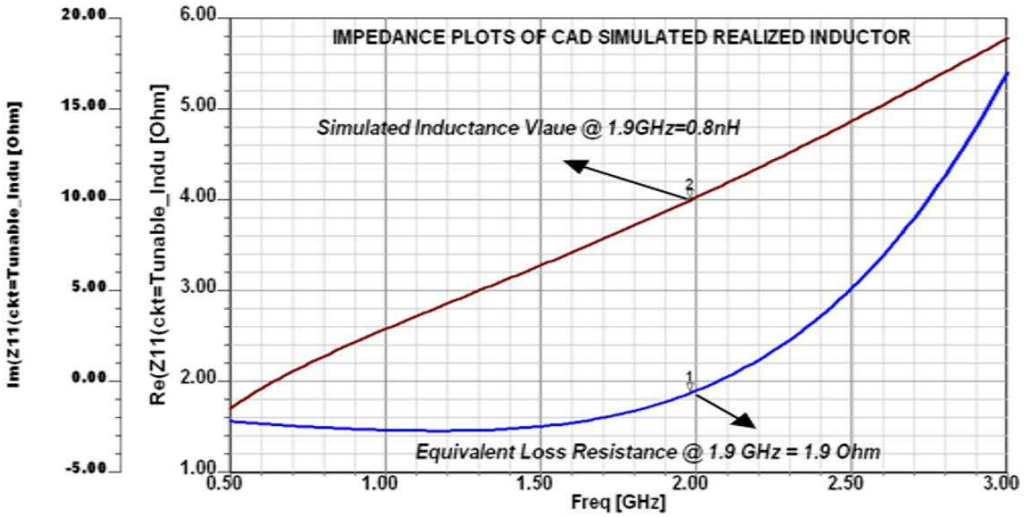

SIMULATED TUNBALE INDUCTOR USING SiGe HBT DEVICE

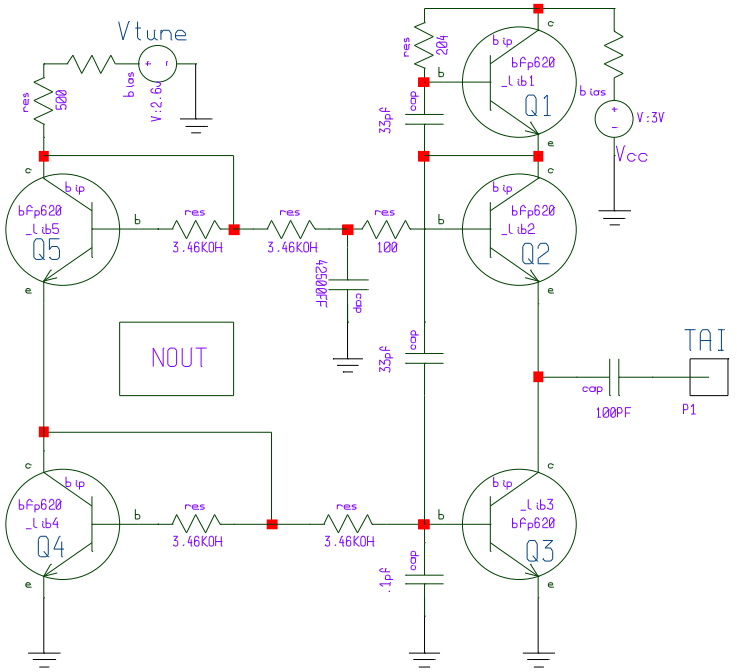

- As shown in the circuit diagram, the value of the realized inductance and associated equivalent loss resistance are 0.8 nH and 1.9 Ω at 1.9 GHz for the operating DC bias condition (3V, 1.8mA) and Vtune (2.5V). The operating DC bias and Vtune are adjusted in such a way that the realized equivalent noise resistance must be positive to avoid the multi-mode oscillations caused by the regenerative effect (if the simulated loss resistance associated with realized inductor has a negative value).

SYNTHESIZED INDUCTOR CIRCUITS

- The graph below shows the comparative phase noise plots for the LC Colpitts oscillator using the lumped LC resonator, the varactor-tuned lumped LC resonator and the synthesized inductor-tuned resonator network for identical inductance value and loss resistance (0.8 nH with series loss resistance 1.9Ω).

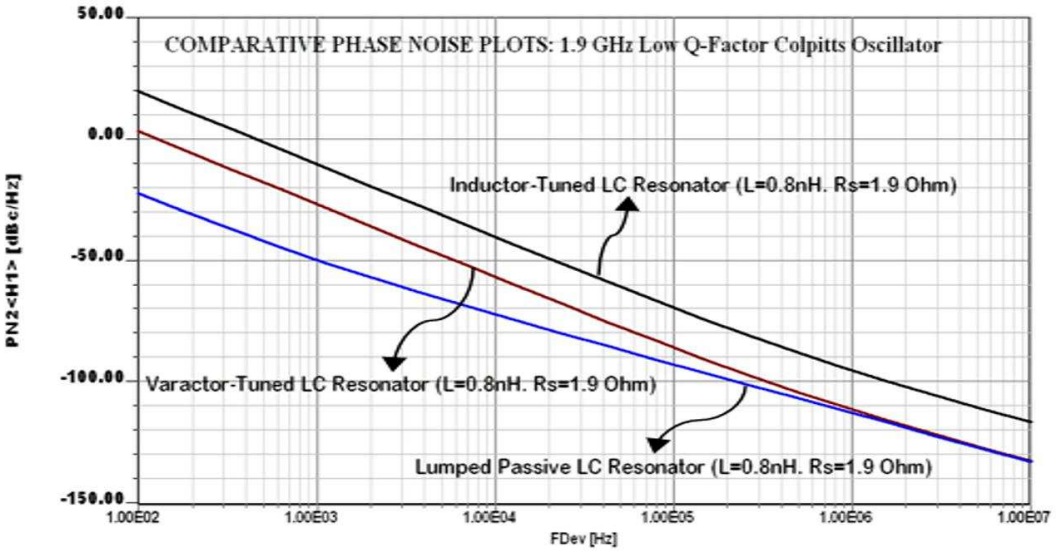

SIMULATED TUNBALE INDUCTOR USING SiGe HBT DEVICE

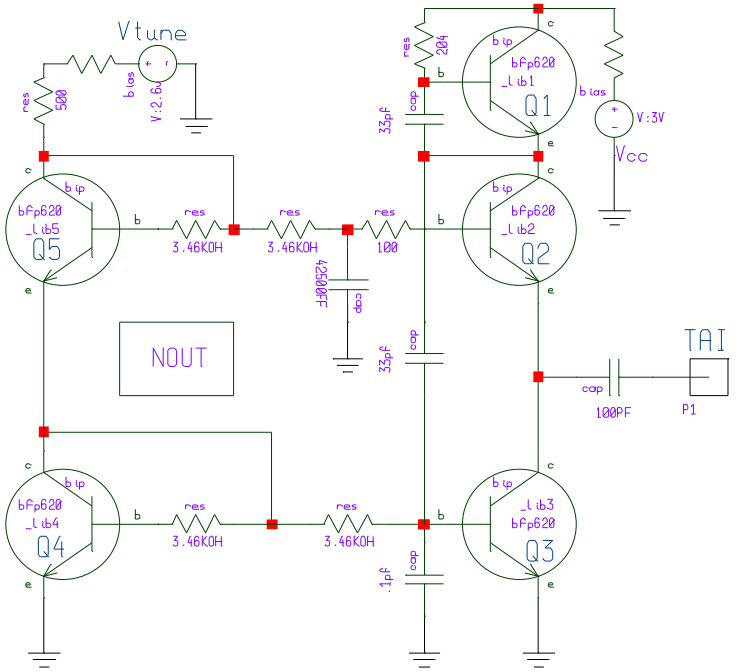

- As shown in the circuit diagram, the value of the realized inductance and associated equivalent loss resistance are 0.8 nH and 1.9 Ω at 1.9 GHz for the operating DC bias condition (3V, 1.8mA) and Vtune (2.5V). The operating DC bias and Vtune are adjusted in such a way that the realized equivalent noise resistance must be positive to avoid the multi-mode oscillations caused by the regenerative effect (if the simulated loss resistance associated with realized inductor has a negative value).

ACTIVE INDUCTOR NOISE

Circuit that transforms a capacitor into an inductor and identifies the noise contribution

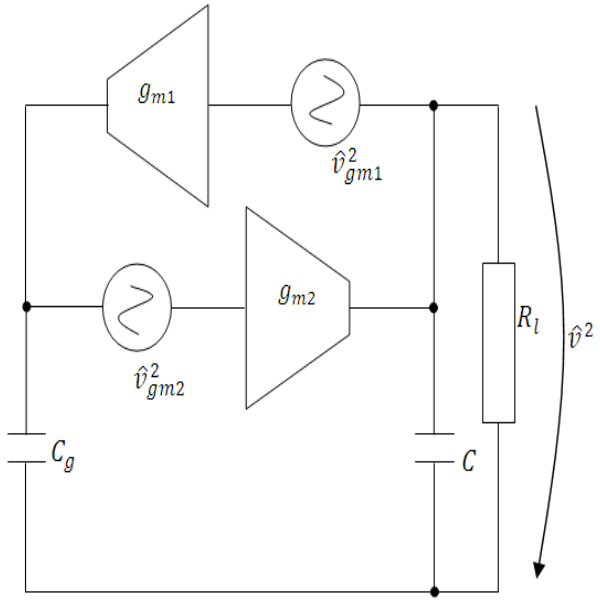

A simplified circuit of active inductor resonator with noise sources

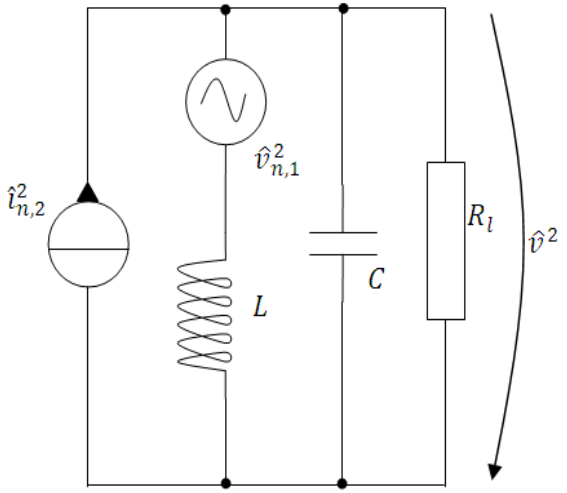

- Vgm1 and Vgm2 are the equivalent noise voltages generated by the transconductances of the Gyrators

ACTIVE INDUCTOR NOISE

- the following applies $\hat{v}_n^2 \cong 4kTr_n|R|, \quad \hat{\imath}_n^2 \cong 4kTg_n|G|$

- where R and G are the negative resistance and conductance values, and the coefficients rn and gn are frequency dependent relative noise resistance and conductance (these give a comparative value of how much noise the active negative resistor produces compared to a passive resistor of the same value).
- The total noise spectral density in voltage squared, of the active inductor resonator is

$$\hat{v}^2 = \frac{\hat{v}_{gm1}^2 + \hat{v}_{gm2}^2 g_{m2}^2 \omega^2 L^2}{\omega^2 L^2 G_l^2 + (\omega^2 LC - 1)^2} \Longrightarrow \hat{v}^2|_{\omega \to \omega_0} = Q_l^2\left(\hat{v}_{gm1}^2 + g_{m2}^2 \hat{v}_{gm2}^2 \omega^2 L^2\right) = 4kT\lambda Q_l^2\left(\frac{1}{g_{m1}} + \frac{g_{m2}}{\omega_0^2 C^2}\right)$$

- The time average Q-factor of active inductor is $\dfrac{\omega_0(1+r_n,g_n)}{\lambda g_{m2}\left(\frac{1}{C}+\frac{1}{C_g}\right)}$

- he time average normalized noise power of an active inductor resonator can be determined by:

$$\overline{v^2} = \int_0^\infty \hat{v}^2 df = \frac{\hat{v}_{gm1}^2}{2\pi}\omega_o \int_0^\infty \frac{d\omega}{[(\omega^2 LC-1)^2 + \omega^2 L^2 G_l^2]} + \frac{\hat{g}_{gm2}^2 \hat{v}_{gm2}^2}{2\pi} \int_0^\infty \frac{\omega^2 L^2 d\omega}{[(\omega^2 LC-1)^2 + \omega^2 L^2 G_l^2]}$$

$$\overline{v^2} \approx \frac{kT\lambda}{C} Q_l \left(\frac{g_{m2}}{g_{m1}}\right)^{1/2}\left[\left(\frac{C_g}{C}\right)^{1/2} + \left(\frac{C}{C_g}\right)^{1/2}\right] = \frac{kT\lambda}{C} Q_l \frac{\omega_o}{g_{m1}}(C + C_g)$$

PHASE NOISE CONTRIBUTION OF THE VARIOUS PARTS OF THE OSCILLATOR USING AN ACTIVE INDUCTOR

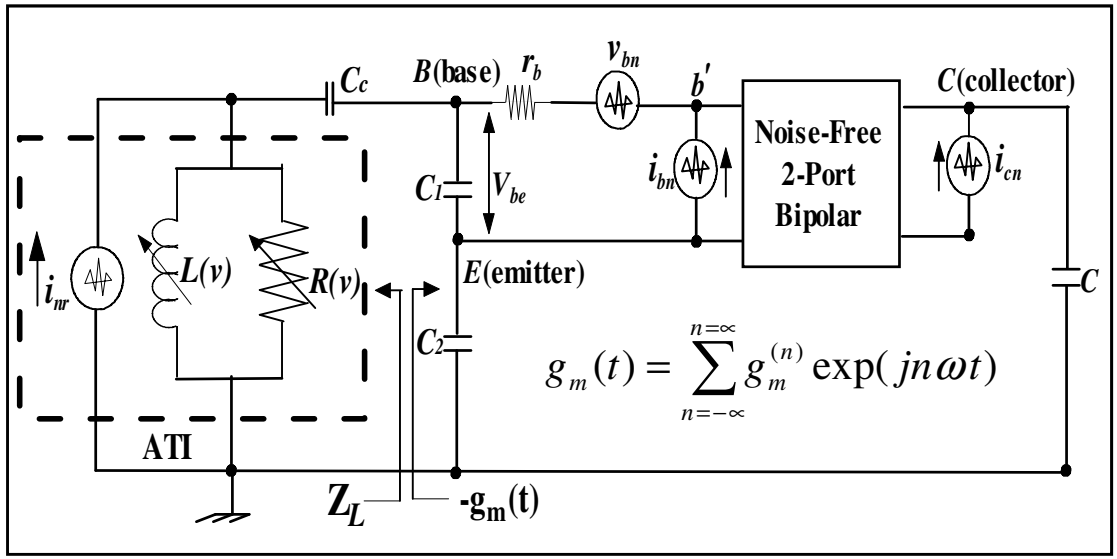

- The total noise voltage power within 1 Hz bandwidth can be described by:

- The first term is related to the active inductor noise due to the active inductor and the second term is related to negative resistance generative active device.

$$\left|\overline{e_n^2(\omega)}\right|_{\omega=\omega_0} = \overline{[e_n^2(\omega_0)]}_{-gm1} + \overline{[e_n^2(\omega_0)]}_{-gm2}$$

PHASE NOISE CONTRIBUTION OF THE VARIOUS PARTS OF THE OSCILLATOR USING AN ACTIVE INDUCTOR

- After some lengthy calculations and minimal approximations, adding shot noise, flicker noise and the loss resistor, the equivalent expression of the phase noise turns out to be

$$\left|\overline{e_{gm2}^2(\omega)}\right|_{\omega=\omega_0} = [4kTR] + \left[\frac{4qI_{c0}g_{m2}^2 + \frac{4K_f I_b^{AF}}{\omega}g_{m2}^2}{\omega_0^2 C_1^2[\omega_0^2(\beta^+)^2 C_2^2 + g_{m2}^2\frac{C_2^2}{C_1^2}]}\right]$$

$$g_{m2} = [Y_{21}^+]\left[\frac{C_1}{C_2}\right]^q$$

$$\beta^+ = \left[\frac{Y_{21}^+}{Y_{11}^+}\right]\left[\frac{C_1}{C_2}\right]^p$$

[4kTR] is the thermal noise of the resonator.

$$g_m(t) = \sum_{n=-\infty}^{n=\infty} g_m^{(n)} \exp(jn\omega t)$$

$$L(\omega) = 10\times\log\left[\left[k_0 + \left(\frac{k^3 k_1\left[\frac{Y_{21}^+}{Y_{11}^+}\right]^2[y]^{2p}}{[Y_{21}^+]^3[y]^{3q}}\right)\left(\frac{1}{(y^2+k)}\right)\right]\left[\frac{[1+y]^2}{y^2}\right]\right]$$

PHASE NOISE CONTRIBUTION OF THE VARIOUS PARTS OF THE OSCILLATOR USING AN ACTIVE INDUCTOR

- Continued from slide before:

$$L(\omega) = 10 \times \log\left[\left[k_0 + \left(\frac{k^3 k_1 \left[\frac{Y_{21}^+}{Y_{11}^+}\right]^2 [y]^{2p}}{\left[Y_{21}^+\right]^3 [y]^{3q}}\right)\left(\frac{1}{(y^2+k)}\right)\right]\left[\frac{[1+y]^2}{y^2}\right]\right]$$

$$k_0 = \frac{kTR}{\omega^2\, \omega_0^2 C_2^2 L_{active-inductor}^2 V_{cc}^2}$$

$$k_1 = \frac{qI_c g_{m2}^2 + \frac{K_f I_b^{AF}}{4\omega} g_{m2}^2}{\omega^2\, \omega_0^4 L_{active-inductor}^2 V_{cc}^2}$$

$$k_2 = \omega_0^4 (\beta^+)^2 \qquad k_3 = \omega_0^2 g_{m2}^2$$

$$k = \frac{k_3}{k_2 C_2^2}$$

$$L_{active-inductor} = \frac{C_1 C_2}{[C_1 + C_2] g_{m1}^2}$$

$$g_m(t) = \sum_{n=-\infty}^{n=\infty} g_m^{(n)} \exp(jn\omega t)$$

$$g_{m2} = \left[Y_{21}^+\right]\left[\frac{C_1}{C_2}\right]^q$$

$$\beta^+ = \left[\frac{Y_{21}^+}{Y_{11}^+}\right]\left[\frac{C_1}{C_2}\right]^p$$

$$y = \frac{C_1}{C_2}$$

- The values of p and q depend upon the drive level.

PHASE NOISE CONTRIBUTION OF THE VARIOUS PARTS OF THE OSCILLATOR USING AN ACTIVE INDUCTOR

- This Figure shows the schematic of self-injection-locked inductor-tuned Colpitts oscillator realized by incorporating phase shifter network in the feedback path, which improves the 1/f noise, including linearization of the large signal drive-level characteristics of the synthesized inductor circuits.
- Injection locked oscillators are frequently used to reduce the wideband noise. The oscillator's tuned-circuit based on its Q reduces the far out noise, while up-multiplication makes the noise worse.
- A variation of the injection locked oscillator is the self-injection, which improves the phase noise further.

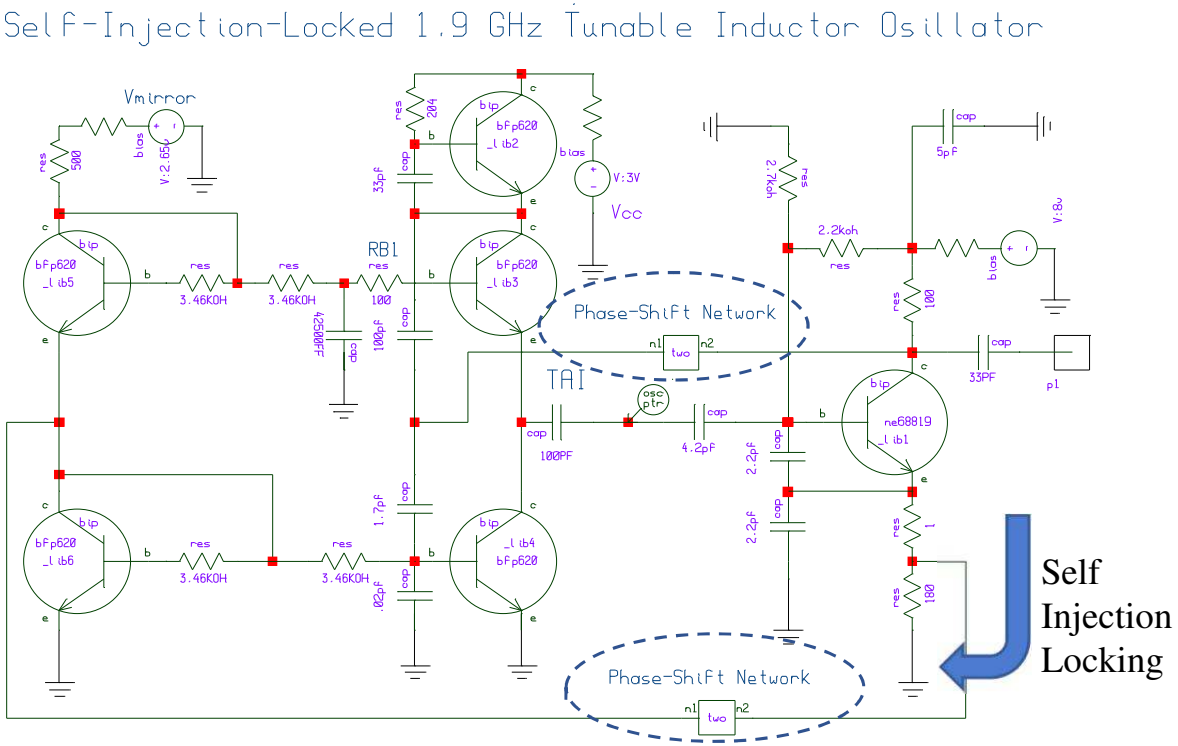

PHASE NOISE CONTRIBUTION OF THE VARIOUS PARTS OF THE OSCILLATOR USING AN ACTIVE INDUCTOR

- The figure at the left above shows the noise improvement simulation based on injection locking which close-in has a 17dB improvement, while further out at 1MHz offset, shows 10dB improvement, and below is the measured phase noise plot of injection locked 1.9 GHz Tunable Active Inductor (TAI).
- The figure at the right side shows the measured phase noise plot (Injection-Locked)

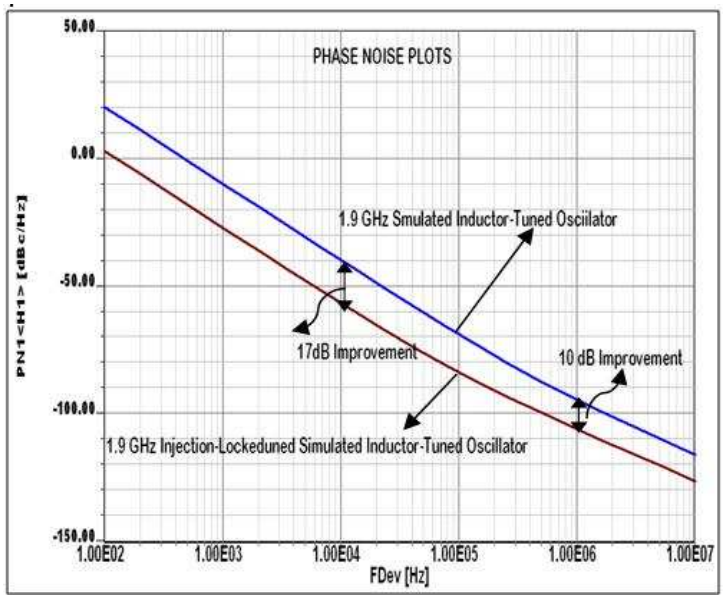

CAD simulated phase noise (WITH AND WITHOUT INJECTION LOCKING)

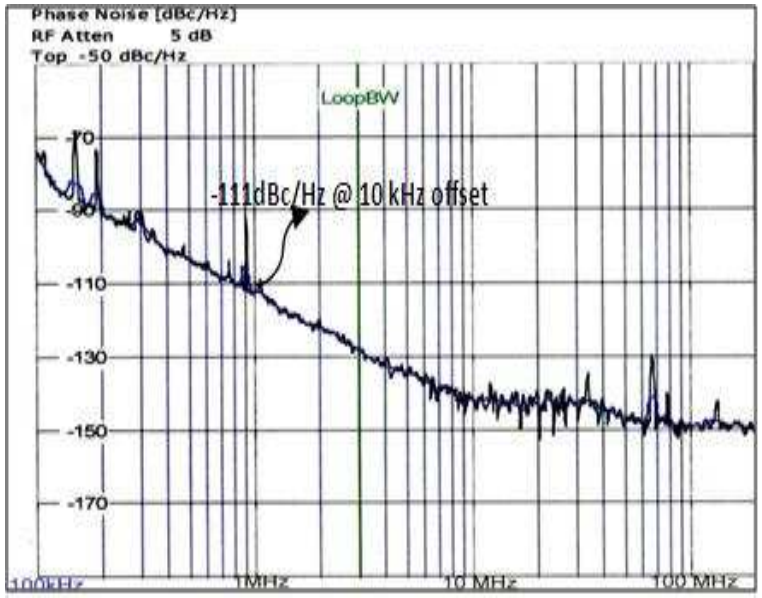

Mesasured phase noise

SUMMARY – Tunable Active Inductors

- This research work demonstrates the state-of-the-art in designing the novel tunable inductor based VCO (voltage controlled oscillator) circuits presented in my dissertation to obtain the Habilitation Status of “Dr.-Ing. habil.” presented to the Faculty 3: Mechanical engineering, Electrical engineering and industrial engineering, Brandenburg University of Technology Cottbus, Germany
  - ✓ Use of TAI (Tunable Active Inductor) resonator is relatively new and its application to replace tuning diodes in VCO (voltage controlled oscillator) have recently begun to be explored
  - ✓ Closed form noise models for TAI VCOs involved complex mathematical treatment due to the convergence problems at large drive-level
  - ✓ Limitation in the dynamic range may restricts the applications in high performance tunable filters, nevertheless by incorporating my novel techniques one can improve the dynamic range up to an accepted limit
  - ✓ The behavior of the TAI (Tunable Active Inductor) oscillator was studied and verified with practical examples.
  - ✓ Intensive studies were conducted to find the optimum configuration for the improvement in the phase noise over the tuning range, and a US Patent application was filed.
  - ✓ The extension of the research work is to increase the tuning range and dynamic range by employing injection mode coupling and noise cancellation techniques in monolithic IC technology.
  - ✓ I expect to see continued research in this field and the use of TAI (Tunable Active Inductor) components as a cost-effective alternative of tuning diodes (Varactor) as a tuning element in filter, resonator, antenna matching network and phase shifter for the applications in concurrent and configurable RF & MW modules/systems.

The Modern Time-Domain Behavior of an Oscillator

- The following is a detailed mathematical analysis of the time-domain behavior of oscillators, intended as a stand-alone mathematical derivation. It was developed between Prof. Rizzoli and team from the University of Bologna, Rowan Gilmore and Prof. Fred Rosenbaum from the University of Washington, St. Louise, and my team at Compact Software, where we introduced the world's first harmonic balance mathematics based simulator, that could handle nonlinear noise in amplifiers, frequency doublers, mixers and finally oscillators.
- The semiconductor noise contribution for the various devices was fairly challenging, and validated.
- The large-signal transfer characteristic affecting the current and voltage of an active device in an oscillator circuit is nonlinear. It limits the amplitude of the oscillation and produces harmonic content in the output signal. The resonant circuit and resulting phase shift sets the oscillation frequency.
- The nonlinear, exponential relationship between the voltage and current of a bipolar transistor is given as

$$i(t) = I_s e^{\frac{qv(t)}{kT}}$$

- I_s is device saturation current , V(t) is the voltage drive applied across the junction, k is Boltzman's constant, q is the electronic charge, and T is the temperature of the device in Kelvins. The bipolar case is mathematically more complex than the FET case. For the FET a similar set of equations exist which can be derived. Since most RFIC's now use SiGe bipolar transistors, the bipolar case has been selected.

The Modern Time-Domain Behavior of an Oscillator

- The voltage V(t) across the base-emitter junction consists of a DC component and a driven signal voltage $V_1\cos(wt)$. It can be expressed as

$$i_e(t) = I_s e^{\frac{qv(t)}{kT}} \qquad i_e(t) = I_s e^{\frac{qV_{dc}}{kT}} e^{\frac{qV_1\cos(wt)}{kT}} \qquad i_e(t) = I_s e^{\frac{qV_{dc}}{kT}} e^{x\cos(wt)}$$

- assuming Ic ≈ Ie (β>10)

$$x = \frac{V_1}{(kT/q)} = \frac{qV_1}{kT}$$

$i_e(t)$ is the emitter current and x is the drive level which is normalized to kT/q

From the Fourier series expansion, $e^{x\cos(wt)}$ is expressed as $e^{x\cos(wt)} = \sum_n a_n(x)\cos(nwt)$

.

The Modern Time-Domain Behavior of an Oscillator

From the Fourier series expansion, $e^{x\cos(wt)}$ is expressed as $e^{x\cos(wt)} = \sum_n a_n(x)\cos(nwt)$

$a_n(x)$ is a Fourier coefficient and given as

$$a_0(x)\big|_{n=0} = \frac{1}{2\pi}\int_0^{2\pi} e^{x\cos(wt)}\,d(wt) = I_0(x) \qquad (6\text{-}89)$$

$$a_n(x)\big|_{n>0} = \frac{1}{2\pi}\int_0^{2\pi} e^{x\cos(wt)}\cos(mwt)\,d(wt) = I_n(x) \qquad (6\text{-}90)$$

$$e^{x\cos(wt)} = \sum_n a_n(x)\cos(mwt) = I_0(x) + \sum_1^{\infty} I_n(x)\cos(mwt) \qquad (6\text{-}91)$$

$I_n(x)$ is the modified Bessel function.

$$\text{As } x \to 0 \Rightarrow I_n(x) \to \frac{(x/2)^n}{n!} \qquad (6\text{-}92)$$

$I_0(x)$ are monotonic functions having positive values for x≥0 and n≥0; $I_0(0)$ is unity, whereas all higher order functions start at zero.

The Modern Time-Domain Behavior of an Oscillator

- The short current pulses are generated from the growing large-signal drive level across the base-emitter junction, which leads to strong harmonic generation. The emitter current represented above can be expressed in terms of harmonics as

$$i_e(t) = I_s e^{\frac{qV_{dc}}{kT}} I_0(x)\left[1 + 2\sum_{1}^{\infty} \frac{I_n(x)}{I_0(x)} \cos(nwt)\right] \quad (6\text{-}93)$$

$$I_{dc} = I_s e^{\frac{qV_{dc}}{kT}} I_0(x) \quad (6\text{-}94)$$

$$V_{dc} = \frac{kT}{q} \ln\left[\frac{I_{dc}}{I_s I_0(x)}\right] \Rightarrow \frac{kT}{q} \ln\left[\frac{I_{dc}}{I_s}\right] + \frac{kT}{q} \ln\left[\frac{1}{I_0(x)}\right] \quad (6\text{-}95)$$

$$V_{dc} = V_{dcQ} - \frac{kT}{q} \ln I_0(x) \quad (6\text{-}96)$$

$$i_e(t) = I_{dc}\left[1 + 2\sum_{1}^{\infty} \frac{I_n(x)}{I_0(x)} \cos(nwt)\right] \quad (6\text{-}97)$$

- V_{dcQ} and I_{dc} are the operating DC bias voltage and the DC value of the emitter current. Furthermore, the Fourier transform of $i_e(t)$, a current pulse or series of pulses in the time domain yields a number of frequency harmonics common in oscillator circuit designs using nonlinear devices.
- The peak amplitude of the output current, the harmonic content defined as $\left[\frac{I_N(x)}{I_1(x)}\right]$, and the DC offset voltage are calculated analytically in terms of the drive level, as shown in Table 6-1 (next slide). It gives good insight of the nonlinearities involved in the oscillator design.

The Modern Time-Domain Behavior of an Oscillator

Drive level [x]	Drive-Voltage [$\frac{kT}{q}$ *x] mV	Offset-Coefficient ln[$I_0(x)$]	DC-Offset $\frac{kT}{q}[\ln I_0(x)]$ mV	Fundamental Current $2[I_1(x)/I_0(x)]$	Second-Harmonic $[I_2(x)/I_1(x)]$
0.00	0.000	0.000	0.000	0.000	0.000
0.50	13.00	0.062	1.612	0.485	0.124
1.00	26.00	0.236	6.136	0.893	0.240
2.00	52.00	0.823	21.398	1.396	0.433
3.00	78.00	1.585	41.210	1.620	0.568
4.00	104.00	2.425	63.050	1.737	0.658
5.00	130.00	3.305	85.800	1.787	0.719
6.00	156.00	4.208	206.180	1.825	0.762
7.00	182.00	5.127	330.980	1.851	0.794
8.00	208.00	6.058	459.600	1.870	0.819
9.00	234.00	6.997	181.922	1.885	0.835
10.00	260.00	7.943	206.518	1.897	0.854
15.00	390.00	12.736	331.136	1.932	0.902
20.00	520.00	17.590	457.340	1.949	0.926

Table 6-1

- From the table, the peak current 2[I1(x)/I0(x)] in column 5 approaches 1.897Idc for a drive level ratio x=10.

for T=300K, $\frac{kT}{q} = 26mV$ (6-98)

and $V_1 = 260mV$ for x=10 (6-99)

The Modern Time-Domain Behavior of an Oscillator

- The second harmonic-distortion $\frac{I_2(x)}{I_1(x)}$ is 85% for a normalized drive level of x=10 and the corresponding DC offset is 205.518mV. When referring to the amplitude, x is always meant as normalized to $\frac{kT}{q}$
- Figure 6-10 is generated with the help of Math-CAD, and shows the plot of the normalized fundamental and second harmonic current with respect to the drive level.

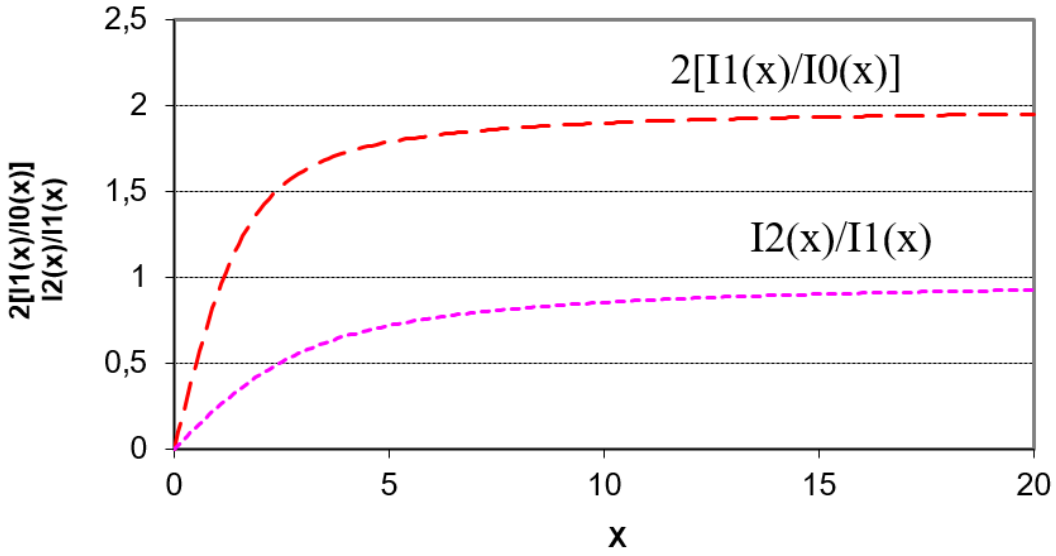

Figure 6-10 Plot of the normalized fundamental current

2I1(x)/I0(x)

andsecond harmonic

I2(x)/I1(x)

with respect to the drive level x.

The Modern Time-Domain Behavior of an Oscillator

- One can notice that as the drive level x increases, the fundamental 2I1(x)/I0(x) and harmonic I2(x)/I1(x) increases monotonically.
- Figure 6-11 shows the plot of the coefficient of offset $[\ln I_0(x)]$ with respect to drive level x so that the DC offset voltage can be calculated at different temperatures by simply multiplying the factor $\frac{kT}{q}$

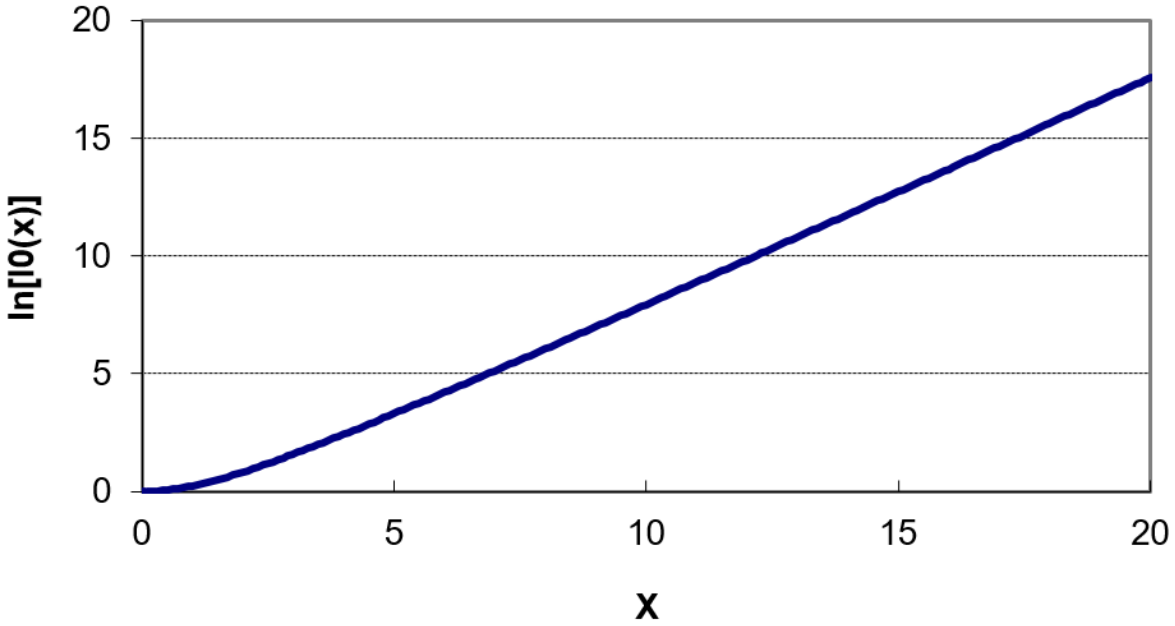

Figure 6-11 Plot of Vs drive level X.

At T= 300K the DC voltage shift is $-26[\ln I_0(x)]mV$

The Modern Time-Domain Behavior of an Oscillator

At T= 300K the DC voltage shift is $-26[\ln I_0(x)]mV$

for x=10

$$V_{dc} = V_{dcQ} - \frac{kT}{q}\ln I_0(x) \qquad (6\text{-}100)$$

$$V_{dc-offset} = \frac{kT}{q}\ln I_0(x) = 206mV \qquad (6\text{-}102)$$

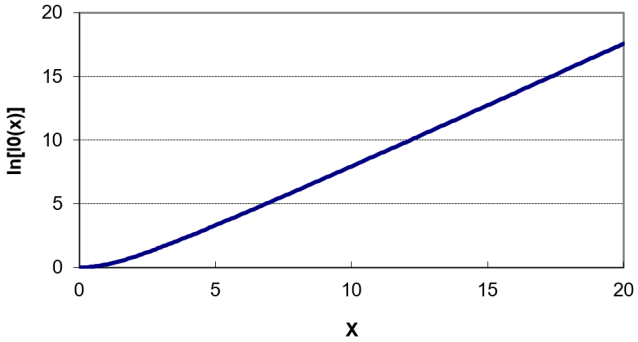

Figure 6-11 Plot of Vs drive level X.

- The harmonic content trade-off is an important consideration in reducing the noise content by using shorter current pulses [64-67].

V_{dcQ} and $V_{dc-offset}$ are the operating bias points and DC offsets due to an increase in the drive level. The DC voltage shift at x=10 is 206mV. Figure 6-12 shows the shape of the output current with respect to the drive level and demonstrates that as the drive level increases, the output current pulse width becomes shorter and the peak current amplitude becomes greater.

$$i_e(t)\big|_{x=10} \to 0\text{, For conduction angle } \geq 60^0 \qquad (6\text{-}103)$$

$$i_e(t)\big|_{x=5} \to 0\text{, For conduction angle } \geq 90^0 \qquad (6\text{-}104)$$

$$i_e(t)\big|_{x=2} \to 0\text{, For conduction angle } > 180^0 \qquad (6\text{-}105)$$

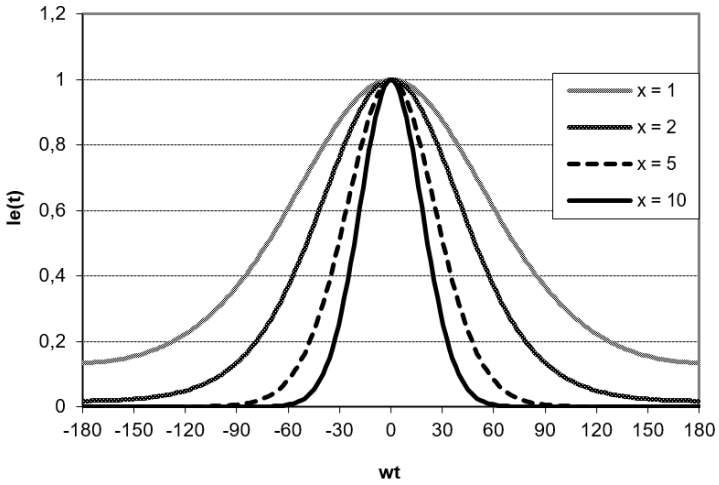

Plot of current with respect to conduction angle- (wt) and drive level X.

Test Case: Design Example of a 100MHz crystal oscillator

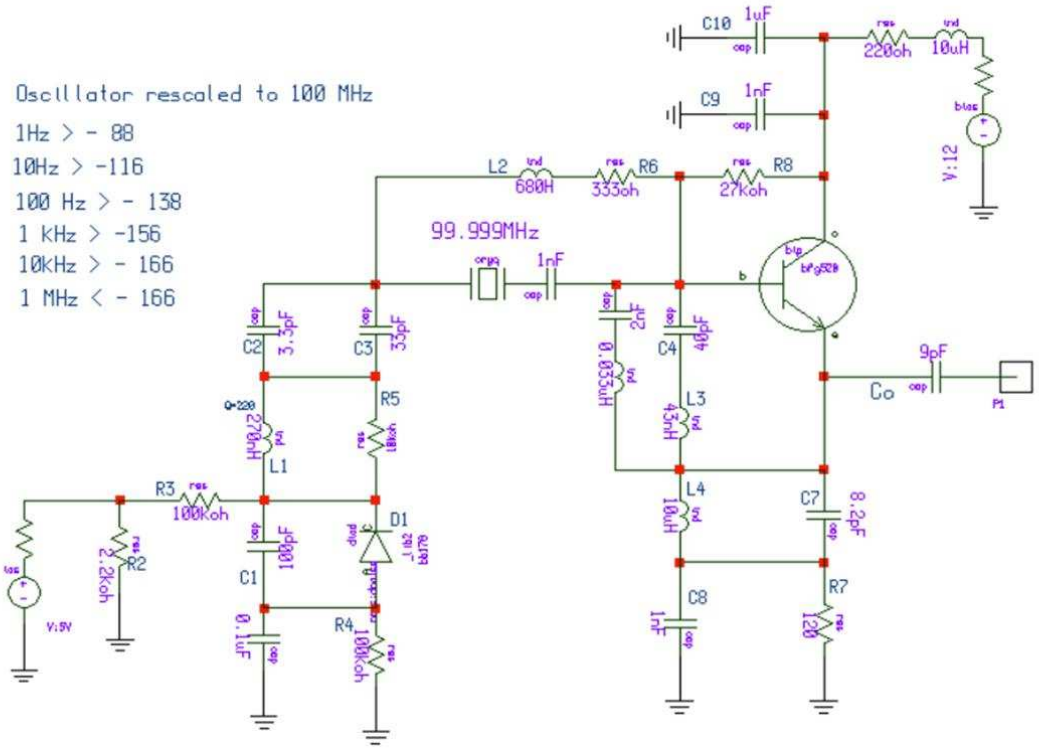

Figure 5-33a: Scaled to 100 MHz based on the 10 MHz HP10811A circuit [17]

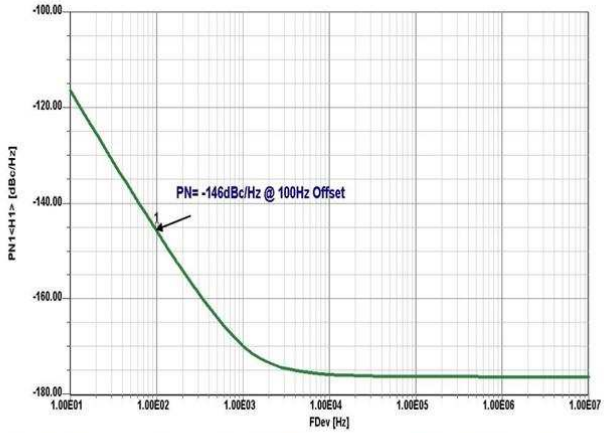

Figure 6-16: CAD simulated Phase Noise Plot of 100 MHz Crystal Oscillator with Buffer Stage [63, Fig 4.16]

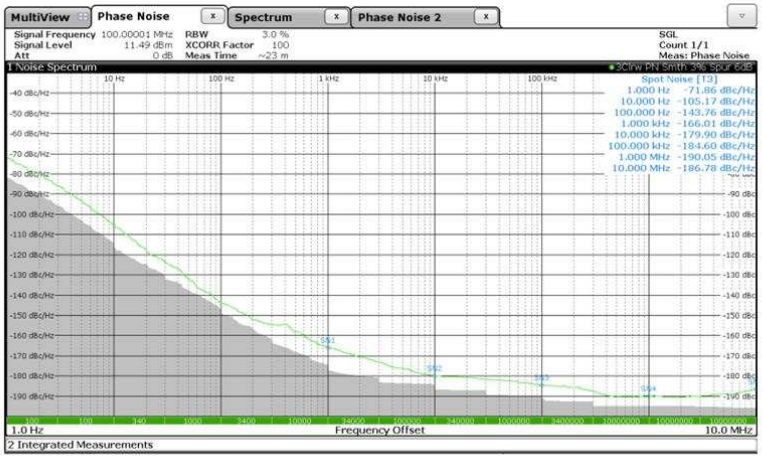

Figure 5-49: Measured phase noise of the 100 MHz crystal oscillator

Phase Noise Analysis Based on the Negative Resistance Model

- The following noise analysis for the oscillator, while based on the approach of Kurokawa, is an attempt to introduce the concept of a “noisy” negative resistance, which is time dependent.
- Kurokawa, addressing the question of synchronized oscillators, provided insight in the general case of a series oscillator.
- The method introduced here is specific for a real oscillator and real noise sources.
- I now take the basic Colpitts oscillator circuit and develop:

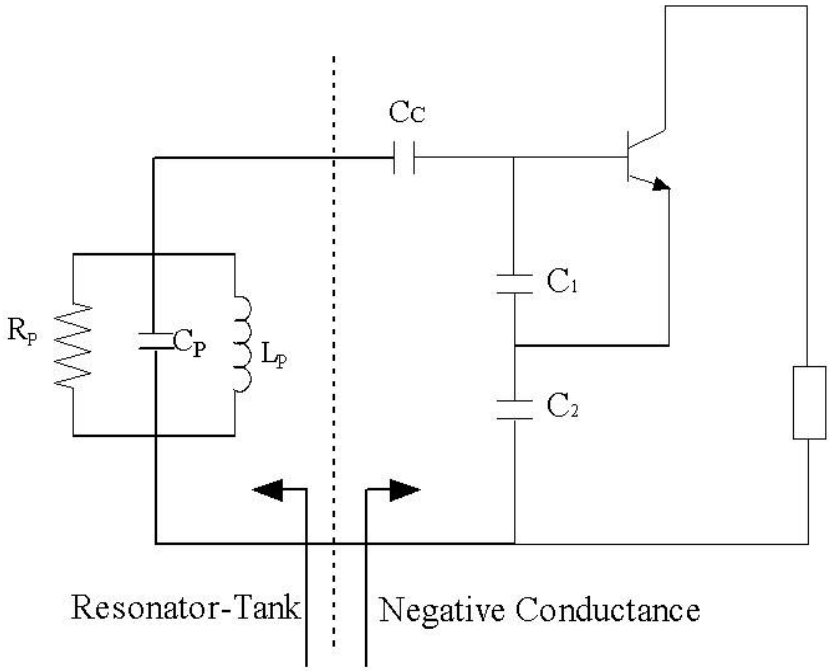

Figure 8-2 Colpitts Oscillator configuration for the intrinsic case, no parasitics assumed, and an ideal transistor considered.

Phase Noise Analysis Based on the Negative Resistance Model

- The following two circuits show the transition from a series tuned circuit connected with the series time-dependent negative resistance and the resulting input capacitance marked CIN.
- Translated, the resulting configuration consists of a series circuit with inductance L and the resulting capacitance C'. The noise voltage $e_N(t)$ describes a small perturbation, which is the noise resulting from R_L and $– R_N(t)$.
- Figure 8-3 shows the equivalent representation of the oscillator circuit in the presence of noise.

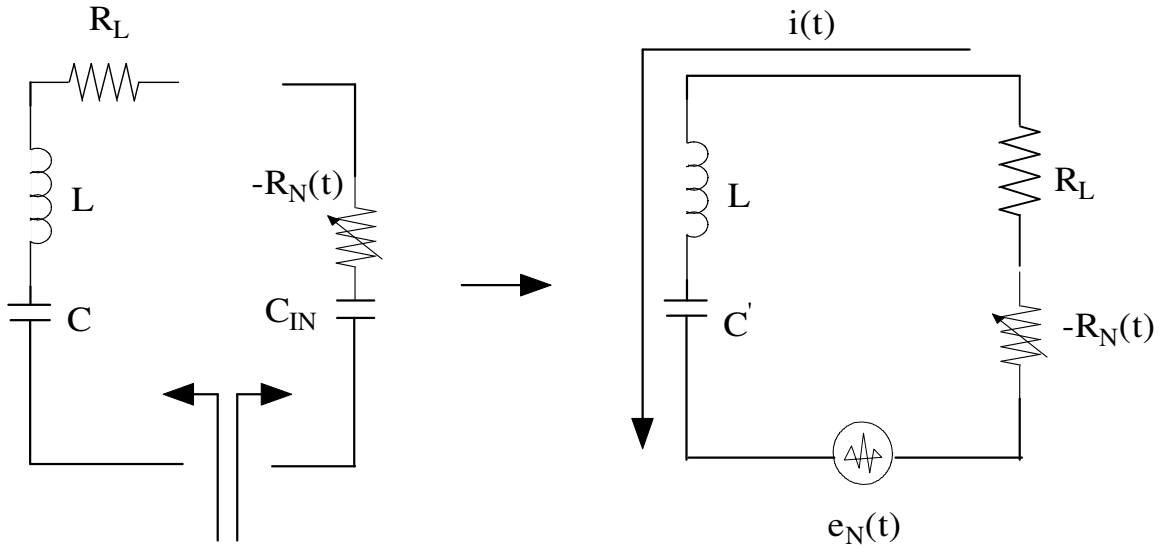

Figure 8-3 Equivalent representation of the oscillator circuit in presence of noise

Phase Noise Analysis Based on the Negative Resistance Model

- The circuit equation of the oscillator circuit of Figure 8-3 can be given as

$$L\frac{di(t)}{dt}+(R_L-R_N(t))i(t)+\frac{1}{C}\int i(t)dt=e_N(t) \quad (8\text{-}11)$$

- where i(t) is the time varying resultant current. Due to the noise voltage eN(t), Equation (8-11) is a nonhomogeneous differential equation. If the noise voltage is zero, it translates into a homogeneous differential equation.
- For a noiseless oscillator, the noise signal $e_N(t)$ is zero and the expression of the free-running oscillator current i(t) can be assumed to be a periodic function of time and can be given as

$$i(t)=I_1\cos(\omega t+\varphi_1)+I_2\cos(2\omega t+\varphi_2)+I_3\cos(3\omega t+\varphi_3)+.....I_n\cos(n\omega t+\varphi_n) \quad (8\text{-}12)$$

where I1, I2 …..In are peak harmonic amplitudes of the current and φ1, φ2…..φn are time invariant phases.

- In the presence of the noise perturbation $e_N(t)$, the current i(t) may no longer be a periodic function of time and can be expressed as

$$i(t)=I_1(t)\cos[\omega t+\varphi_1(t)]+I_2(t)\cos[2\omega t+\varphi_2(t)]+I_3(t)\cos[3\omega t+\varphi_3(t)]+$$
$$....I_{n-2}(t)\cos[(n-2)\omega t+\varphi_{n-2}(t)]+I_{n-1}(t)\cos[(n-1)\omega t+\varphi_{n-1}(t)]+I_n(t)\cos[n\omega t+\varphi_n(t)]$$

where I1(t), I2(t)…..In(t) are time variant amplitudes of the current and φ1(t), φ2(t)…..φn(t) are time variant phases.

Phase Noise Analysis Based on the Negative Resistance Model

- Considering that In(t) and φn(t) do not change much over the period of 2π/nω; each corresponding harmonic over one period of oscillation cycle remains small and more or less variant.
- The solution of the differential equation becomes easy since the harmonics are suppressed due to a Q > 10, which prevents i(t) to flow for the higher terms.

After the substitution of the value of $\frac{di}{dt}$ and $\int i(t)dt$, the complete oscillator circuit equation, as given in Equation (8-11), can be rewritten as

$$L\{-I_1(t)(\omega+\frac{d\varphi_1(t)}{dt})\sin[\omega t+\varphi_1(t)]+\frac{dI_1(t)}{dt}\cos[\omega t+\varphi_1(t)]+$$
$$-I_2(t)(2\omega+\frac{d\varphi_2(t)}{dt})\sin[2\omega t+\varphi_2(t)]+\frac{dI_2(t)}{dt}\cos[2\omega t+\varphi_2(t)]+$$
$$-I_3(t)(3\omega+\frac{d\varphi_3(t)}{dt})\sin[3\omega t+\varphi_3(t)]+\frac{dI_3(t)}{dt}\cos[3\omega t+\varphi_3(t)]+\ldots$$
$$-I_n(t)(n\omega+\frac{d\varphi_n(t)}{dt})\sin[n\omega t+\varphi_n(t)]+\frac{dI_n(t)}{dt}\cos[n\omega t+\varphi_n(t)]\}+$$
$$[(R_L-R_N(t))i(t)]+$$

$$\frac{1}{C}\left\{\left[\frac{I_1(t)}{\omega}-\frac{I_1(t)}{\omega^2}\left(\frac{d\varphi_1(t)}{dt}\right)\right]\sin[\omega t+\varphi_1(t)]+\frac{1}{\omega^2}\left(\frac{dI_1(t)}{dt}\right)\cos[\omega t+\varphi_1(t)]\right\}+$$
$$\frac{1}{C}\left\{\left[\frac{I_2(t)}{2\omega}-\frac{I_2(t)}{4\omega^2}\left(\frac{d\varphi_2(t)}{dt}\right)\right]\sin(2\omega t+\varphi_2(t)+\frac{1}{4\omega^2}\left(\frac{dI_2(t)}{dt}\right)\cos(2\omega t+\varphi_2(t))\right\}+$$
$$\frac{1}{C}\left\{\left[\frac{I_3(t)}{3\omega}-\frac{I_3(t)}{9\omega^2}\left(\frac{d\varphi_3(t)}{dt}\right)\right]\sin[3\omega t+\varphi_3(t)]+\frac{1}{9\omega^2}\left(\frac{dI_3(t)}{dt}\right)\cos[3\omega t+\varphi_3(t)]\right\}+\ldots$$
$$\frac{1}{C}\left\{\left[\frac{I_n(t)}{n\omega}-\frac{I_n(t)}{n^2\omega^2}\left(\frac{d\varphi_n(t)}{dt}\right)\right]\sin[n\omega t+\varphi_n(t)]+\frac{1}{n^2\omega^2}\left(\frac{dI_n(t)}{dt}\right)\cos[n\omega t+\varphi_n(t)]\right\}=e_N(t)$$

Phase Noise Analysis Based on the Negative Resistance Model

- Because Q > 10 we approximate:.

$$\frac{di(t)}{dt} = -I_1(t)(\omega + \frac{d\varphi_1(t)}{dt})\sin[\omega t + \varphi_1(t)] + \frac{dI_1(t)}{dt}\cos[\omega t + \varphi_1(t)] + (\text{slowly varying function at higher order harmonics of a very small amount})$$

$$\int i(t)dt = \left[\frac{I_1(t)}{\omega} - \frac{I_1(t)}{\omega^2}\left(\frac{d\varphi_1(t)}{dt}\right)\right]\sin[\omega t + \varphi_1(t)] + \frac{1}{\omega^2}\left(\frac{dI_1(t)}{dt}\right)\cos[\omega t + \varphi_1(t)] + \quad (\text{slowly varying function at higher order harmonics of a very small amount})$$

After the substitution of the value of $\frac{di}{dt}$ and $\int i(t)dt$, the oscillator circuit Equation (8-14) can be rewritten as

$$L\left[-I_1(t)(\omega + \frac{d\varphi_1(t)}{dt})\sin[\omega t + \varphi_1(t)] + \frac{dI_1(t)}{dt}\cos[\omega t + \varphi_1(t)]\right] + \left[(R_L - R_N(t))I(t)\right] + \left|\right.$$

$$\frac{1}{C}\left\{\left[\frac{I_1(t)}{\omega} - \frac{I_1(t)}{\omega^2}\left(\frac{d\varphi_1(t)}{dt}\right)\right]\sin[\omega t + \varphi_1(t)] + \frac{1}{\omega^2}\left(\frac{dI_1(t)}{dt}\right)\cos[\omega t + \varphi_1(t)]\right\} = e_N(t) \qquad (8\text{-}15)$$

Phase Noise Analysis Based on the Negative Resistance Model

$$L\left[-I_1(t)(\omega+\frac{d\varphi_1(t)}{dt})\sin[\omega t+\varphi_1(t)]+\frac{dI_1(t)}{dt}\cos[\omega t+\varphi_1(t)]\right]+[(R_L-R_N(t))I(t)]+|$$

$$\frac{1}{C}\left\{\left[\frac{I_1(t)}{\omega}-\frac{I_1(t)}{\omega^2}\left(\frac{d\varphi_1(t)}{dt}\right)\right]\sin[\omega t+\varphi_1(t)]+\frac{1}{\omega^2}\left(\frac{dI_1(t)}{dt}\right)\cos[\omega t+\varphi_1(t)]\right\}=e_N(t) \qquad (8\text{-}15)$$

For simplification purposes, the equations above are multiplied with $\sin[\omega t+\varphi_1(t)]$ or $\cos[\omega t+\varphi_1(t)]$ and integrated over one period of the oscillation cycle, which will give an approximate differential equation for phase $\varphi(t)$ and amplitude i(t) as

$$\left[\frac{2}{IT_0}\right]\int_{t-T_0}^{t}e_N(t)\sin[\omega t+\varphi(t)]dt=-\frac{d\varphi}{dt}\left[L+\frac{1}{\omega^2 C'}\right]+\left[-\omega L+\frac{1}{\omega C'}\right] \qquad (8\text{-}16)$$

$$\left[\frac{2}{T_0}\right]\int_{t-T_0}^{t}e_N(t)\cos[\omega t+\varphi(t)]dt=\frac{dI(t)}{dt}\left[L+\frac{1}{\omega^2 C'}\right]+\left[R_L-\overline{R_N(t)}\right]I(t) \qquad (8\text{-}17)$$

where $\overline{R_N(t)}$ is the average negative resistance under large signal condition. $\overline{R_N(t)}=\left[\frac{2}{T_0 I}\right]\int_{t-T_0}^{t}R_N(t)I(t)\cos^2[\omega t+\varphi)]dt$

- Since magnitude of the higher harmonics are not significant, the subscript of $\varphi(t)$ and $I(t)$ are dropped. We now determine the negative resistance

Calculation of the Region of the Nonlinear Negative Resistance

- Under steady-state free running oscillation condition, $\frac{dI(t)}{dt} \to 0$ implies steady current, and $e_N(t) \to 0$

with I = fundamental RF current. Solving the now homogeneous differential equation

for $R_L - R_N(t)$ and inserting the two terms into 8-17, we obtain

$$\left[\frac{2}{T_0}\right]\int_{t-T_0}^{t} e_N(t)\cos[\omega t+\varphi(t)]dt = \frac{dI}{dt}\left[L+\frac{1}{\omega^2 C'}\right]+\left[R_L-\overline{R_N(t)}\right]I(t) \qquad (8\text{-}19)$$

$$\text{term} \to 0$$

now we introduce γ; $\gamma = \frac{\Delta R}{\Delta I}$; for $\Delta \to 0$, $\gamma \to 0$ and

$$[R_L-\overline{R_N(t)}] = \gamma\ \Delta I\ ,\ \gamma \to 0 \Rightarrow [R_L-\overline{R_N(t)}]I(t) \to 0 \qquad (8\text{-}20)$$

$$R_L-\overline{R_N(t)} = R_{Load} - \left[\frac{2}{T_0}\right]\int_{t-T_0}^{t} R_N(t)\cos^2[\omega t+\varphi(t)]dt \to 0 \qquad (8\text{-}21)$$

Calculation of the Region of the Nonlinear Negative Resistance

$[R_L - \overline{R_N(t)}]I(t) \rightarrow 0$ gives the intersection of $[\overline{R_N(t)}]$ and $[R_L]$. This value is defined as I_0 which is the minimum value of the current needed for the steady-state sustained oscillation condition.

Figure 8-4 shows the plot of the nonlinear negative resistance, which is a function of the amplitude of the RF current. As the RF amplitude gets larger the conducting angle becomes more narrow.

For a small variation of the current ΔI from I_0, the relation above is expressed as

$$[R_L - \overline{R_N(t)}] = \gamma\ \Delta I$$

$\gamma\ \Delta I$ can be found from the intersection on the vertical axis by drawing the tangential line on $[\overline{R_N(t)}]$ at $I = I_0$. $|\Delta I|$ decreases exponentially with time for $\gamma > 0$.

Hence, I_0 represents the stable operating point. On the other hand, if $[\overline{R_N(t)}]$ intersects $[R_L]$ from the other side for $\gamma < 0$ then $|\Delta I|$ grows indefinitely with time. Such an operating point does not support stable operation].

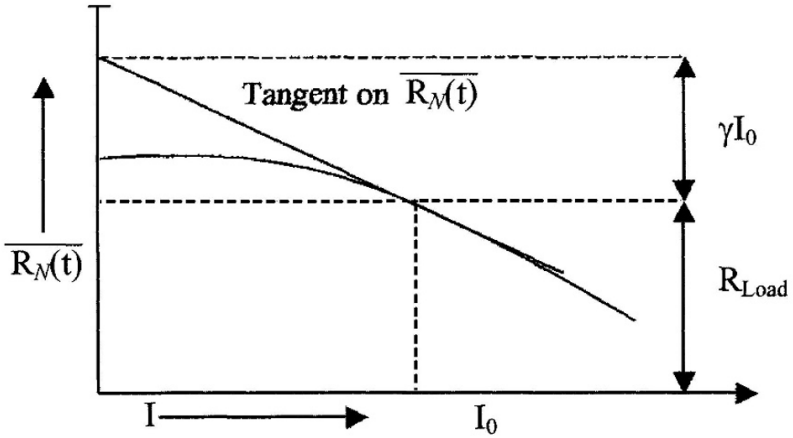

- ***Figure 8-4 Plot of negative resistance of [$\overline{R_N(t)}$] vs. amplitude of current I.***

Design Example of an Oscillator for Best Phase Noise and Good Output Power

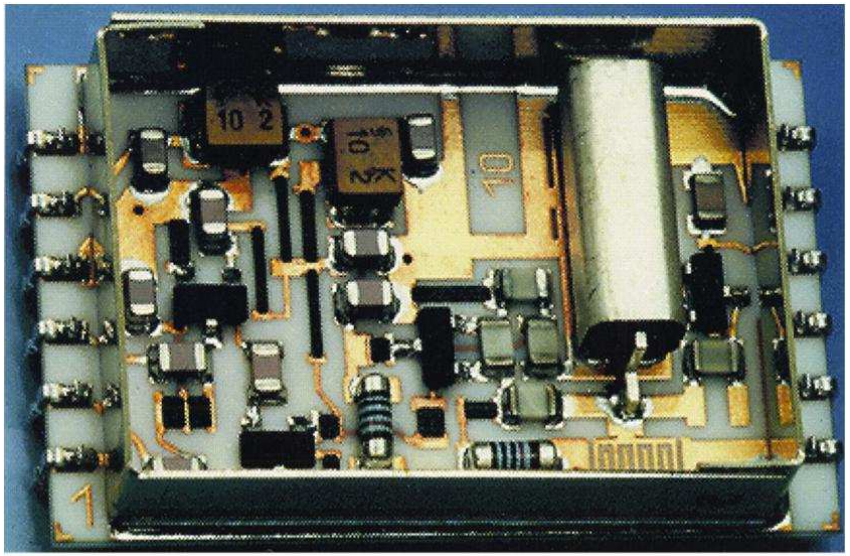

Parallel-tuned Colpitts oscillator circuit, which has to be designed with the following specifications. The unit was also built and measured. It uses a ceramic resonator and its equivalent circuit is shown.

- Requirements:
  - output power requirement: 13 dBm
  - operating frequency: 1000 MHz
  - load: 50 Ω
  - phase noise –124 dBc/Hz @10KHz

Design Example of an Oscillator for Best Phase Noise and Good Output Power

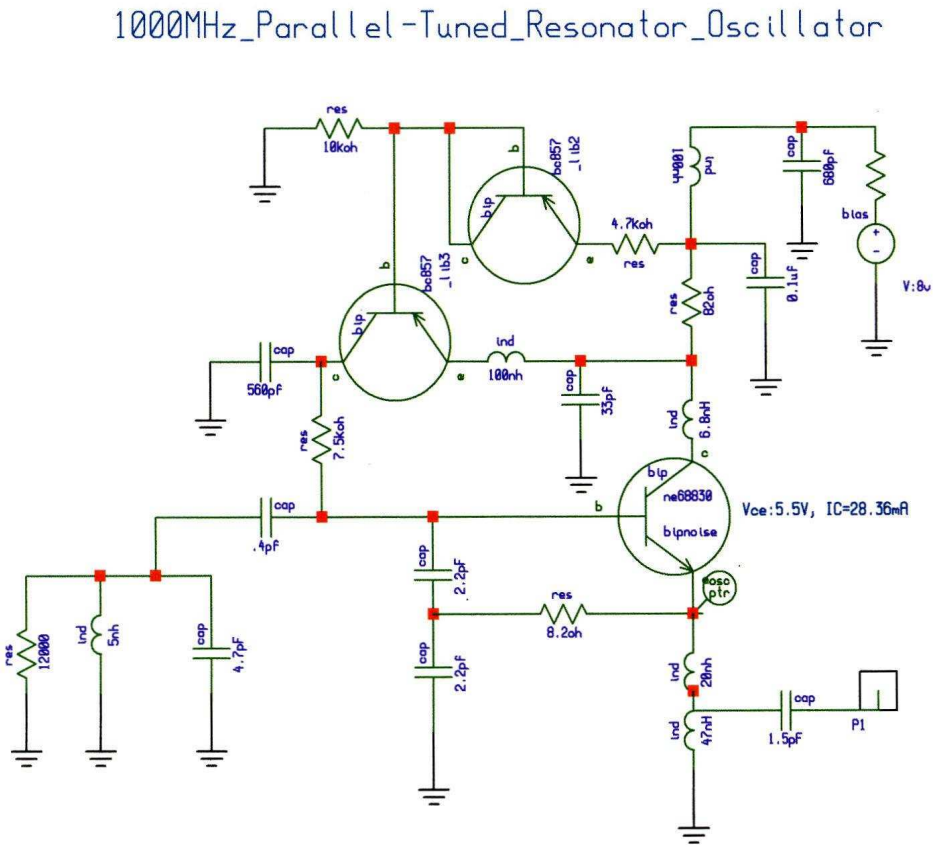

Schematic of the 1000 MHz oscillator.

Design Example of an Oscillator for Best Phase Noise and Good Output Power

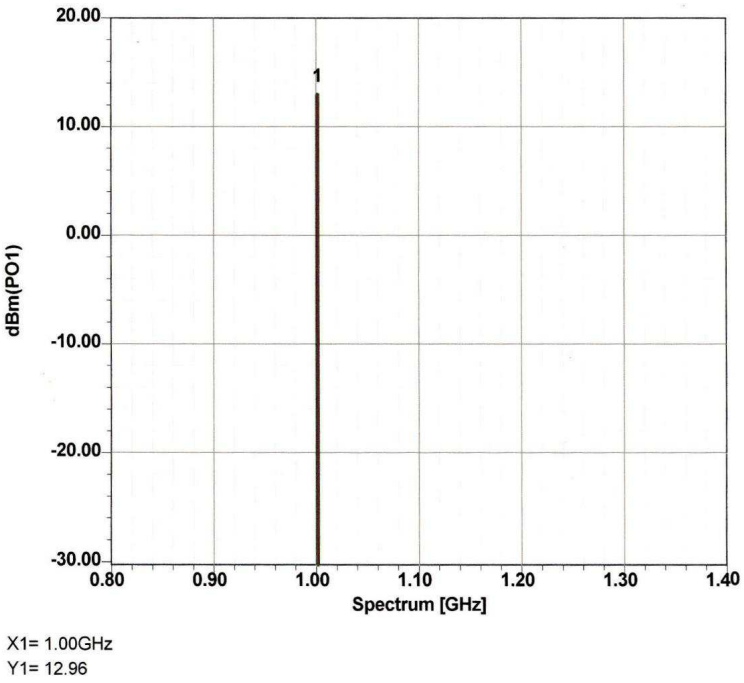

Predicted output power of the oscillator.

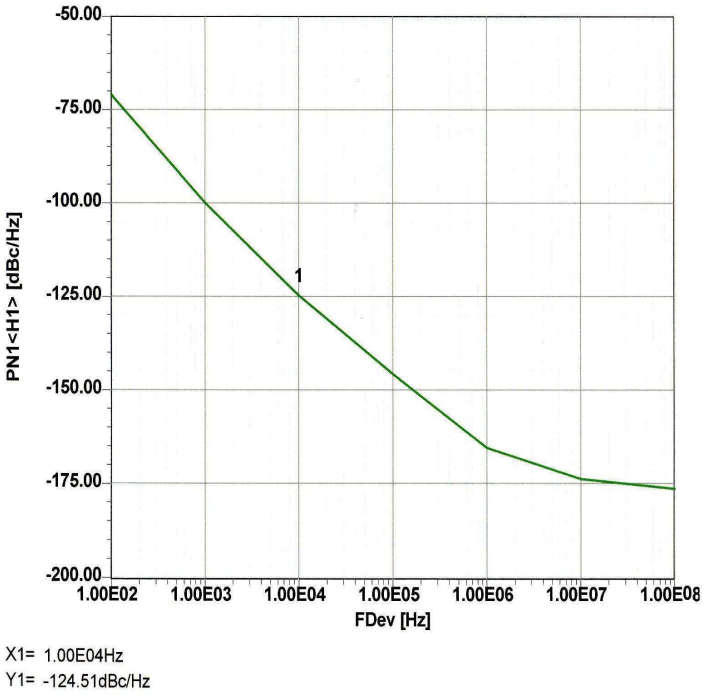

Predicted phase noise of the oscillator

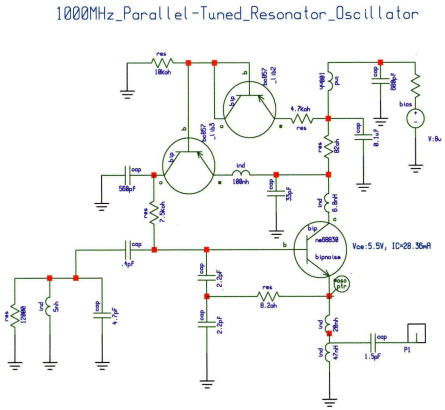

Schematic of the 1000 MHz oscillator.

Design Example of an Oscillator for Best Phase Noise and Good Output Power

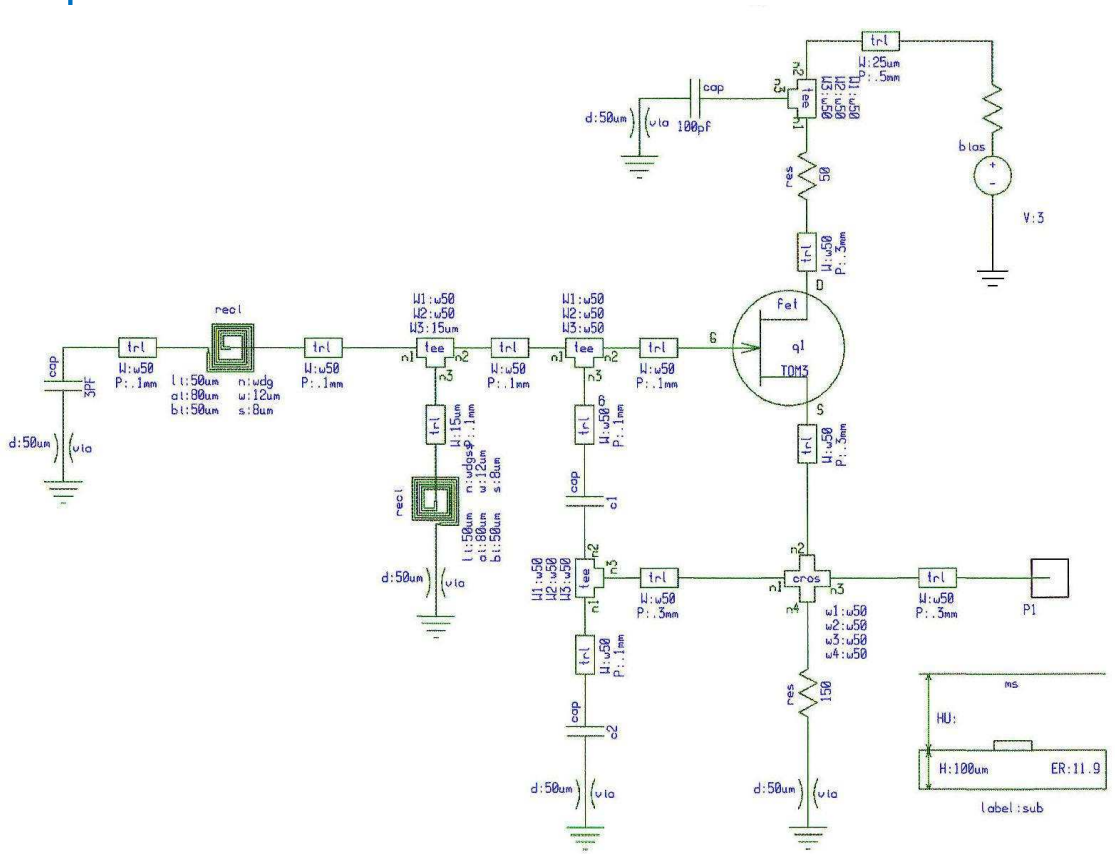

Circuit schematic of a 2 GHz GaAs FET oscillator built on GaAs substrate with very fine resolution of the components

Design Example of an Oscillator for Best Phase Noise and Good Output Power

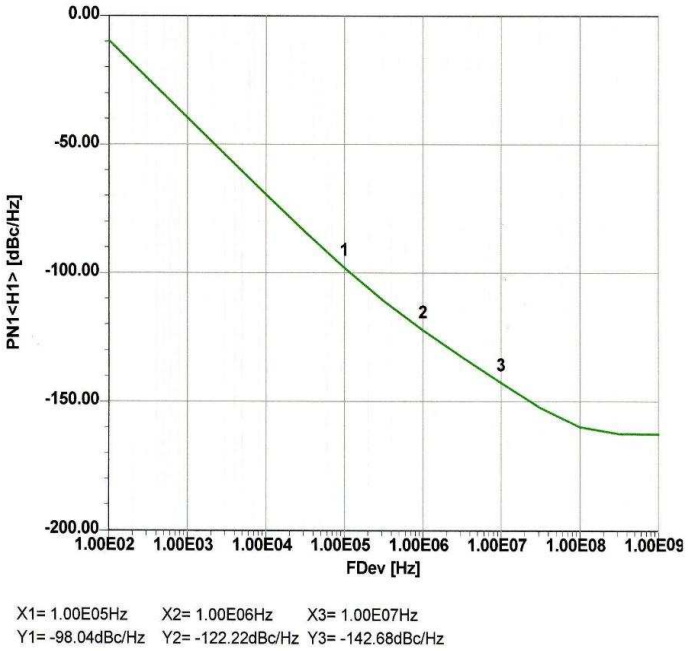

Predicted phase noise of this oscillator. The measured values were 100 dBc/Hz at 100 kHz and 120 dBc/Hz at 1 MHz. There is a deviation of about 2 dB compared to simulation.

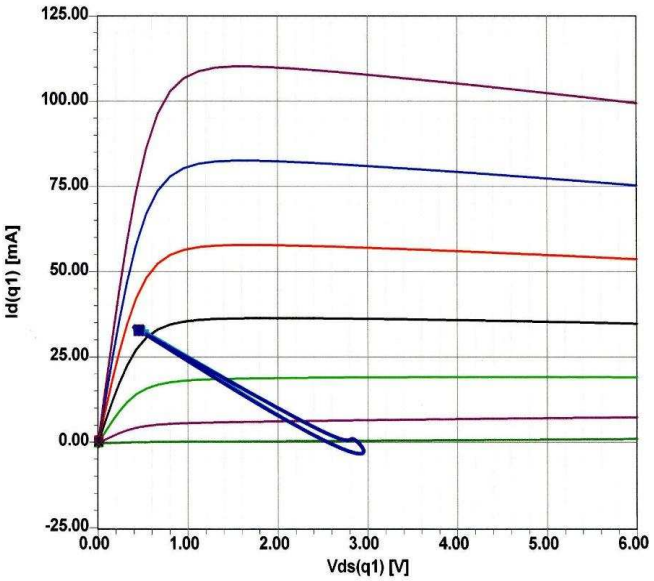

Shows the DC-IV and the load line for the GaAs FET oscillator.

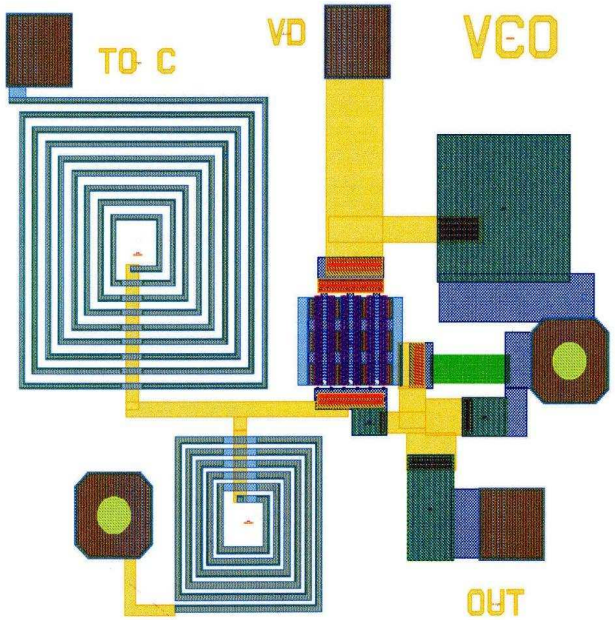

Layout of the 2 GHz GaAs FET oscillator

Further Design Examples

2400 MHz MOSFET-Based Push-Pull Oscillator

A Symmetric LC Oscillator

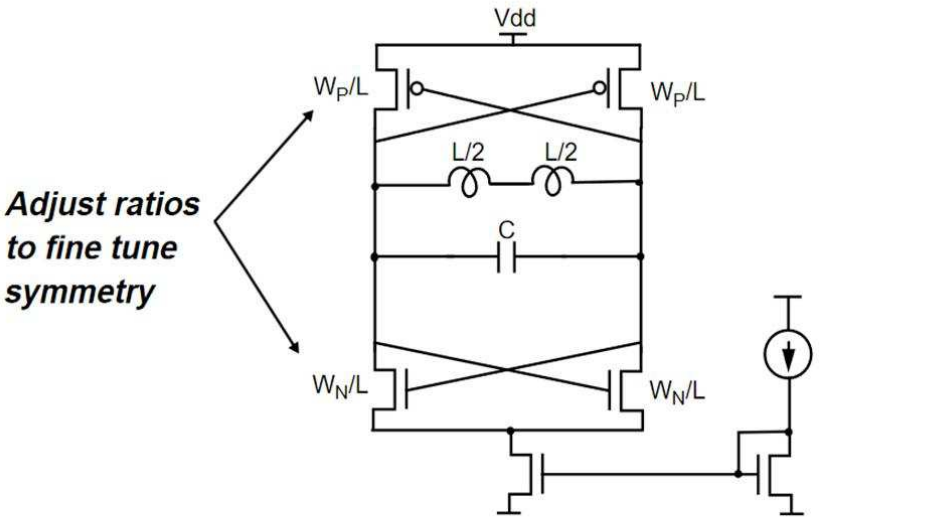

Uses the same current twice for high transconductance.

[Also appears in: J.Craninckx, *et al*, Proceedings of CICC 97.]

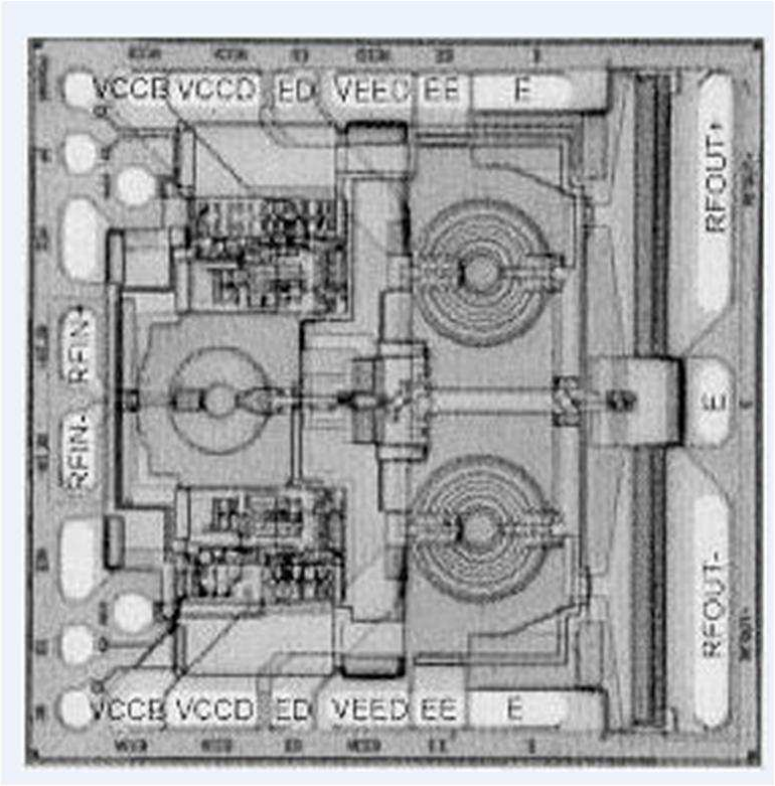

Summary

- We made a quite detailed survey through major topics with respect to Oscillator design.
- A variety of circuits have been discussed.
- Different type of resonators were introduced which are strongly influencing the design and the performance of oscillators.
- A detailed mathematical modelling was explained describing major effects within oscillators.
- Modern simulation tools can precisely predict the technical parameters of a design.

Key References

1. M. Odyniec, Editor, *RF and Microwave Oscillator Design*, Chapter 5: Modern Harmonic-Balance Techniques for Oscillator Analysis and Optimization, by V. Rizzoli, A. Neri, A. Costanzo, F. Mastri, Artech House, 2002.
2. U.L. Rohde, C.R Chang, J. Gerber, "Design and Optimization of Low-Noise Oscillators Using Nonlinear CAD Tools," IEEE Frequency Control Symp. Proc., pp 548-554, 1994.
3. U. L. Rohde, C. R. Chang, J. Gerber, "Parameter Extraction for Large Signal Noise Models and Simulation of Noise in Large Signal Circuits Like Mixers and Oscillators," Proceedings of the 23rd European Microwave conference, Madrid, Spain, Sept. 6-9, 1993.
4. V. Rizzoli, F. Mastri, C. Cecchefti, "Computer-Aided Noise Analysis of MESFET and HEMT Mixers," IEEE Trans. Microwave Theory and Techniques, Vol. MTT-37, pp 1401-1410, Sept. 1989.
5. V. Rizzoli, A. Lippadni, "Computer-Aided Noise Analysis of Linear Multiport Networks of Arbitrary Topology," IEEE Trans. Microwave Theory and Techniques, Vol. MTT-33, pp 1507-1512, Dec. 1985.
6. V. Rizzoli, F. Mastri, D. Masotti, "General-Purpose Noise Analysis of Forced Nonlinear Microwave Circuits," Military Microwave, 1992.
7. W. Anzill, F. X. Kärtner, P. Russer, "Simulation of the Single-Sideband Phase Noise of Oscillators," Second International Workshop of Integrated Nonlinear Microwave and Millimeterwave Circuits, 1992.
8. U. L. Rohde, Matthias Rudolph RF/Microwave Circuit Design for Wireless Applications, Second Edition, Wiley, 2013
9. Anisha M. Apte, "A New Analytical Design Method of Ultra-low-noise Voltage Controlled VHF Crystal Oscillators and it's Validation", Ph.D. Dissertation Brandenburgischen Technischen Universität Cottbus–Senftenberg, February, 2020
10. Fundamentals of RF and Microwave Techniques and Technologies Kindle Edition by Hans L. Hartnagel, Rüdiger Quay, Ulrich L. Rohde, Matthias Rudolph, Springer 2023
11. Microwave Circuit Design Using Linear and Nonlinear Techniques 3rd Edition by George D. Vendelin, Anthony M. Pavio, Ulrich L. Rohde, Matthias Rudolph, Wiley 2021
12. Microwave and Wireless Synthesizers: Theory and Design, 2nd Edition by Ulrich L. Rohde, Enrico Rubiola, Jerry C. Whitaker Wiley, 2021
13. Wolfgang Griebel, " Space Qualified 5MHz Crystal Oscillators with Maximum Stability between 1 and 10 Seconds", Ph. D. dissertation Brandenburgischen Technischen Universität Cottbus–Senftenberg, April, 2021

Thank you very much for your attention

Questions?